

Interscience Research Network

Interscience Research Network

Conference Proceedings - Full Volumes

IRNet Conference Proceedings


11-11-2011

International Conference on MECHATRONICS, ROBOTICS AND MANUFACTURING

Prof. Srikanta Patnaik, Mentor

Prof. Subhasis Bhaumik Professor

Follow this and additional works at: https://www.interscience.in/conf_proc_volumes

 Part of the [Aerospace Engineering Commons](#), [Automotive Engineering Commons](#), [Electrical and Computer Engineering Commons](#), and the [Mechanical Engineering Commons](#)

Proceedings
Of
International Conference
on
**MECHATRONICS, ROBOTICS AND
MANUFACTURING**

(ICMRM-2011)

11th & 12th December, 2011

Editor-in-Chief

Prof. (Dr.) Srikanta Patnaik

President, IRNet India and Chairman IIMT
Interseince Campus, Bhubaneswar
Email: patnaik_srikanta@yahoo.co.in

Prof(Dr) Subhasis Bhaumik

Associate Professor, Aerospace Engg. & Applied Mechanics
Bengal Engineering and Science University

Organized by:



About ICMRM 2011

As on today, for mechatronic systems, the main issue is no more how to implement a control system, but how to implement actuators and what is the energy source. The most advanced mechatronics systems are the well known camera autofocus system or camera anti-shake systems. With regards to energy sources of mechatronics systems, most of the applications presently use batteries. But there is a paradigm shift in this approach and now the concept is the energy harvesting, allowing transforming into electricity mechanical energy from shock, vibration, or thermal energy from thermal variation, and so on.

Secondly, robotics has become a popular tool in raising interests primarily among mechanical and computer science engineers. In practice, it is usually an electro-mechanical machine which is guided by computer or electronic programming, and is thus able to do tasks on its own. Another common characteristic is that by its appearance or movements, a robot often conveys a sense that it has intent or agency of its own. This conference also addresses various issues of robotic systems.

Manufacturing system refer to a range of human activity, from handicraft to high tech, but is most commonly applied to industrial production, in which raw materials are transformed into finished goods on a large scale. Such finished products may be used for manufacturing other, more complex products, such as aircraft, household appliances or automobiles. Modern manufacturing includes all intermediate processes required for the production and integration of a product's components.

The conference shall address to the broad areas of **Mechatronics, Robotics, and Manufacturing**. This will cover industrial applications, such as mechanical product manufacturing; applications in the automotive, aircraft, aerospace, machine tools, mould and die industries; consumer electronics product manufacturing; computers, semiconductor and communication industries and regulated product manufacturing; and biomedical, food, pharmaceutical and packaging industries.

The objective of ICMRM-2011 is to establish a channel of communication to disseminate knowledge between academics/researchers and industry practitioners about the advances in mechatronics, robotics, sensors and controls applications in modern manufacturing processes and systems.

Area of Coverage

Topics include, but are not limited to, the following:

- Agent-based manufacturing systems
- Artificial intelligence methods for manufacturing
- Advanced machining systems
- Autonomous and adaptive control systems
- Automated manufacturing systems
- Computer aided and integrated manufacturing methods
- Computer aided inspection and quality control systems
- Computers in manufacturing
- Computational methods and optimisation
- Software design for intelligent manufacturing
- Robotics in manufacturing
- Micro and nanomechatronics systems for manufacturing
- Hybrid manufacturing processes and systems
- Intelligent and smart machining systems
- Layered manufacturing
- Micro and nanomanufacturing systems
- Modern engineering of manufacture
- Process modelling and monitoring
- Sensors and actuators for manufacturing systems
- Virtual and rapid prototyping
- Network technologies in manufacturing

EDITORIAL BOARD

Editor-in-Chief

Prof. (Dr.) Srikanta Patnaik

President, IRNet India and Chairman IIMT
Interscience Campus, Bhubaneswar
Email: patnaik_srikanta@yahoo.co.in

Prof (Dr) Subhasis Bhaumik

Associate Professor, Aerospace Engg. & Applied Mechanics
Bengal Engineering and Science University

Members of Editorial Board

Dr. Anthony Tzes

Professor & Department Head 2009-11
University of Patras
Electrical & Computer Engineering Department
6 Eratosthenous Str. Rio, Achaia 26500
GREECE.

Dr. Costas Tzafestas

Assistant Professor,
National Technical University of Athens (NTUA)
School of Electrical and Computer Engineering
Division of Signals, Control and Robotics
Zographou Campus 15773, Athens, Greece.

Dr. Prabhat K. Mahanti

Professor, Computer science
University of New Brunswick
100 Tucker Park Road, Saint John, N.B., E2L 4L5
Canada
Email: pmahanti@unb.ca
URL: www.unb.ca

Prof. Joseph Davis

School of Information Technologies
The University of Sydney
AUSTRALIA

Kostas J. Kyriakopoulos

Professor
Control Systems Lab, Mechanical Eng. Dept.
National Technical University of Athens
9 Heroon Polytechniou Str., Zografou
Athens 15700, Greece.

Organizing Committee

Chief Patron:

Prof. (Dr.) Srikanta Patnaik

President, IRNet India and Chairman IIMT
Interseince Campus, Bhubaneswar
Email: patnaik_srikanta@yahoo.co.in

Programme Chair:

Prof. (Dr.) B. B. Biswal.

Department of Mechanical Engineering
National Institute of Technology, Rourkela
India, Email: bibhuti.biswal@gmail.com

Secretary IRNet:

Prof. Pradeep Kumar Mallick

IIMT, Bhubaneswar
Email:pradeepmallick84@gmail.com
Mobile No: 08895885152

Conference Coordinator:

Rashmi Ranjan Nath, IRNet, Bhubaneswar

Event Manager

Prof. Sharada Prasad Sahoo, IIMT, Bhubaneswar

Publication

Prof. Sushanta Kumar Panigrahi, IIMT, Bhubaneswar
Prof. Mritunjay Sharma, IIMT, Bhubaneswar

Post Conference Coordinator

Bibhu Prasad Mohanty, IRNet, Bhubaneswar
Mob:08895995279

Head (System & Utilities)

Prof. Sanjay Sharma, IIMT, Bhubaneswar

Members of IRNet

Miss. Ujjayinee Swain, Sagarika Ray, Akash Kumar Bhoi,
Bikash Kumar Rout & Pritika Mohanty.

First Impression : 2011

(c) Interscience Research Network

Proceedings of International Conference on Mechatronics, Robotics And Manufacturing

No part of this publication may be reproduced or transmitted in any form by any means, electronic or mechanical, including photocopy, recording, or any information storage and retrieval system, without permission in writing from the copyright owners.

DISCLAIMER

The authors are solely responsible for the contents of the papers compiled in this volume. The publishers or editors do not take any responsibility for the same in any manner. Errors, if any, are purely unintentional and readers are requested to communicate such errors to the editors or publishers to avoid discrepancies in future.

ISBN : 978-93-81693-07-0

Published by :

IPM PVT. LTD., Interscience Campus
At/PO.: Kantabada, Via: Janla, Dist: Khurda, Pin- 752054
Publisher's Website : www.interscience.in
E-mail: ipm.bbsr@gmail.com

Typeset & Printed by :

IPM PVT. LTD.

TABLE OF CONTENTS

Sl. No.	Topic	Page No.
	Editorial	
	- <i>Prof. (Dr.) Srikanta Patnaik</i>	
	- <i>Prof(Dr) Subhasis Bhaumik</i>	
1	Overview of Friction Stir Welding - <i>Biswajit Parida & Sukhomay Pal</i>	01-08
2	Path Planning and Navigation for Mobile Robot Using Modified Active Bat IPS - <i>Md. Reaz Ashraful Abedin</i>	09-15
3	Oil Spill Reduction using Sea Swarm Technique - <i>Swapnil Sarode, Gaurav Ranade & Yashraj Sahasrabudhe</i>	16-18
4	Fusion of Hard and Soft Control Strategies for a Double Inverted Pendulum - <i>Alex N. Jensen, Chandrasekhar Potluri, & D. Subbaram Naidu</i>	19-23
5	Investigation and Development of Mathematical Correlations of Cutting Parameters for Machining Titanium with CNC WEDM - <i>Bazani Shaik & S. V. Ramana</i>	24-28
6	Robust Adaptive Control For Two Robot Manipulators Handling An Object - <i>E. Balasubramanian, S. Riyaz Ahammed & S. Abilash</i>	29-35
7	A Nonlinear Model to Study Selectively Deformable Wing of an Aircraft - <i>M. Thangavel¹ & C. Thangavel²</i>	36-42
8	Need for Computer Integrated Manufacturing – A Review - <i>Mohd.Abdul Shoeb, Mirza Hussain Baig, Md. Thajuddin & Dr.T. Srihari</i>	43-48
9	Gesture Based Communication -A Gesture Humanoid - <i>G S L K CHAND, G JAGADEESH & Ch SARVANA KUMAR</i>	49-52
10	Micro Robots For Minimally Invasive Surgery – A Review - <i>Deiva Ganesh. A & Thangavel. M</i>	53-60
11	Mechanical Design of Omni-Directional Robot Suitable for Swarm Based Application - <i>M. Thangavel & T. Vinny Daniel David</i>	61-68

Editorial

Every engineering discipline is becoming multidisciplinary in nature. Even the advanced industrial products or consumer products also holistic in their development and utility. In the world of automation the entire focus is to properly manifest a computational model with sharp edge of intelligence that can drive the mechanically designed capital goods meant for manufacturing or some process of intermediate products. The conference is addressing these three disciplines like Mechatronics, Robotics and Manufacturing which are integrated disciplines in many instances. Mechatronics is the combination of mechanical engineering, electronic engineering, computer engineering, software engineering, control engineering, and systems design engineering in order to design, and manufacture useful products^{[1][2]}. Mechatronics is a multidisciplinary field of engineering, that is to say it rejects splitting engineering into separate disciplines. Originally, mechatronics just included the combination between mechanics and electronics; hence the word is only a portmanteau of mechanics and electronics. However, as technical systems have become more and more complex the word has been "updated" during recent years to include more technical areas. French standard NF E 01-010 gives the following definition: "approach aiming at the synergistic integration of mechanics, electronics, control theory, and computer science within product design and manufacturing, in order to improve and/or optimize its functionality. The application areas include Machine vision , Automation and robotics, Servo-mechanics Sensing and control systems, Automotive engineering, automotive equipment in the design of subsystems such as anti-lock braking systems, Computer-machine controls, such as computer driven machines like IE CNC milling machines, Expert systems Industrial goods.

Robotics is the branch of technology that deals with the design, construction, operation, structural disposition, manufacture and application of robots. Robotics is related to the sciences of electronics, engineering, mechanics mechatronics, and software. The concept and creation of machines that could operate autonomously dates back to classical times, but research into the functionality and potential uses of robots did not grow substantially until the 20th century. Today, robotics is a rapidly growing field, as we continue to research, design, and build new robots that serve various practical purposes, whether domestically, commercially, or militarily. A first particular new innovation in robot design is the open sourcing of robot-projects. To describe the level of advancement of a robot, the term "Generation Robots" can be used. This term is coined by Professor Hans Moravec, Principal Research Scientist at the Carnegie Mellon University Robotics Institute in describing the near future evolution of robot technology. First generation robots, Moravec predicted in 1997, should have an intellectual capacity comparable to perhaps a lizard and should become available by 2010. Because the first generation robot would be incapable of learning, however, Moravec predicts that the second generation robot would be an improvement over the first and become available by 2020, with the intelligence maybe comparable to that of a mouse. The third generation robot should have the intelligence comparable to that of a monkey. Though fourth generation robots, robots with human intelligence, professor Moravec predicts, would become possible, he does not predict this happening before around 2040 or 2050.

Manufacturing Engineering is a very broad area which includes the design and development of products. The manufacturing engineering discipline has very strong overlaps with mechanical engineering, industrial engineering, electrical engineering, electronic engineering, computer science, materials management, and operations management. Manufacturing engineers' success or failure directly impacts the advancement of technology and the spread of innovation. This field of engineering emerged in the mid to late 20th century, when industrialized countries introduced factories with:

- Advanced statistical methods of quality control: These factories were pioneered by the American mathematician William Edwards Deming, who was initially ignored by his home country. The same methods of quality control later turned Japanese factories into world leaders in cost-effectiveness and production quality.
- Industrial robots on the factory floor, introduced in the late 1970s: These computer-controlled welding arms and grippers could perform simple tasks such as attaching a car door quickly and flawlessly 24 hours a day. This cut costs and improved production speed

Many manufacturing companies, especially those in industrialized nations, have begun to incorporate computer-aided engineering (CAE) programs into their existing design and analysis processes, including 2D and 3D solid modeling computer-aided design (CAD). This method has many benefits, including easier and more exhaustive visualization of products, the ability to create virtual assemblies of parts, and ease of use in designing mating interfaces and tolerances.

Other CAE programs commonly used by product manufacturers include product life cycle management (PLM) tools and analysis tools used to perform complex simulations. Analysis tools may be used to predict product response to expected loads, including fatigue life and manufacturability. These tools include finite element analysis (FEA), computational fluid dynamics (CFD), and computer-aided manufacturing (CAM).

The conference is designed to stimulate the young minds including Research Scholars, Academicians, and Practitioners to contribute their ideas, thoughts and nobility in these three integrated disciplines. Even a fraction of active participation deeply influences the magnanimity of this international event. I must acknowledge your response to this conference. I ought to convey that this conference is only a little step towards knowledge, network and relationship.

I congratulate the participants for getting selected at this conference. I extend heart full thanks to members of faculty from different institutions, research scholars, delegates, IRNet Family members, members of the technical and organizing committee. Above all I note the salutation towards the almighty.

Editor-in-Chief

Prof. (Dr.) Srikanta Patnaik

President, IRNet India and Chairman IIMT
Interscience Campus, Bhubaneswar
Email: patnaik_srikanta@yahoo.co.in

Prof. (Dr) Subhasis Bhaumik

Associate Professor, Aerospace Engg. & Applied Mechanics
Bengal Engineering and Science University

Overview of Friction Stir Welding

Biswajit Parida & Sukhomay Pal

Mechanical Engineering, IIT Guwahati, India-781039.

Abstract - In this study the various factors affecting Friction Stir Welding (FSW) process has been reviewed. This can be broadly differentiated into five categories including the introductory part. After an introduction to FSW, the parameters influencing this process such as tool geometry, tool rotational speed, tool traverse rate, applied forces and forces generated have been reviewed. Then the various models developed by a number of researchers in order to stabilize the FSW process have been discussed. The effect of friction stir welding process on microstructure and properties of the welded parts along with the tool condition monitoring during the operation have been reviewed. Finally the purpose of this review and the scope for future work on this emerging joining technique has been discussed.

Key words - Friction stir welding, FSW thermal history, different welding zone, micro-structure, micro-hardness.

I. INTRODUCTION

Friction Stir Welding (FSW) is a solid state welding method without using filler material. In this process the joined material is plasticized by heat generated by friction between the surface of the plates to be welded and the contact surface of a special tool. The tool is composed of two main parts, namely; shoulder and pin. Shoulder is responsible for the generation of heat and for containing the plasticized material in the weld zone, while pin mixes the material of the components to be welded, thus creating a joint. Though tools designed for different applications may have slightly different shapes of the tool pin and shoulder, all tools maintain this same two elements design. This process was invented by The Welding Institute (TWI), Cambridge, UK in 1991 [1] and has been one of the most significant joining technology developments in the last two decades.

FSW creates weld by the combined action of frictional heating and mechanical deformation. The maximum temperature reached is of the order of 0.8 of the melting temperature of base metal. It is being considered as a thermo-mechanical process, which transforms heterogeneous microstructure of base metal to more homogeneous microstructure. The process is most suitable for critical applications like joining of structural components made of aluminum and its alloys. It involves complex interactions between a variety of simultaneous thermo-mechanical processes and parameters, which affect the heating and cooling rate, plastic deformation and material flow, dynamic recrystallization phenomena and mechanical integrity of the joint. The friction stir welding is shown in Fig. 1.

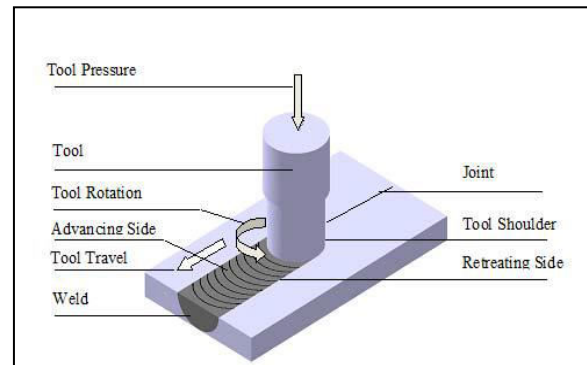


Fig.1 : Friction stir welding process.

Ma [2] studied the friction stir processing technology which is developed based on the basic principles of FSW. He has concluded that intense plastic deformation and thermal exposure during friction stir processing (FSP) causes the creation of fine, uniform, and pore-free structure. The process causes intense plastic deformation, material mixing, and thermal exposure. It results in significant microstructural refinement, densification, and homogeneity of the welded zone. It is energy efficient, environment friendly, and versatile. It can be developed to be a generic metalworking technique that can provide the localized modification and control of microstructures in the near-surface layers of metallic components.

II. EFFECT OF PROCESS PARAMETERS

In FSW the material flow pattern and temperature distributions are greatly influenced by various welding parameters, tool geometry, and joint design which in turn influence the microstructural evolution of material.

This section contains some of the major factors affecting FSW process, such as tool geometry, welding parameters, joint design etc.

In material flow the tool geometry plays a vital role which governs the traverse rate at which FSW can be conducted. The tool design also governs the heat generation, plastic flow, the power required and the uniformity of microstructure and mechanical properties. The heating results primarily from the friction between pin and workpiece in the initial stage of tool plunge. The function of the tool is to 'stir' and 'move' the material at the same time the shoulder provides confinement for the heated volume of material. Two very important parameters in FSW process are the tool rotation rate in clockwise or counter-clockwise direction and the tool traverse speed. The heat generation rate, temperature field, cooling rate, force, torque, and the power depend on these variables. Another important process parameter is the angle that the tool makes with the vertical axis. A suitable tilt of the spindle towards trailing direction ensures that the shoulder of the tool holds the stirred material and moves it efficiently from the front to the back of the pin. Further, the insertion depth of pin into the workpieces is important for producing sound welds.

Wang and Liu [3] studied the Friction stir welding of aluminum plates which were welded at various rotational speeds (850 – 1860 rpm) and travel rates of 30 to 160 mm/min. The welding forces were ranging from 2.5 MPa to 10 MPa and the welding head dimensions were different. They found that dimensions of the tool probe are critical to produce sound weld. The microstructure of the weld is characterized by its much finer and equi-axed grains as compared to the parent Aluminum plate. 10% higher micro-hardness was obtained than the parent metal. It was found that the travel rate of welding head pin has a strong effect on micro-hardness and tensile strength. Scialpi *et. al.* [4] studied the influence of shoulder geometry on microstructure and mechanical properties of friction stir welded 6082 aluminum alloy. The experiments were carried out on AA 6082 T6 sheet of 1.5 mm thick with a tool rotational speed of 1810 rpm and at a feed rate of 460 mm/min. Three types of shoulder geometries were taken into consideration. They concluded that tool with fillet and cavity (TFC) crown is the best in terms of crown quality. Tool with fillet and scroll (TFS) and TFC showed a higher strength and elongation. They also concluded that the TFC can be considered the best tool with 460 mm/min and 1810 rpm. Fujii *et. al.* [5] studied the effect of tool shape on mechanical properties and microstructure of friction stir welded aluminum alloys. The welding of 1050-H24, 5083-O and 6061-T6 aluminum alloys was performed by using the simplest shape (column without threads), the ordinary shape (column with threads) and the triangular prism shape

pins as shown in Fig. 2, were used to weld three types of aluminum alloys. The conclusions achieved were for 1050-H24 whose deformation resistance is very low, a columnar tool without threads produces weld with the best mechanical properties. For 6061-T6 whose deformation resistance is relatively low, the tool shape does not significantly affect the microstructures and mechanical properties of the joints. At a high rotation speed (1500 rpm), the triangular prism tool is the best; at the middle rotation speed (800 rpm), the column with threads is the best. For a low rotation speed (600 rpm), the tool shape does not significantly affect the microstructures and mechanical properties of the joints.

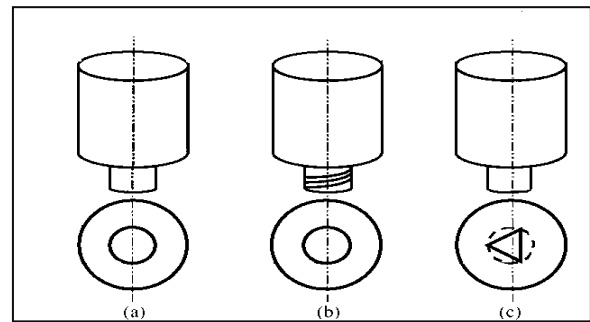


Fig. 2 : FSW tool shape: (a) column without threads, (b) column with threads, (c) triangular prism

Boz and Kurt [6] carried out the welding processes with five different stirrers, four of them were screw type with 0.85, 1.10, 1.40 and 2.0 mm pitch and one was a bar with 5mm x 5 mm square cross-section. The stirrers with 1.40 mm and 2.0 mm pitch acted like a drill rather than a stirrer and compelled the weld metals outwards. As a result of this weld metal was accumulated towards the stirrer shoulder and therefore the welding process could not be affected. The weld metal accumulated between tool pin and shoulder is shown in Fig. 3. The best bonding was obtained with 0.85 mm and 1.10 mm pitched stirrers. Specimens were welded using 0.85 mm and 1.10 mm pitched stirrers exhibited the same mechanical and metallographic properties. The square cross-section stirrer showed poor mechanical and metallographic properties. Sakthivel *et. al.* [7] studied the effect of Welding Speed on Micro-structure and Mechanical Properties of Friction-stir Welded Aluminum in which the welds were made at various welding speed by using a hardened steel FSW tool. They have concluded that the micro-structure of the weld nugget consists of fine equiaxed grains and are more homogenous at lower welding speed than at higher welding speed. The size of the weld zone becomes wider when decreasing the traverse speed as a result of a large amount of frictional heat easy material flow. The

hardness slightly increases with the increase of welding speed. The ultimate tensile strength is observed to increase when decreasing the traverse speed. The best mechanical properties are obtained at lower traverse speed due to the occurrence of homogenous grains and higher heat input.

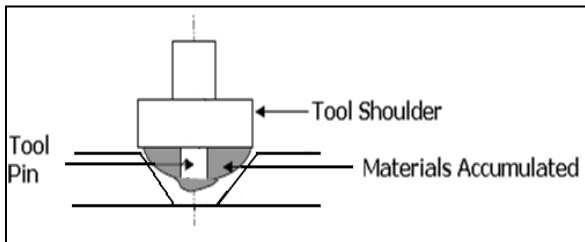


Fig. 3 : Weld metal accumulated between tool pin and shoulder.

Adamowski and Szkodo [8] studied the FSW of aluminum alloy (AW6082-T6) in terms of the properties and micro-structural changes in welds in function of varying process parameters. The test welds were produced with various combinations of process parameters without the possibility of controlling the downward force. They concluded that the mechanical resistance of welds increases with the increase of travel speed. Softening of the material in the weld nugget and heat affected zone was observed. The hardness of both the heat affected zone and the weld nugget is lower than that of the base metal. Sato *et al.* [9] joined the 6063-T4 aluminum alloy using FSW process. They considered different rotation speeds and a constant transverse speed study the temperature variation, measured by using thermocouples. It was found that the maximum temperature attained in the nugget zone (NZ) and rose sharply with increasing rotation speed up to 2000 rpm. The grain size of the NZ increased exponentially with increasing maximum temperature. The hardness values in the as-welded condition were distributed homogeneously in the weld.

Kim *et al.* [10] investigated the effect of the welding speed and the rotation speed on the microstructure in the stir zone by measuring the Si particle distribution in the Aluminum die casting alloys. Four millimeter thick ADC12 aluminum die casting alloy plates were welded keeping the tilt angle as 3° , and the tool plunge downforce as 14.2 kN. The tool rotation speed in the clockwise direction and the welding speed were varied from 750 to 1750 rpm and from 250 to 1000 mm/min, respectively. The conclusions obtained from the above experimentations are that the stir zone has fine recrystallized grains without a dendritic structure. The number of finer Si particles increases during the FSW. The size of the Si particles in the bottom is smaller than that in the top or the middle, while the size in the retreating side is almost the same as that in the

advancing side. The Si particles size decreases with the increasing welding speed.

III. MODELING OF FSW PROCESS

This section includes the review of the understanding of mechanical and thermal processes during FSW. In FSW process the heat is generated by friction between the tool and the work-piece. This results in intense plastic deformation and temperature increase within and around the stirring zone. Due to this a significant microstructural evolution, including grain size, grain boundary character, dissolution and coarsening of precipitates, breakup and redistribution of dispersoids, and texture takes place.

Durdanovic *et al.* [11] developed a mathematical model which describes the heat generated in various stages of FSW process. Parameters involving proper welded joint creation are just the same parameters in heat generation. The amount of heat generated directly depend on the geometrical parameters of the tool, rotational and traversal speed, pressure, shear stress and friction co-efficient. It was concluded from various models that determination of precise amount of heat generated during friction stir welding process is complicated since there are various uncertainties, assumptions and simplifications of mathematical models that describes the welding process. Hwang *et al.* [12] explored the thermal histories and temperature distributions in a work piece during a FSW process involving the butt joining of aluminum 6061-T6. Regression analysis by the least squares method was used to predict the temperature and it was found that the temperatures inside the pin can be regarded as a uniform distribution. The heat transfer starts from the rim of the pin to the edge of the workpiece, approximately following a second-order polynomial equation. The appropriate temperatures ranges for a successful FSW process are between 365°C and 390°C . The temperatures on the advancing side are slightly higher than those on the retreating side. The tensile strength and the hardness at the thermo-mechanically affected zone are about one-half of the base metal.

McNelley *et al.* [13] used two restoring models for hot working of metals to interpret microstructure and micro-texture data for two aluminum alloys subjected to FSP. They concluded that due to recrystallization, grain refinement occurs during FSW process.

III. MICROSTRUCTURE AND MECHANICAL PROPERTIES OF FRICTION STIR WELDED JOINT

The heat associated with FSW process results in significant microstructural evolution within and around the three zones as shown in Fig. 4 namely- nugget zone

(NZ), thermo-mechanically affected zone (TMAZ), and heat affected zone (HAZ). This leads to substantial change in post weld mechanical properties such as strength, ductility, fatigue, and fracture toughness. Aluminum alloys are classified into heat-treatable alloys and non heat-treatable (solid-solution-hardened) alloys. FSW creates a softened region around the weld center in a number of precipitation-hardened aluminum alloys. A number of investigations demonstrated that the change in hardness in the friction stir welds is different for precipitation-hardened and solid-solution-hardened aluminum alloys.

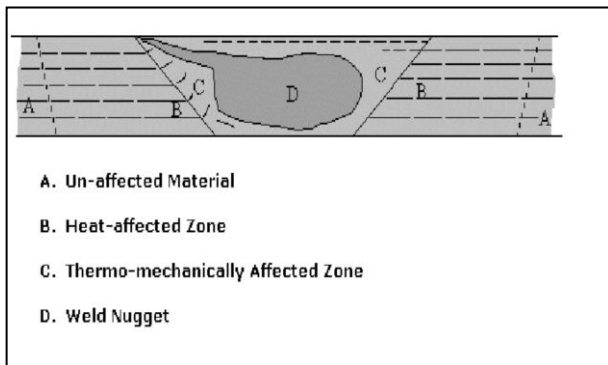


Fig. 4 : FSW weld with four distinct zones

Cerri and Leo [14] studied the warm and room temperature deformation of friction stir welded thin aluminum sheets. In this work the Friction stir welded joints of 2024T3– 2024T3, 6082T6–6082T6 and 6082T6–2024T3 of very thin thickness (0.8mm) were investigated at room and warm temperatures of deformation by tensile tests and microhardness measurements. They concluded that all the thin FSW joints showed the capability to undertake tensile stress at room temperature and at warm temperatures of deformation. The stress has decreased with increasing temperature and decreasing strain rate. The ductility of the thin joints was quite independent of temperature and strain rate. Cabibbo *et. al.* [15] studied the microstructure and mechanical properties of AA6056 friction stir welded plates using polarized optical and transmission electron microscopy techniques. FSW was carried out for 10-mm thick plates at a rotational speed of 1800 rpm and tilt angle of 3° and with a translational speed of 15 mm/s. The conclusions obtained are that the grain structure is fine equi-axed in the nugget at the weld centre, highly elongated with very small cells in the retreating side TMAZ and in the narrow advancing side, and slightly elongated coarse grains in the HAZ and the parent material. Strain rate and temperature gradients are much steeper in the advancing side than in the retreating. Mechanical properties of the welded region are quite good, the ultimate strength is about 90%

and yield strength is about 66% of the values in the base alloy. Su *et al.* [16] have reported in AA7050 the transformation of elongated grains with 1–2 μm cells in the TMAZ into 1 – 4 μm equiaxed structure with many HAB in the nugget. Prangnell *et al.* [17] shown that the crystallite size in the nugget is consistent with structures developed in torsion to the same strain at equivalent temperatures and strain rates.

Sarsilmaz and Caydas [18] studied the statistical analysis on mechanical properties of Friction Stir Welded AA1050/AA5083 couples. The parameters taken into consideration were spindle rotation speed, traverse speed and stirred geometry. During experiments, the tool rotational speed and traverse speed were varied while screw and triangular profiles were used for stirrer geometry. The ultimate tensile strength and hardness of the welded joints were determined. The relative effect of each factor and combination of factors on responses was obtained using analysis of variance. They concluded that the ultimate tensile strength and nugget hardness increases with traverse speed but decreases with tool rotational speed. The most important factor on ultimate tensile strength was found as traverse speed with (relative effect of 71.62%), then the rotational speed (relative effect of 10.59%) and finally the stirrer geometry (7.03%). The most important factor on nugget hardness was found as traverse speed (72.57%), then the rotational speed (21.19%) and finally the stirrer geometry (0.89%). Sakhivel *et. al.* [7] concluded that the best mechanical properties are obtained at lower traverse speed due to the occurrence of homogenous grains and higher heat input. The grains are refined and equiaxed in weld nugget of average diameter 1-5 μm . This refinement is due to the dynamic recrystallization [28, 29, 30], which is a combined action of high rate strain and elevated temperatures. Such a structure is characterized by a very low level of residual stresses, excellent ductility and mechanical properties superior to those of HAZ [31]. Rodrigues *et. al.* [19] studied the influence of FSW parameters on the micro-structural and mechanical properties of AA 6016-T4 thin welds. The welds produced in 1 mm thick plates with two different tools, were analyzed and compared concerning the micro-structure and mechanical properties. For each tool the welding parameters were optimized in order to achieve non-defective welds. They concluded that the differences in tool geometry and welding parameters induced significant changes in the material flow path during welding as well as in the microstructure in the weld nugget. The welds produced shoulder displayed a larger nugget grain size with few coarsened precipitates. It opposed to the welds done with the scrolled shoulder which showed a smaller grain size containing many coarsened precipitates. The differences in micro-structure conducted to a reduction

in hardness around 15% in the cold welds contrary to the hot welds where an even match condition was reached. Despite the mechanical heterogeneity, the cold weld blanks displayed good deep drawing behavior. Sato and Kokawa [20] tried to clarify dominant microstructural factors governing the global tensile properties of the welded joint. This is by the estimation of the distribution of the local tensile properties in the joint including extensive regions from the stir zone to the unaffected base material region. In this study an extruded 6063-T5 Al, 4 mm thickness plates were friction stir welded keeping the travel speed and the tool shoulder diameter as 10 mm/s and 15 mm respectively. They concluded that the minimum hardness determined global yield and ultimate tensile strengths of the welded joint. A tensile fracture occurred in the minimum hardness region in a joint having heterogeneous hardness such as an as welded joint.

Yeni *et. al.* [21] examined the effect of post weld aging on microstructure, hardness and tensile properties. The welding was carried out using two different helical angles of the threaded pin, namely right and left helical. For right helical pin, two different shoulders were utilized. They concluded that the nugget zone exhibited a recrystallized fine grain structure with grain sizes increasing moving from the weld region to the base metal. Post weld aging process compensates the hardness decrease observed in as welded joints; no significant decrease in hardness is obtained throughout the weld region. It was been seen that the left helical screw yields higher mechanical properties when tested at the same shoulder diameter. Rhodes *et. al.* [22] studied the fine-grain evolution in friction-stir processed 7050 aluminum. They found that the fine grains are initiated by recrystallization. The increase in tool speed has resulted in increased deformation as well as increased frictional and deformation heating to the extent that recrystallization has occurred. The heat generated by the rotating tool is a function of the rotation speed and the external cooling rate. At slower cooling rates and/or faster tool rotation speeds, recrystallization of the deformed aluminum occurs. Fonda *et. al.* [23] studied the initial microstructural evolution during FSW process. In this study an aluminum single crystal was friction stir welded in four different directions. The conclusions drawn from the above work is that the shear deformation generated by the FSW process gradually rotates regions of the single crystal. It grows in size and mis-orientation as the welding deformation continues. This rotation continues until these new grains achieve an easily-sheared orientation. Further development of this grain structure has been obscured by conventional recrystallization and deformation near the tool.

Fonda and Bingert [24] investigated the thermo-mechanically affected zone/heat-affected zone (TMAZ/HAZ) boundary of a friction stir weld 2519 Al to determine their contributions to the properties of that region. Two plates of 25 mm thick 2519-T87 aluminum alloy were friction stir welded along the rolling direction with a conventional pin tool under load control. The welding was performed with a rotational speed of 175 rpm and a tool translational speed of 1.1 mm/s. The microhardness map revealed that the soft band, corresponding to the typical fracture location in friction stir welds of this alloy, is located at the boundary between the TMAZ and HAZ. The primary cause of softening at the TMAZ/HAZ boundary was determined to be due to coarsening and transformation of the strengthening precipitates during the welding process. Locations within the TMAZ achieve temperatures during welding that are sufficient to at least partially dissolve the precipitates, leading to the precipitation of very fine GP zones during cooling.

IV. TOOL CONDITION MONITORING

In FSW there is no appreciable tool consumption for many systems for which there do not seem to be any literature reports of systematic studies of tool condition. The issue of tool condition for extended processing will become an important concern especially where abrasive particles are involved since there is increasing interest in aerospace, automotive and marine system applications for advanced metal matrix composite use.

Yang *et. al.* [25] developed a monitoring algorithm to detect gaps in friction stir butt welding operations. During the operation they conducted experiments to determine how the process parameters like tool rotation rate and tool traverse speed and the gap width affect the welding process more particularly, the plunge force acting vertically downward. Three different welding scenarios were considered.

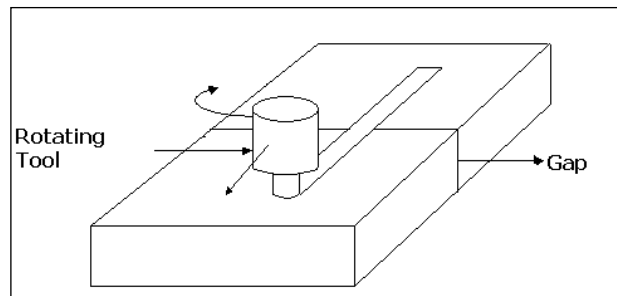


Fig. 5 : Schematics of FSW process.

In the first one tool friction stirs a solid piece of material. The second scenario consists of two sheets which are firmly pushed together such that there is no gap and then are welded that represents the ideal

welding condition. For the third scenario two sheets are separated by shims such that there is a constant known gap and then are welded. The monitoring algorithm was applied to friction stir butt welding operations of 2024 Al alloy. They concluded that the algorithm is able to detect the presence of gaps in FSW operations reliably for tool traverse speeds below 4.233 mm/s and gap sizes above 0.3048 mm. Prado *et. al.* [26] studied the tool wear and the rate of wear for hardened, steel, right-hand screws rotating at 1000 rpm in the FSW of Al 6061+20 vol. %Al₂O₃ particles. They concluded that the welding of above material using threaded tool steel screw weld pins produces a self optimized shape with no threads which continues to produce excellent welds but without any additional tool wear. The self optimized shape changes with increase in weld speed and at a constant tool rotation speed of 1000 rpm. They also concluded that the rate of tool optimization increases with increasing weld speeds which in their study were as high as 9 mm/s and very favorable in terms of commercial welding speeds. Tool optimization occurs for smooth tool shapes with no threads or screw features especially in metal matrix composites FSW. Chen *et. al.* [27] discussed acoustic emission (AE) based monitoring of FSW process. They mentioned that the fast fourier transform method is not appropriate for the monitoring of FSW process as the signal is time variant. Their research focused on the investigation of AE signals using wavelet transforms by having abrupt changes in the workpiece geometry. Finally, they concluded that the different types of defect yield different features in a specific range of frequencies and the band energy variation can provide an indication of gap-induced defects. They also mentioned that the largest problem in using AE to monitor FSW is that a large number of components are involved in generating the AE signals, making it very difficult to extract the valuable features from the AE signals.

V. OUTLOOK AND REMARKS

Current developments in process modeling, microstructure and mechanical properties of the weld, monitoring of FSW process have been addressed in this review. Despite considerable interests in this technology in past decade, the basic physical understanding of the process is still lacking. Some important areas, including material flow, tool geometry design, tool wear, microstructural stability, welding of dissimilar alloys and metals, require understanding. With better quantitative understanding of the principles of heat transfer, material flow, tool-work-piece contact conditions and effects of various process parameters, efficient tools can be standardized. Current FSW process sub-models are complex, time consuming, and difficult to be used in real time. And also they all suffer

from lack of reliability of the predicted results because the physics is highly complex and the current phenomenological models do not contain any model component designed to ensure a good agreement with experimental results. With further research efforts and an increased understanding of the process, an increasing number of applications will be found in the fabrication and processing of materials.

ACKNOWLEDGEMENTS

The authors would like to thank Dr. P. Biswas (IIT,Guwahati), Dr. M. M. Mohapatra (IIT,Roorkee) and Dr. N. R. Mandal (IIT,Kharagpur) for many helpful discussions and their interest in this work.

REFERENCES

- [1] Thomas, W. M., Nicholas, E. D., Needham, J. C., Murch, M. G., Temple-Smith, P., and Dawes, C. J. Friction welding. Patent Application No. 9125978.8, December, 1991
- [2] Z Y Ma, "Friction Stir Processing Technology: A Review", Metallurgical and Materials Transactions, Volume 39A, March 2008 642-658.
- [3] Wang Deqing, Liu Shuhua, "Study of Friction stir welding of aluminum", Journal of Materials Science, Volume 39 (2004) 1689 – 1693.
- [4] Scialpi, L.A.C. De Filippis, P. Cavaliere, "Influence of shoulder geometry on microstructure and mechanical properties of friction stir welded 6082 aluminum alloy", Journals for Materials and Design, Volume 28 (2007) 1124-1129 DOI:10.1016/j.matdes.2006.01.031.
- [5] Hidetoshi Fujii, Ling Cui, Masakatsu Maeda, Kiyoshi Nogi, "Effect of tool shape on mechanical properties and microstructure of friction stir welded aluminum alloys ", Journal of Material Science and Engineering, Volume A 419 (2006),Pages 25-31
- [6] Mustafa Boz, Adem Kurt, "The Influence of Stirrer Geometry on Bonding and Mechanical Properties in friction stir welding process", Journal of Materials and Design, Volume 25 (2004), Pages 343-347.
- [7] T Sakhivel, G S Senegar, J Mukhopadhyay, "Effect of Welding Speed on Micro-structure and Mechanical Properties of Friction-stir Welded Aluminum", International Journal of Advanced Manufacturing Technology (2008), DOI 10.1007/s00170-008-1727-7.

- [8] J. Adamowski, M Szkodo, “ Friction-stir-welds (FSW) of Aluminum alloy AW6082-T6 ”, *Journal of Achievements in materials and Manufacturing Engineering*, Volume 20, Issue 1-2, January-February 2007.
- [9] Sato YS, Urata M, Kokawa H. Parameters controlling microstructure and hardness during friction-stir welding of precipitation-hardenable aluminum alloy 6063. *Metall Mater Trans A* 2002;33(3):625–35.
- [10] Y.G. Kim a, H. Fujii, T. Tsumura, T. Komazaki, K. Nakata, “Effect of Welding Parameters on Microstructure in the Stir Zone of FSW Joints of Aluminum die Casting Alloy ”, *Journals for Materials Letters* Volume 60 (2006) 3830–3837 DOI:10.1016/j.matlet.2006.03.123.
- [11] M B Durdanovic, M M Mijajloric, D S Milcic, D S Stamenkovic, “Heat Generation during Friction-stir-welding (FSW) process”, *Tribology in Industry*, Volume 31, No. 1 & 2, 2009.
- [12] Yeong-Maw Hwang, Zong-Wei Kang, Yuang-Cherng Chiou, Hung-Hsiou Hsu, “Experimental study on temperature distributions within the workpiece during friction stir welding of aluminum alloys”, *International Journal of Machine Tools & Manufacture Design, Research and Application*, Volume 48 (2008) 778–787.
- [13] T R McNelley, S Swaminathan and J Q Su, “Recrystallization mechanisms during friction stir welding/processing of aluminum alloys”, Elsevier Science Ltd. (2007), Doi:10.1016/j.scriptamat.2007.09.064.
- [14] E. Cerri , P. Leo, “Warm and room temperature deformation of friction stirwelded thin aluminum sheets”, *Journals for Materials and Design* (2009) Volume 31 1392-1402.
- [15] M. Cabibbo, H.J. McQueenb, E. Evangelista, S. Spigarelli, M. Di Paola, A. Falchero, “Microstructure and mechanical property studies of AA6056 friction stir welded plate”, *Journal of Materials Science and Engineering*, Volume A 460-461 (2007), Pages 86-94.
- [16] J.-Q. Su, T.W. Nelson, R. Mishra, M. Mahoney, *Acta Mater.* 51 (2003) 713–729.
- [17] Kh.A.A. Hassan, B.P.Wynne, P.B. Prangnell, In the TWI, Cambridge, UK. The paper was presented at the 4th int FSW symp. Park City Utah, May 2003.
- [18] Furkan Sarsilmaz – Ulas caydas, “Statistical Analysis on Mechanical Properties of Friction Stir Welded AA1050/AA5083 couples”, *International Journal of Advanced Manufacturing Technology* (2008), DOI 0.1007/s00170-008-1716-x.
- [19] D M Rodrigues, A Loureiro, C Leitao, R M Leal, B M Chaparro, P Vilaca, “Influence of Friction Stir Welding Parameters on the Micro-structural and Mechanical properties of AA 6016-T4 Thin Welds”, *Journals for Materials and Design* (2008), DOI 10.1016/j.matdes.2008.09.016.
- [20] Yutaka S Sato and Hiroyuki Kokawa, “Distribution of Tensile Property and Microstructure in Friction stir Weld of 6063 Aluminum”, *Metallurgical and Materials Transactions*, Volume 32A, December 2001-3023.
- [21] C Yeni, S sayer, O Ertugrul, M Pakdil, “Effect of Post Weld-aging on the Mechanical and Micro-structural Properties of Friction-stir Welded Aluminum alloy 7075”, *Achieves of Material Science and Engineering*, Volume 34, Issue 2, December 2008, Pages 105-109.
- [22] C G Rhodes, M W Mahoney, W H Bingel, M Calabrese, “Fine-grain Evolution in Friction-stir Processed 7050 Aluminum”, Elsevier Science Ltd. (2003), Doi:10.1016/S1359-6462(03)00082-4.
- [23] R.W. Fonda, J.A. Wert, A.P. Reynolds and W. Tang, “Initial Microstructural Evolution during Friction Stir Welding”, *Material Science and Technology* 2007 175-177.
- [24] R.W. Fonda and J.F. Bingert, “Micro-structural Evolution in the Heat-Affected Zone of a Friction Stir Weld”, *Metallurgical and Materials Transactions*, Volume 35A, May 2004-1487.
- [25] Yu Yanga, Prabhanjana Kalyab, Robert G. Landersb, K. Krishnamurthy, “Automatic gap detection in friction stir butt welding operations”, *International Journal of Machine Tools & Manufacture, Design, Research and Application*, Volume 48 (2008) 1161–1169.
- [26] R.A. Prado, L.E. Murr, K.F. Soto, J.C. McClure, “Self-optimization in tool wear for friction-stir welding of Al 6061 +20% Al₂O₃ MMC”, *Material Science and Engineering*, Volume A349 (2003) 156-165.
- [27] Changming Chen, Radovan Kovacevic, Dragana Jandgric, “Wavelet transform analysis of acoustic emission in monitoring friction stir welding of 6061 aluminum”, *International Journal of Machine Tools & Manufacture, Design, Research and Application*, Volume 43 (2003) 1383–1390

- [28] J-Q. Sua, T.W. Nelson, C.J. Sterling, Microstructure evolution during FSW/FSP of high strength aluminum alloys, *Materials Science and Engineering A* 405 (2005) 277–286.
- [29] Barcellona, G. Buffa, L. Fratini, D. Palmeri, On microstructural phenomena occurring in friction stir welding of aluminium alloys, *Journal of Materials Processing Technology* 177 (2006) 340–343.
- [30] J. Ouyang, E. Yarrapareddy, R. Kovacevic, Microstructural evolution in the friction stir welded 6061 aluminum alloy (T6-temper condition) to copper, *Journal of Materials Processing Technology* 172 (2006) 110–122.
- [31] H.G. Salem, Friction stir weld evolution of dynamically recrystallized AA2095 weldments, *Scripta Materialia* 49 (2003) 1103-1110.



Path Planning and Navigation for Mobile Robot Using Modified Active Bat IPS

Md. Reaz Ashraful Abedin

Electronics and Communication Engineering Discipline, Khulna University, Khulna, Bangladesh
E-mail : abedin.reaz@gmail.com

Abstract - This research introduces with a new approach to efficient navigation of mobile robots in indoor environment. We have used Active Bat indoor positioning system (IPS) for localization of a robot which eliminates a lot of complexities regarding probabilistic mapping. Till now Active Bat system is being used for only positioning of an object with much higher precision than Global Positioning System. But we have proposed some modification in this method so that it can also be used to direct a mobile robot to the right way and can make the navigation problem easier. We have developed path planning algorithm and simulations of the algorithm have shown how much feasible our plans are.

Keywords- *Active Bat, Mobile robot, Navigation, Path planning, algorithm.*

I. INTRODUCTION

With the escalating exploitation of mobile robots in laboratories, industries and for many other purposes (like guidance in an exhibition, exploring through unidentified dangerous places, collecting samples etc), navigation becomes a serious issue for research. The problem of navigation can be solved by making certain three facts to the mobile robot: the robot's position on the environment, position of its destination and the path through which it has to go. To deal with these three facts mobile roboticists generally used three different types of approaches. In first approach, the robot is provided with the map of the environment. The map building is done by using the sensors of the robot. Sensors are used to acquire information about the robot's environment or even directly measure a robot's global position [1]. With the information acquired, a map can be built so that the robot can use the map for further localization and navigation. In second approach, the robot can have the information about its position from an informer and can follow the informer's guidance to reach at the destination. In third approach, the robot is assumed to be like a human who can explore the environment and make a map of the environment in his mind (not mapped before) and simultaneously can localize itself. This approach is typically known as SLAM [16].

The term which deals with the current position of the robot in the environment is known as localization. The robot must determine its position in the

environment to navigate properly. Significant advances have been achieved in this term in the past decade because localization has received the greatest research attention. Till now several localization methodologies have been developed. Among them decomposition strategies [2][3], Markov localization [4], Kalman filter localization [14], landmark based system [15], positioning beacon systems [1], route-based localization are most popular.

The localization problem can be made obviated if a GPS sensor is attached with a mobile robot. The information about its position in the global coordinate is immediately available in this approach. But GPS system has some limitations. Firstly, GPS signals can not travel through walls and obstacles easily and suffer from signal attenuation. It makes GPS system inappropriate for indoor applications [11]. There are some other factors that can degrade GPS signal. Those are Ionosphere and troposphere delays, multipath signals, receiver clock error, orbital error, satellite geometry/shading etc [12]. Furthermore the existing GPS network provides precision to within more than a few meters, which is intolerable for localizing human-scale mobile robot [1].

II. THE ACTIVE BAT SYSTEM

A. Why Active Bat?

Because of several limitations we can't use GPS for localization or navigation of a mobile robot in indoor environment. Here we introduce an indoor positioning

system named Active Bat which was developed in Cambridge University Computer Laboratory [5]. Active bat uses broadband ultrasonic positioning system for 3-D localization. The Active Bat system is based on the principle of Trilateration. Trilateration is a method of position finding by measurement of distances of the object which has to be localized from other three known reference points. Detail calculations of Trilateration are presented in [10].

In this system a transmitter is attached with the object that has to be located. The transmitter transmits a short pulse of ultrasound which is received by receivers mounted at known points on the ceiling. Now the times of flight of the pulse to the receivers from the transmitter can be measured. As we know the speed of sound in air, so it's easy to calculate the distances from the transmitter to each receiver.

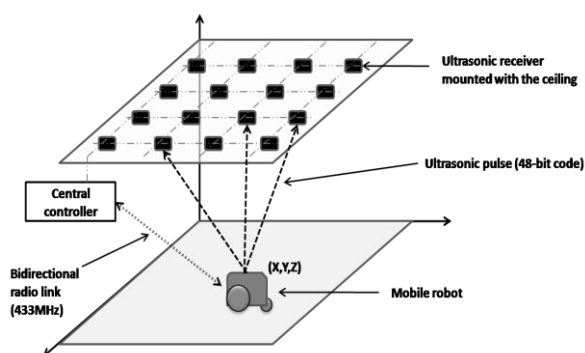


Figure 1. The Active Bat System

If we have three or more such distances, we have enough information to determine the 3D position of the object to which the transmitter is attached. We can also calculate the orientation of the object by finding the relative positions of two or more bats attached to the object. The transmitter is called the Bat. Active bat system provides 3cm of precision in each dimension which is highly appreciable. It is a low power, wireless and relatively inexpensive system [13].

B. Modified Active Bat System

The Active Bat system was mainly designed for tracking an object or a person or something other which has mobility. In this case the object or person does not conscious about their position. They are just tracked by the system. But in case of mobile robots, it must has to know where it is and in which direction it has to move to reach at the goal. So the Active Bat system should be modified if we want to use this system for mobile robot navigation.

Before discussing about the modifications we need to know something more about active bat system. In

active bat system each Bat has a unique 48-bit code, and is linked with the fixed location system infrastructure using a bidirectional 433MHz radio link. The receivers are connected by a high-speed serial network. The serial network is terminated by a DSP calculation board, which collects results from the receivers and uses them to compute transmitter's position. The Bats and the receiver chains are coordinated by a central controller [5].

For using in mobile robot navigation, modification of Active Bat system should be done in the way so that the robot can continuously be informed about its position on the environment. We propose that the bat should be embedded with the robot and controlled by the robot itself, not by the central controller. Thus the robot will be able to know about its position at any moment. Actually during navigation the robot needs to be informed about its position continuously. Typically in active bat system when it is necessary to know the position of a bat, the central controller addresses the bat over the radio link, and at a known time it transmits a pulse of ultrasound. When its position has been found by the DSP calculation boards, the controller passes the resulting location sighting to client middleware and applications, not to the bat. But in modified Active Bat system the central controller will inform the robot about its position and orientation through the radio link.

III. MAP REPRESENTATION

There are several methods used by mobile roboticists to represent map in robot's memory. Among those continuous valued line representation of EPFL, exact cell decomposition, fixed decomposition, adaptive decomposition, occupancy grid map, topological representation, probabilistic map are most popular [1]. Here we recommend using a different type of map representation which can make the navigation process using Active Bat system appreciably simple and efficient.

First of all we represent the whole indoor environment with three dimensional coordinate system. We can assume the environment has rectangular shape and the plane upon which the robot will move (floor) is XZ plane in the X, Y, Z coordinate.

The robot needs to know the coordinate position of its destination to reach there. Now, there may be more than one path to reach the destination point. Then which way the robot will chose? So we need path planning and algorithm to follow the path. By embedding two bats with the robot it is possible to determine the orientation of the robot. So we can determine the angle by which the robot has to move its front side and then follow a straight line to reach its destination point by using the

formulas of coordinate geometry. The robot can track its position anytime it wants to check whether the way through which it is moving is write or wrong. If there is not any obstacle and distance is short the robot can perform the task in two ways. One is to calculate possible coordinate points on the line from starting point to destination point and matching frequently the robots position when moving with those calculated points to keep precision. Other way is to calculate the distance between the starting and end point and then calculating the moved distance from the spin of the robots wheel. In this case, if the robot is distracted by wheel slippage or collision, then it has to recalculate its position and follow a new path. For legged mobile robot the first approach is better to follow. But what about long distance and if there are static obstacles on the straight line?

In this case we need to assign some predefined nodes in the map that is depicted on robot’s memory which we call here “stations”. The coordinate positions of the stations are based on the positions of the static and permanent obstacles. The robot will follow the stations to reach its destination. In that case the robot should know that which the efficient way is. That means in which way it needs least time to reach the goal. But there may be more than one path to reach a desired place. So the robot needs the information about the adjacent stations of any station and the distances from one station to its adjacent stations. It’s quite simple to calculate the distances from the formulas of coordinate geometry. But information about the adjacency of the stations should be inputted manually in robots memory. We need to do programming to do this job. It will be easier to use tree algorithm to keep information about the stations.

To observe the efficiency of these two algorithms a hypothetical environment is considered. Any one of the corners of the rectangular floor can be assumed as the origin. Here we have considered a 3600 square meter (60 meters × 60 meters) area with several obstacles. We can split up the whole environment with numerous circles having 3 cm diameter as the active bat system can provide 3cm of precision. As the robot we are considering is not a flying robot and it just moves on a flat plane, we will consider that in the 3D position information provided by the central controller, value of Y coordinate will be always same for simplicity of calculation.

In the following diagram we depict our hypothetical environment in the coordinate system.

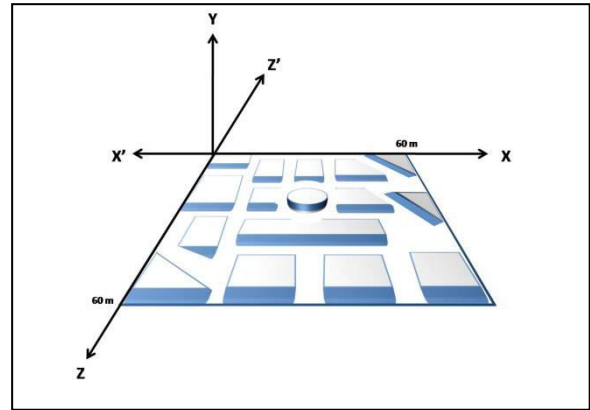


Fig. 2 : Coordinate representation of the environment with obstacles

Now we have to define the stations at required positions so that the robot can follow the stations as temporary destinations to reach at final destination. Top view of the environment is illustrated in Fig. 3. There are 15 different rooms with one or more entrances for each room. We have defined 54 stations in the environment, coordinate positions of which can be calculated by using the Bat before writing in robot’s memory. So there are numerous numbers of path through which a robot can move from one position to another (Fig. 4).

But we need to find the most efficient path. To do so, firstly we can gather information about coordinate positions of all stations as well as the adjacent stations for each case (Table I).

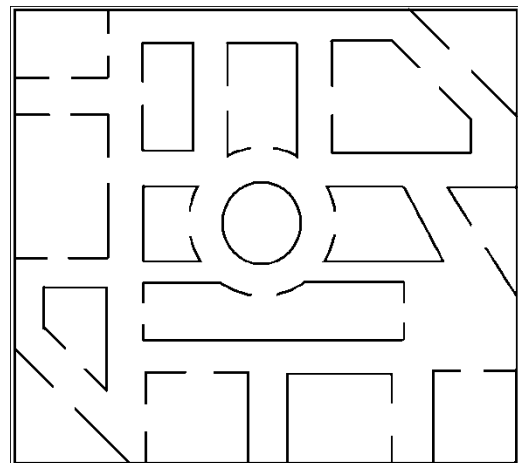


Fig. 3 : Top view of the Robot’s environment

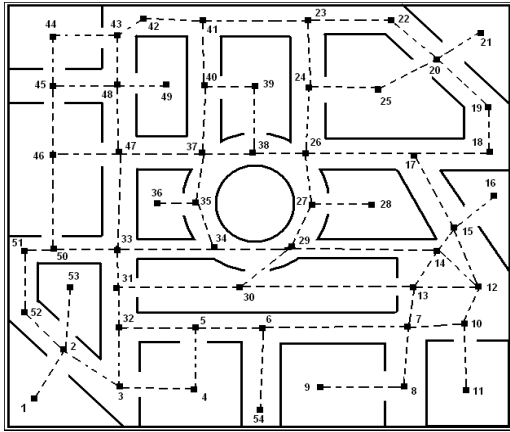


Fig. 4: Paths through which the robot can move

TABLE : 1 COORDINATE POSITIONS OF THE STATIONS AND THEIR ADJACENT STATIONS

Station	Coordinate position		Adjacent stations and distances (m)							
	X	Z	St	Ds	St	Ds	St	Ds	St	Ds
1	3.8	55.3	2	7.47						
2	7.1	48.6	3	8.22	52	6.81	53	8.85	1	7.47
3	13.7	53.5	2	8.22	4	8.71	32	8.20		
4	22.4	53.9	3	8.71	5	8.40				
5	22.6	45.5	6	7.80	32	8.90	4	8.40		
6	30.4	45.5	5	7.80	7	17.20	54	11.30		
7	47.6	45.5	6	17.20	10	6.52	8	8.02	13	5.74
8	47	53.5	9	9.70	7	8.02				
9	37.3	53.7	8	9.70						
10	54.1	45	7	6.52	11	9.10	12	5.57		
11	54.1	54.1	10	9.10						
12	55.8	39.7	10	5.57	13	7.50	14	6.86	15	8.57
13	48.3	39.8	12	7.50	14	5.55	7	5.74	30	20.60
14	50.9	34.9	15	3.91	29	17.31	13	5.55	12	6.86
15	53	31.6	17	11.41	14		12	8.57	16	6.22
16	57.4	27.2	15	6.22						
17	48.1	21.3	15	11.41	18	8.91	26	12.70		
18	57	21	17	8.91	19	6.40				
19	56.8	14.6	18	6.40	20	9.14				
20	50.8	7.7	19	9.14	21	6.27	22	7.21	25	8.35
21	56	4.2	20	6.27						
22	45.7	2.6	20	7.21	23	10.00				
23	35.7	2.7	22	10.00	24	9.20	41	12.10		
24	35.9	11.9	25	8.02	23	9.20	26	9.21		
25	43.9	12.4	20	8.35	24	8.02				

26	35.4	21.1	24	9.21	17	12.70	27	6.70	38	6.10
27	36.4	28.4	28	6.70	26	6.70	29	6.53		
28	43.1	28.3	27	6.70						
29	33.6	34.3	27	6.53	14	17.31	30	8.07	34	8.80
30	27.7	39.8	31	14.40	13	20.60	29	8.07		
31	13.3	39.6	30	14.40	33	5.00	32	5.71		
32	13.7	45.3	3	8.20	5	8.90	31	5.71		
33	13.4	34.6	34	11.40	31	5.00	50	7.41	47	13.40
34	24.8	34.4	33	11.40	35	6.86	29	8.80		
35	22.6	27.9	34	6.86	37	6.96	36	4.46		
36	18.2	28.6	35	4.46						
37	23.5	21	47	9.80	38	5.80	35	6.96	40	9.50
38	29.3	21	39	9.20	37	5.80	26	6.10		
39	29.5	11.8	40	6.01	38	9.20				
40	23.5	11.5	39	6.01	41	8.80	37	9.50		
41	23.6	2.7	42	7.10	23	12.10	40	8.80		
42	16.5	2.5	43	3.80	41	7.10				
43	13.4	4.7	42	3.80	44	7.40	48	7.00		
44	6	4.9	43	7.40	45	7.00				
45	6.1	11.9	44	7.00	48	7.30	46	9.40		
46	6	21.3	45	9.40	47	7.70	50	13.00		
47	13.7	21.2	48	9.50	46	7.70	37	9.80	33	13.40
48	13.4	11.7	49	5.80	47	9.50	43	7.00	45	7.30
49	19.2	11.7	48	5.80						
50	6	34.3	51	3.54	46	13.00	33	7.41		
51	2.5	34.8	50	3.54	52	8.60				
52	2.7	43.4	51	8.60	2	6.81				
53	8	39.8	2	8.85						
54	30.3	56.8	6	11.30						

IV. ALGORITHM

Now, for determining the most efficient path we need to develop algorithm. First of all, information of all stations and their position is needed to be put together in a single variable. Considering the environment described above we have used a 3x54 matrix to represent those information. Suppose the variable is denoted by s_t . Then

$$s_t = \begin{pmatrix} \text{Station 1} & \text{Station 2} & \text{Station 3} & \dots & \dots & \text{Station 54} \\ \text{X-pos of Station 1} & \text{X-pos of Station 2} & \text{X-pos of Station 3} & \dots & \dots & \text{X-pos of Station 54} \\ \text{Z-pos of station 1} & \text{Z-pos of station 2} & \text{Z-pos of station 3} & \dots & \dots & \text{Z-pos of station 54} \end{pmatrix}$$

$$= \begin{vmatrix} 1 & 2 & 3 & . & . & . & 54 \\ 3.8 & 7.1 & 13.7 & . & . & . & 30.3 \\ 53.3 & 48.6 & 53.5 & . & . & . & 56.8 \end{vmatrix}$$

Then another 5×54 matrix is initialized to represent all adjacent stations of each station. Here five rows are considered as no station has more than four adjacent stations.

$$a_n = \begin{vmatrix} 1 & 2 & 3 & . & . & . & 54 \\ 2 & 3 & 2 & . & . & . & 6 \\ 0 & 52 & 4 & . & . & . & 0 \\ 0 & 53 & 32 & . & . & . & 0 \\ 0 & 1 & 0 & . & . & . & 0 \end{vmatrix}$$

Step 1: Start from the robot's current position (c_p). Suppose robot's destination station is d_s . Search for the adjacent stations of current position. This data can be extracted from the variable a_n .

Step 2: Calculate the distances from current position to adjacent stations. We can define function to do this calculation like following,

Function Distance ($c_p, a_n[i]$)

Extract X-position of c_p (xc_p), Z-position of c_p (zc_p), X-position of a_n ($xa_n[i]$) and Z-position of a_n ($za_n[i]$) from s_t .

$$\text{dis}[i] = \sqrt{(\text{sqr}(xc_p - xa_n[i]) + \text{sqr}(zc_p - za_n[i]))}$$

Here, i = iterative value which can be found from matching the values of a_n with s_t .

Step 3: Set previous distance (p_d) equals to zero and initial position (i_p)= c_p . Now calculate total distance from the following equation, $t_d = p_d + \text{dis}[i]$

Step 4: Record each route information in a 3×54 matrix variable rt_k where $k=1$ to infinity. Like

$$rt_1 = \begin{vmatrix} I_p & a_n[1] & . & . & . \\ \text{dis}(i_p, c_p) & \text{dis}(c_p, a_n[1]) & . & . & . \\ 0 & T_d & . & . & . \end{vmatrix}$$

Step 5: Set $c_p = a_n$ and $p_d = t_d$. Initialize a set of traversed stations T_r . Assign the values of a_n to T_r .

Step 6: Search for adjacent stations. Repeat step 2 and get the distances.

Step 7: Calculate total distances like step 3 but this time p_d has nonzero values.

Step 8: Check for whether $a_n \in t_r$. if $a_n \in t_r$, so there are multiple paths to go to a_n from i_p . Compare t_d of those routes and terminate the route having higher distance (so that no station will be traversed more than one).

Step 9: Check whether $c_p = d_s$. If 'yes', then save the route as rt_{ds} and check whether $rt_k \geq rt_{ds}$. If 'yes', then stop executing the algorithm and set rt_{ds} as the most efficient route. If rt_k (not necessarily all routes but at least one) $< rt_{ds}$, then halt calculating rt_{ds} and go to step 5. If $c_p \neq d_s$, then also go to step 5.

V. SIMULATION

The algorithm will be clearer from simulations. Consider a fact that the robot is at station no 51. It needs to go to station no 37. At first stage, we get 2 adjacent stations of 51. Those are 50 and 52 having distances 3.50m and 8.60m sequentially. At second stage, node 50 has 2 adjacent nodes 46 and 33 having distances 13.00m and 7.41m making total distances 16.50m and 10.91m sequentially. Node 52 has one adjacent Station 2 having distance 6.81m making total distance 15.41m. In this way path calculation will be continued. We can depict this method by a tree diagram (Fig. 5).

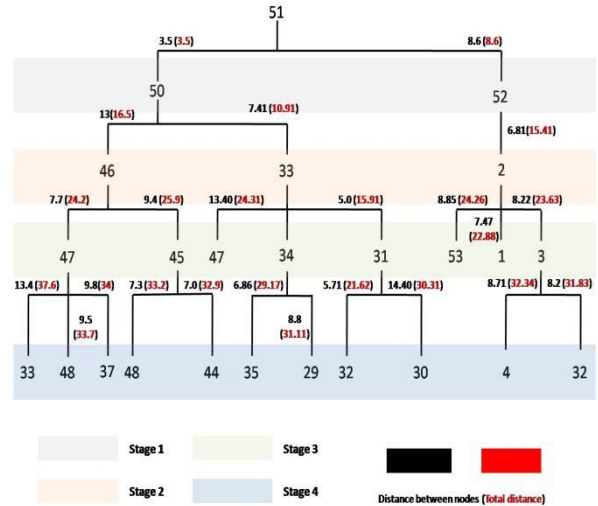


Fig. 5 : Tree diagram representation of algorithm execution

From the tree diagram (Fig. 5), it is easy to realize that the shortest route from node 51 to 35 is 51-50-33-34-35 and the distance is 29.17m. Each time the robot calculates the shortest path between two stations it will be saved in its memory so that it will not need to

recalculate for next time. We have seen that node 47 appears in two ways: from 46 and from 33. In this case as the total path from 51 to 47 has two different values. So longer path (24.31m) is omitted and traversing continues through shorter path.

We have developed program in MATLAB to simulate the whole process. From the simulation we have seen that the robot can calculate and chooses the optimal route. Below is the simulation result when the robot needs to go from station 1 to station 21.

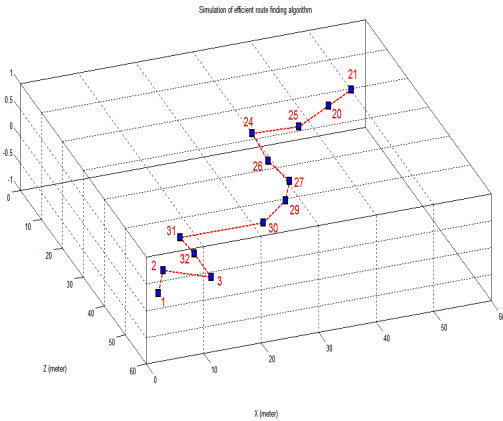


Fig. 6 : Simulation of efficient route finding algorithm

From the simulation, total calculated distance from station 1 to 21 through the shortest path is 92.15 meters. Manual calculation of the most efficient path ensures the effectiveness of our algorithm.

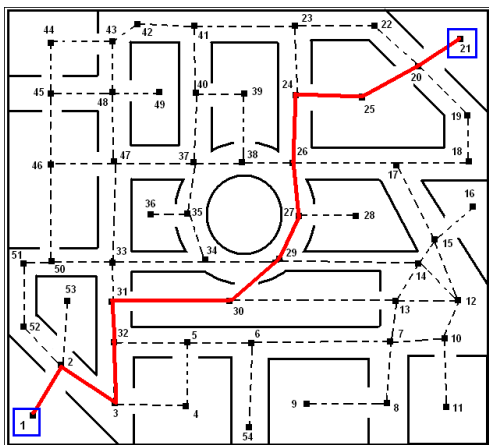


Figure 7. The robot has chosen the optimal route

But does the robot can go to a place other than the predefined stations? The answer is “yes”. We have developed another algorithm for doing this task. Suppose the robot needs to go at coordinate position

$X=45, Z=25$. Then the robot will search for any node within the square area having (45, 25) point at the middle and 5meters on each side. The robot will get two different stations 17 and 28 within this area (Fig. 8). Then it has to determine which node is less far from its current position. If it can not find any node within this area then it can search for nodes within a larger square area. Following the nearest node the robot can go straightly to its desired position even though the node is not predefined.

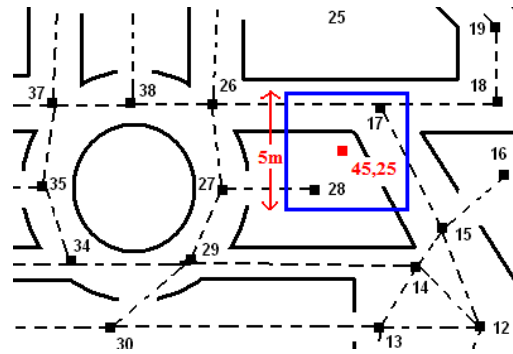


Fig. 8. : Searching predefined station near non-predefined position

Now it is time to be concerned about obstacle avoidance. The obstacles may be static or dynamic. There are several obstacle avoidance methods such as vector field histogram method [6], bubble band method [7], dynamic window approach [8] etc. But we found the bug algorithm most compatible with our path planning. In bug2 algorithm (improved bug algorithm) the robot starts to follow the obstacle’s contour, but departs immediately when it is able to move directly toward its destination [9]. So after avoiding collision the robot can again set its nearest station as temporary goal and go further. As localization is so much simple in this system, the robot can make correction of its route anytime after suffering from wheel slippage or unavoidable collision.

VI. CONCLUSION

We have done path planning and developed algorithms which allow a mobile robot to be informed about its position in the environment by Active Bat system and navigate in indoor environment in efficient way. In this method the robot is free from uncertainty about its position in the environment. It does not need to build and follow a probabilistic map. It can know its position with 3-5cm precision anytime it wants which overcome the problem of using GPS for navigation. This method deals with localization problem so simply and improves navigation efficiency significantly.

VII. FUTURE WORK

We propose to improve this method as future research. There are few problems which should be solved. In current Active Bat system there are large number of ultrasonic receivers are used [5] which can be minimized by using better technology. Moreover in our proposed method, the robot can not determine whether there is any static obstacle or not between the position of its destination (not predefined station) and the nearest station that lies within the searched square area before going there. So it needs to change its final station to another station that is near to the goal and also lies within the square area. The robot will be able to use its time more efficiently if this problem can be solved.

REFERENCES

- [1] Roland Siegwart, Illah R. Nourbakhsh, "Introduction to Autonomous Mobile Robots", ISBN 0-262-19502-X, MIT press, pp. 89 & 180-298, 2004.
- [2] H. Moravec and A.E. Elfes, "High Resolution Maps from Wide Angle Sonar", in Proceedings of the IEEE International Conference on Robotics and Automation, At.-Louis, MO, pp. 115-120, March 1985.
- [3] J.C. Latombe, "Robot Motion Planning", Norwood, MA, Kluwer Academic Publishers, 1991.
- [4] W. Burgard, D. Fox, D. Henning, "Fast Grid-Based Position Tracking for Mobile Robots", in Proceedings of the 21th German Conference on Artificial Intelligence (KI97), Freiburg, Germany, Springer-Verlag, 1997.
- [5] "The Bat Ultrasonic System", Archive of AT&T Laboratories, Cambridge. Available at: <http://www.cl.cam.ac.uk/research/dtg/attarchive/bat/>.
- [6] J. Borenstein, Y. Koren, "The Vector Field Histogram Fast Obstacle Avoidance for Mobile Robots", IEEE Journal of Robotics and Automation, pp. 275-290, 1991.
- [7] O. Khatib, S. Quinlan, "Elastic Bands: Connecting, Path Planning and Control", in Proceedings of IEEE International Conference on Robotics and Automation, Atlanta, GA, May 1993.
- [8] D. Fox, W. Burgard, S. Thrun, "The Dynamic Window Approach to Collision Avoidance", IEEE Robotics and Automation Magazine, pp. 20-35, 1997.
- [9] V. Lumelsky, T. Skewis, "Incorporating Range Sensing in the Robot Navigation Function", IEEE Transactions on Systems, Man, and Cybernetics, vol 20, no 5, pp. 1055-1070, 1990.
- [10] Dimitris E. Manolakis, "Efficient solution and performance analysis of 3D position estimation by trilateration", IEEE transactions on Aerospace and electronic systems, vol 32, no 4, October 1996.
- [11] Diego Martinez and Yong K. Cho, "Framework to Improve Mobile Robot's Navigation Using Wireless Sensor Modules", 26th International Symposium on Automation and Robotics in Construction, 2009.
- [12] Ronald W Phoebus Jr., "GPS and Trilateration: A basic understanding of a complex system and the algebra Used to determine position", 2003. Available:<http://online.redwoods.cc.ca.us/instruct/bwagner/previous/math45/>
- [13] Rainer MAUTZ, "Combination of Indoor and Outdoor Positioning", International Conference on Machine Control & Guidance, 2008.
- [14] Maybeck, P.S., "The Kalman Filter: An Introduction to Concepts", in "Autonomous Robot Vehicles", New York, Spinger Verlag, 1990.
- [15] A. Lazanas, J.C. Latombe, "Landmark-Based Robot Navigation", in Proceedings of the 10th National Conference on AI, San Jose, CA, July 1992.
- [16] Hugh Durrant-Whyte, Tim Bailey, "Simultaneous Localisation and Mapping (SLAM): PartI The Essential Algorithms", Robotics and Automation Magazine, 13 (2), pp. 99-110.



Oil Spill Reduction using Sea Swarm Technique

Swapnil Sarode¹, Gaurav Ranade² & Yashraj Sahasrabudhe³

¹Dept. of Electronics, V.E.S. Institute of Technology, Mumbai - 400 074, India

²Dept. of Electronics and Telecommunications, K. J. Somaiya College of Engineering, Mumbai - 400022, India

³Dept. of Electronics, K.C. College of Engineering, Thane - 400 603, India

Abstract - Seaswarm is intended to work as a fleet, or “swarm” of vehicles, which communicate their location through GPS and WiFi in order to create an organized system for collection that can work continuously without human support. Because they are smaller than commercial skimmers attached to large fishing vessels, they are able to navigate hard to reach places like estuaries and coast lines. Seaswarm works by detecting the edge of a spill and moving inward until it has removed the oil from a single site before joining other vehicles that are still cleaning.

I. INTRODUCTION

Recently, oil spill accidents are seen relatively frequent and becomes a severe threat to coastal and marine ecosystems and causes gross adverse impacts on coastal and marine water quality. Thus, active surveillance and rapid response to marine oil spills is important and essential to environment protection. Oil spills happen when people make mistakes or are careless and cause an oil tanker to leak oil into the ocean. There are a few more ways an oil spill can occur. Equipment breaking down may cause an oil spill. If the equipment breaks down, the tanker may get stuck on shallow land. When they start to drive the tanker again, they can put a hole in the tanker causing it to leak oil.

II. SEA SWARMING TECHNIQUE

By autonomously navigating the water’s surface, Seaswarm proposes a new system for ocean-skimming and oil removal. Seaswarm uses a photovoltaic powered conveyor belt made of a thin nanowire mesh to propel itself and collect oil. The nanomaterial, patented at MIT, can absorb up to 20 times its weight in oil. The flexible conveyor belt softly rolls over the ocean’s surface, absorbing oil while deflecting water because of its hydrophobic properties. The robots move on the water’s surface autonomously, and the cells generate enough energy to keep the bots moving for a few weeks. The conveyor belt constantly rotates and gathers pollutants, gathering the oil in the head of the robot and putting the cleaned belt back into rotation. The nanowire-covered belt is then compressed to remove the oil. As the clean part of the belt comes out of the head it immediately begins absorbing oil, making the collection process seamless and efficient. The robots work together to cover a large area of the water and communicate with one another and with land-bound researchers. Seaswarm is intended to work as a fleet, or “swarm” of vehicles,

which communicate their location through GPS and WiFi in order to create an organized system for collection that can work continuously without human support.

Prototype:

The robot is 16 feet long by 7 feet wide and can gather up to 20 times its weight in oil. The first prototype was successfully tested by MIT research group in Boston's Charles River in August, and it responded well to the water's changing surface. The prototype used a nanowire fabric capable of absorbing up to 20 times its weight in oil. This entirely hydrophobic material is resistant to water but can remove lipids like oil from the ocean. Then the fabric can be heated so the oil can be removed. Once the oil is removed, the nanowire mesh can be recycled again and again.

III. SIMPLE SWARMING ALGORITHM

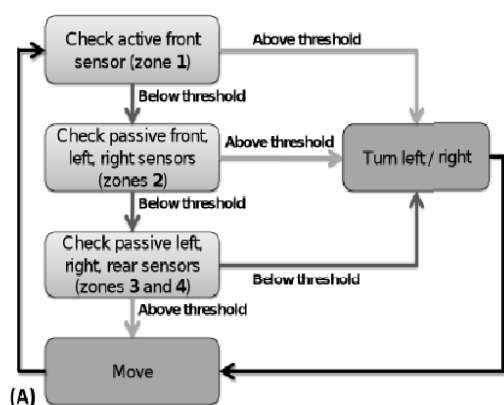
Each robot in the swarm periodically emits IR-pulses. The robots then react (move straight, turn left or turn right) depending on information from their active and passive IR-sensors. These sensors are polled periodically and the returned values are then checked against predefined thresholds (Fig. 1B) in a simple subsumption architecture (Fig. 1A).

First, the active IR-value for the front sensor is polled to find out whether there is an obstacle in front. If the value for the reflected IR-light is above a certain threshold, the robot turns away in a random direction. This is the basic collision avoidance of our robots.

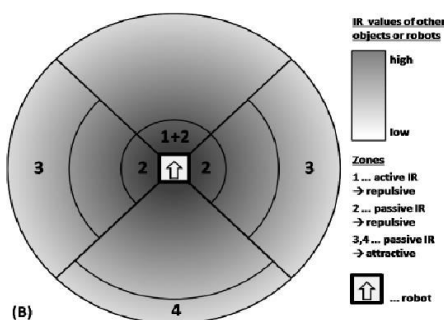
If there are no objects in its way, the robot checks the passive IR-values of all sensors. If the front, left or right sensor is above a certain threshold, the robot turns away from what is presumably another robot which is

too close. This rule is usually referred to as the separation rule in flocking algorithms.

If there is no other robot too close, the robot checks the passive IR-values of its left, right and rear sensors. For every sensor that returns a value that is above the environmental IR-light threshold but below the threshold which defines the maximally desired distance to another robot in that sector, the robot performs a basic vector addition and adds up all turns. It then decides to turn in a direction depending on whether there were more left or more right turns. Robots in the rear zone trigger a random turn reaction. This rule is usually referred to as the cohesion rule in flocking algorithms.



The third rule in flocking algorithms is usually the alignment rule which generates the common direction of movement in a flock. Since we wanted our algorithm to be as simple as possible we wanted to exclude complex communication or image recognition procedures and implemented a method which generates emergent alignment. To achieve this we adjusted the thresholds for the cohesion rule so that robots tend to follow other robots. This is done by simply shifting the threshold for the rear sensor more outwards in comparison to the threshold for the left and right sensors (zones 3 and 4 in Fig. 1B).



Depending on the position and heading of two approaching robots, one robot will be behind the other

robot. When both robots move, the robot behind will turn towards the robot in front before the robot in front reacts and turns around. This creates a leader robot and a follower robot, purely by chance. These two robots will then move around in the arena without separating. If the path of these two robots is blocked by an obstacle or another robot joins the flock, the arrangement can change instantly. If two robots approach frontally, they will avoid each other, only to turn back to each other shortly after, which can create a deadlock situation. To prevent such situations, we implemented a random-turn reaction which means that robots will randomly turn either left or right when avoiding other robots in front (zone 1 in Fig. 1B).

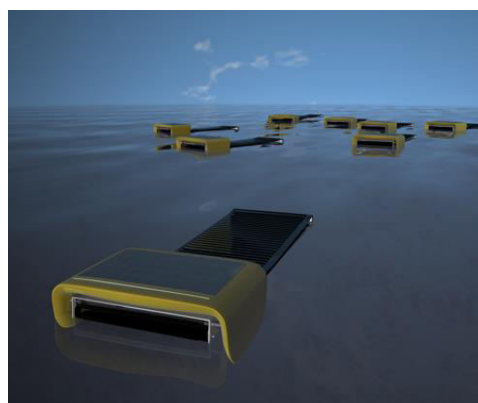
IV. ADVANTAGES

This process is more streamlined than current ocean-skimming technologies because the robots can operate autonomously and don't need to return to the shore for constant maintenance. As the vehicles work in unison they can cover large areas and by communicating with each other and researchers on land, they can coordinate their collection efforts.

V. FUTURE PROSPECTIVE

Combination with already existing Technology :

Swarm Technique can be developed to combine the already developed Satellite Remote Sensing to enhance the performance. Once the site of spill is located the Swarm can be addressed from the nearest location from the spot. Applications can be added to this technology with the help of new developments in the research field. There are numerous additions such as Rescue operation, Study of Weather conditions, Study of Marine Life, Water Salinity check and many more. In other words, if it is capable of combining all the latest developments then it will be a great combination from technology to save the environment.



The Swarm, as seen in a simulation.

CONCLUSION

The Boom technique used for oil containment takes a lot of time and needs to be attended at regular intervals. Also the efficiency of this method is lower. The Prototype experimented has proved to be more efficient than this technique.

REFERENCES

- [1] <http://senseable.mit.edu>
- [2] <https://ieeexplore.ieee.org>
- [3] Control of a robotic swarm for the elimination of marine oil pollutions. Swarm Intelligence Symposium, 2007. SIS 2007,IEEE.



Fusion of Hard and Soft Control Strategies for a Double Inverted Pendulum

Alex N. Jensen, Chandrasekhar Potluri, & D. Subbaram Naidu

Measurement and Control Engineering Research Center (MCERC), College of Engineering,
Idaho State University, Pocatello, Idaho 83209, USA
E-mail: jensalex@isu.edu, potlchan@isu.edu, naiduds@isu.edu

Abstract - A double inverted pendulum is a useful system to test a controller. The pendulum works well to test controllers because of its non-linear nature that can make it difficult to control. This paper looks into solving the problem of balancing a double inverted pendulum with process and measurement noise is addressed. This is accomplished by a fuzzy controller, information fusion, and a Kalman filter. The Kalman filter is used to find the best state estimate. The information from higher order (six) inputs is fused together to form lower order (two) inputs. Simulations using Simulink™ for the double inverted pendulum show superior faster response and considerably less overshoot.

I. INTRODUCTION

A double inverted pendulum is a useful system to test a controller. The pendulum is an ideal test platform because it is a nonlinear multivariable or multi parameter system, absolute instability, and is a non-minimum phase system. This problem is extensively used in control laboratories to show the effectiveness and accuracy of the control systems [1], [2] and [3]. The higher order non linearity's makes the pendulum difficult to control which makes it an ideal benchmark to test controllers. Many controllers over shoot and are instability because of the non-linear of the system [3]. Most of the controllers are designed on the energy principle and the robust control methods [1]. Past researches stipulate the training of neural networks and the use of fuzzy logic yields better results in the control of double inverted pendulum. In this paper we are using the fuzzy logic and the optimal control strategies to control the double inverted pendulum. This schemed control strategy is yielding better results.

A double inverted pendulum is a classic control system to test controllers on and has been extensively tested. Current research is limited on using optimal control strategies such as a Kalman filter to control they system [4], [5] and [6]. An example of more current use of inverted pendulums can be seen in walking biped robot as in [7]. For a walking robot process noise is very likely will maneuvering in uneven terrain with wind or other environmental changes.

The controller purposed in [3] will be used with added noise. Process noise and measurement noise will be added to the system to simulate noise that can occur

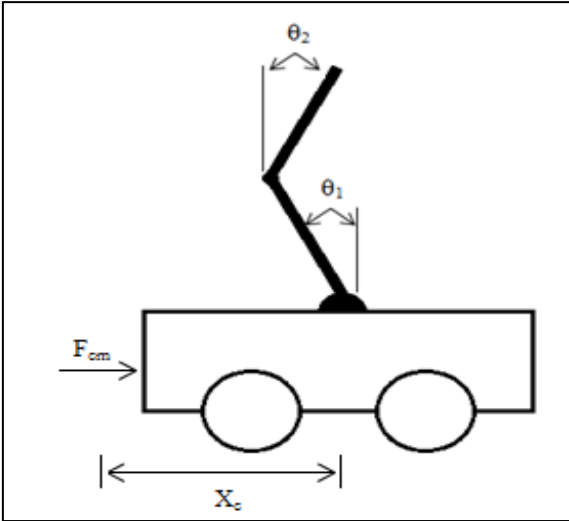
in a system. Process error could be wind or other external elements acting on the system that would occur in actual operation. Measurement error could represent instrumentation error in measurement from bad leads to the sensor or faulty wires. A Kalman filter, an optimal control method, is used to filter out the noise and create a best estimation of the state. The outputs are graphed and compared to the original system to judge the performance of the Kalman filter compared to the original system. Section II. System and Controller covers the original system with the assumptions and the setup of the basic controller. III. Proposed Controller Design goes through the modified state-space with added noise to the process and measurement along with the Kalman filter design. IV. Simulation and Results shows the controller and how the proposed design out preforms the original controller. V. Conclusion summarizes the result of the previous section explaining how the proposed system out preforms the previous method because it has reduced the overshoot dramatically along with the settling time.

II. SYSTEM AND CONTROLLER

The model of the double inverted pendulum is shown below in Figure 1. The two linkages attached to the base of the cart qualify the system to be a double inverted pendulum. X_c is the displacement of the car relative to a reference point. θ_1 is pendulum 1's or the bottom pendulum's reference angle and θ_2 is pendulum 2's or the top pendulum's reference angle.

In Equations (1) and (2) is the state-space of the inverted pendulum system [3]

$$\dot{x} = A^*x(t) + B^*u(t) \quad (1)$$



$$y = C^*x(t) + D^*u(t) \quad (2)$$

$$A = \begin{bmatrix} 0 & 0 & 0 & 1 & 0 & 0 \\ 0 & 0 & 0 & 0 & 1 & 0 \\ 0 & 0 & 0 & 0 & 0 & 1 \\ 0 & 0 & 0 & 0 & 0 & 0 \\ 0 & 70.1505 & -20.0972 & 0 & 0 & 0 \\ 0 & -35.0752 & 34.5486 & 0 & 0 & 0 \end{bmatrix} \quad (3)$$

$$B = [0 \ 0 \ 0 \ 1 \ 5..1075 \ -0.0537]^T \quad (4)$$

$$C = \begin{bmatrix} 1 & 0 & 0 & 0 & 0 & 0 \\ 0 & 1 & 0 & 0 & 0 & 0 \\ 0 & 0 & 1 & 0 & 0 & 0 \\ 0 & 0 & 0 & 1 & 0 & 0 \\ 0 & 0 & 0 & 0 & 1 & 0 \\ 0 & 0 & 0 & 0 & 0 & 1 \end{bmatrix} \quad (5)$$

$$D = [0 \ 0 \ 0 \ 0 \ 0 \ 0]^T \quad (6)$$

$$Q = \begin{bmatrix} 200 & 0 & 0 & 0 & 0 & 0 \\ 0 & 100 & 0 & 0 & 0 & 0 \\ 0 & 0 & 100 & 0 & 0 & 0 \\ 0 & 0 & 0 & 0 & 0 & 0 \\ 0 & 0 & 0 & 0 & 0 & 0 \\ 0 & 0 & 0 & 0 & 0 & 0 \end{bmatrix} \quad (7)$$

$$R = 1 \quad (8)$$

Given the plant as in Equation (1) the performance index will be written as:

$$J(t) = \frac{1}{2} s(t) + \frac{1}{2} \int_0^{\infty} (x'(t)Qx(t) + u'(t)Ru(t))dt \quad (9)$$

A step by step procedure will be followed to create the Kalman filter as done in [3]. Steps taken from [8]

Step 1: Solving the matrix differential Riccati equation:

$$\begin{aligned} \dot{P}_e(t) &= A(t)P_e(t) + P_e(t)A'(t) - \\ &P_e(t)C'(t)R_v^{-1}(t)C(t)P_e(t) + B_w(t)Q_w(t)B_w'(t) \end{aligned} \quad (10)$$

where $P_e(t=0) = P_{e0}$,

Q_w and R_v are unknown so the values were assigned as $Q_w = \text{diag}([200,100,100,0,0,0])$ and $R_v = 1$.

$\dot{P}(t)$ was computed using the differential Riccati equation by using MATLAB™:

$$P_c(t) = \begin{bmatrix} 1.198 & -0.016 & -0.019 & 0.797 & -0.034 & -0.010 \\ -0.016 & 1.252 & 0.424 & -0.075 & 9.485 & -0.891 \\ -0.019 & 0.424 & 2.196 & -0.063 & 0.197 & 11.075 \\ 0.797 & -0.075 & -0.068 & 1.193 & 0.119 & 0.108 \\ -0.034 & 9.485 & 0.197 & 0.119 & 77.923 & -23.176 \\ -0.010 & -0.891 & 11.075 & 0.108 & -23.176 & 63.831 \end{bmatrix} \quad [11]$$

Step 2: Obtain the optimal estimator (filter) gain:

$$K_e(t) = P_e(t)C'(t)R_v^{-1}(t) \quad (12)$$

$$K_e(t) = \begin{bmatrix} 1.198 & -0.008 & -0.006 & 0.199 & -0.007 & -0.002 \\ -0.016 & 0.626 & 0.141 & -0.019 & 1.897 & -0.149 \\ -0.019 & 0.212 & 0.732 & -0.016 & 0.039 & 1.846 \\ 0.797 & -0.038 & -0.021 & 0.298 & 0.024 & 0.018 \\ -0.034 & 4.742 & 0.0656 & 0.030 & 15.585 & -3.863 \\ -0.010 & -0.445 & 3.691 & 0.027 & -4.635 & 10.638 \end{bmatrix}$$

III: OPTIMAL STATE ESTIMATE \hat{x} :

$$\dot{\hat{x}}(t) = A(t)\hat{x}(t) + B(t)u(t) + K_e(t)[y(t) - C(t)\hat{x}(t)] \quad 14)$$

$$\hat{x}(t_0) = \bar{x}_0$$

Step 4: Solving the matrix differential Riccati equation:

$$\begin{aligned} \dot{P}_c(t) &= -P_c(t)A(t) - A'(t)P_c(t) - Q(t) + \\ &P_c(t)B(t)R^{-1}(t)B'(t)P_c(t) \end{aligned} \quad (15)$$

Compute $\dot{p}(t)$ the solution of the differential Riccati equation

$$P_c(t) = 1 * e^{3t} \begin{bmatrix} 0.215 & 0.046 & -0.433 & 0.115 & -0.021 & -0.084 \\ 0.046 & 0.414 & -0.815 & 0.070 & 0.005 & -0.145 \\ -0.433 & -0.815 & 2.550 & -0.381 & 0.045 & 0.469 \\ 0.115 & 0.070 & -0.381 & 0.085 & -0.014 & -0.073 \\ -0.021 & 0.005 & 0.045 & -0.014 & 0.004 & 0.009 \\ -0.084 & -0.145 & 0.469 & -0.073 & 0.009 & 0.087 \end{bmatrix} \quad (16)$$

Step 5: Obtain the optimal control $u^*(t)$ as:

$$K_c(t) = R^{-1}(t) * B'(t) * P_c(t) \quad (17)$$

We are interested in $K(t)$. Solving $K(t)$ in MATLAB™:

$$K_c(t) = R^{-1} B' P$$

$$K = [K_x, K_{\theta_1}, K_{\theta_2}, K_{\dot{x}}, K_{\dot{\theta}_1}, K_{\dot{\theta}_2}]$$

$$K_c = [14.142 \quad 104.897 \quad -175.072 \quad 15.193 \quad 3.252 \quad -30.610]$$

Step 6: Closed-loop optimal control:

$$u(t) = -K_c(t) \hat{x}(t) \quad (18)$$

To finish the steps done in [3] the fusion algorithm is created by taking the K gain in Step 5 and F which equals:

$$F(x) = \begin{bmatrix} k_1/k_3 & k_2/k_3 & 1 & 0 & 0 & 0 \\ 0 & 0 & 0 & k_4/k_6 & k_5/k_6 & 0 \end{bmatrix} \quad (19)$$

III. PROPOSED CONTROLLER DESIGN

Given the continuous-time, stochastic dynamics or process as:

$$\dot{x}(t) = A(t)x(t) + B(t)u(t) + B_w(t)w(t) \quad (20)$$

where $w(t)$ is the process noise

The observation or measurement model as:

$$y(t) = C(t)x(t) + v(t) \quad (21)$$

where $v(t)$ is the measurement noise

Where $w(t) \sim [0, Q_w(t)]$ and $v(t) \sim [0, R_v(t)]$ are uncorrelated dynamics and measurement noises.

$$Q_w(t) = 1 \text{ and } R_v(t) = \text{diag}([1, 2, 3, 4, 5, 6]);$$

With the added noise a Kalman filter will be used to find the optimal states of the system. An estimated gain was calculated from the original system with the new noise values shown in this section. With these estimated Kalman filter gains new A_f, B_f, C_f, D_f matrices were created.

$$A_f = \begin{bmatrix} -1.198 & 0.008 & 0.006 & 0.801 & 0.007 & 0.002 \\ 0.016 & -0.626 & -0.141 & 0.019 & -0.897 & 0.149 \\ 0.019 & -0.212 & -0.732 & 0.016 & -0.039 & -0.846 \\ -0.797 & 0.038 & 0.021 & -0.298 & -0.024 & -0.018 \\ 0.034 & 65.408 & -20.163 & -0.03 & -15.585 & 3.863 \\ 0.010 & -34.63 & 30.857 & -0.027 & 4.635 & -10.638 \end{bmatrix} \quad (22)$$

$$B_f = \begin{bmatrix} 1.198 & -0.008 & -0.006 & 0.199 & -0.007 & -0.002 \\ -0.016 & 0.626 & 0.141 & -0.019 & 1.897 & -0.149 \\ -0.019 & 0.212 & 0.732 & -0.016 & 0.039 & 1.846 \\ 0.797 & -0.038 & -0.021 & 0.298 & 0.024 & 0.018 \\ -0.034 & 4.742 & 0.066 & 0.03 & 15.585 & -3.863 \\ -0.010 & -0.445 & 3.691 & 0.027 & -4.635 & 10.638 \end{bmatrix} \quad (23)$$

$$C_f = \begin{bmatrix} 1 & 0 & 0 & 0 & 0 & 0 \\ 0 & 1 & 0 & 0 & 0 & 0 \\ 0 & 0 & 1 & 0 & 0 & 0 \\ 0 & 0 & 0 & 1 & 0 & 0 \\ 0 & 0 & 0 & 0 & 1 & 0 \\ 0 & 0 & 0 & 0 & 0 & 1 \\ 1 & 0 & 0 & 0 & 0 & 0 \\ 0 & 1 & 0 & 0 & 0 & 0 \\ 0 & 0 & 1 & 0 & 0 & 0 \\ 0 & 0 & 0 & 1 & 0 & 0 \\ 0 & 0 & 0 & 0 & 1 & 0 \\ 0 & 0 & 0 & 0 & 0 & 1 \end{bmatrix} \quad (24)$$

$$D_f = 0 \quad (25)$$

The performance measure to minimize the mean-squared error (MSE) of the state estimate as:

$$J(t) = \text{trace}\{P_e(t)\} \quad (26)$$

Using the Equation (9) the performance index a feedback gain will be made. The Kalman filter gain will be calculated using the LQR of A_f, B_f, Q_w and R_v .

This gain is called K_k .

$$K_k = \begin{bmatrix} 13.133 & -0.003 & -0.028 & 0.597 & 0.001 & -0.001 \\ -0.014 & 2.133 & 1.078 & 0.002 & -0.080 & -0.046 \\ 0.001 & 0.499 & 2.045 & 0.005 & -0.037 & -0.086 \\ 0.559 & -0.042 & -0.041 & 0.035 & 0.002 & 0.002 \\ 0.017 & 2.468 & 0.296 & 0.008 & -0.082 & -0.013 \\ 0.023 & 0.075 & 2.520 & 0.008 & -0.028 & -0.106 \end{bmatrix} \quad (27)$$

IV. SIMULATION AND RESULTS

With steps 1 through step 6 and the Kalman filter that estimated the best states with the added noise the controller will be constructed. The controller will have the fuzzy controller, a subsystem that does the information fusion, added noise and a Kalman filter for parameter estimation. In Figure 2 shows the controller that was created. This controller is used to balance a double inverted pendulum on a movable trolley.

The controller consists of a fuzzy controller that uses information fusion to simplify the data. The information fusion takes a six dimensional state variable and uses a fusion function to generate two variables. These two variables are error and the variation of error. The information fusion simplifies the fuzzy controller because it reduces the amount of states that need to be considered. A Kalman filter was used in Figure 2 to find the best estimation of parameters because of noise. Process noise was added to the input and measurement noise was added to the output.

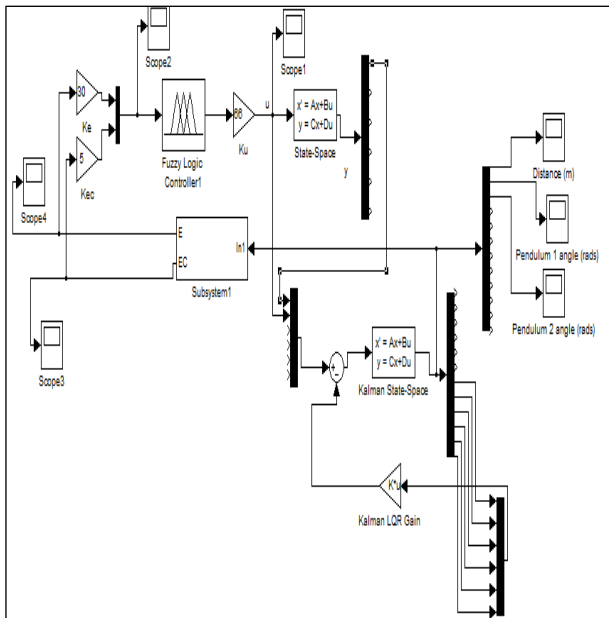


Figure 2: Inverted Pendulum Controller with Kalman Filter

The outputs of the original system before the noise was added are in Figure 3. The output of the system

with the added noise and the Kalman filter are in Figure 4. From the figures it can be seen that the trolley does not settle as quickly as the original system without noise. As for the pendulum angles 1 and 2 it can be seen that the angles are near stabilize within about 1 second. The Kalman system is not able to bring the pendulum to a perfect balance without moving the cart but is able to bring the angles of the pendulum to a steady state quicker than the original system could. Depending on the design requirements of the system the Kalman method would be desirable if overshoot and settling time within a given percentage was critical. If absolute settling is required and overshoot is not an issue then this method would not be desirable.

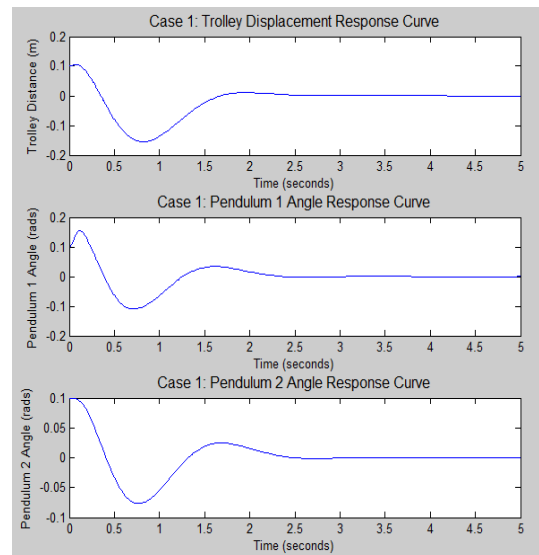


Figure 3: Simulation Results without Kalman filter

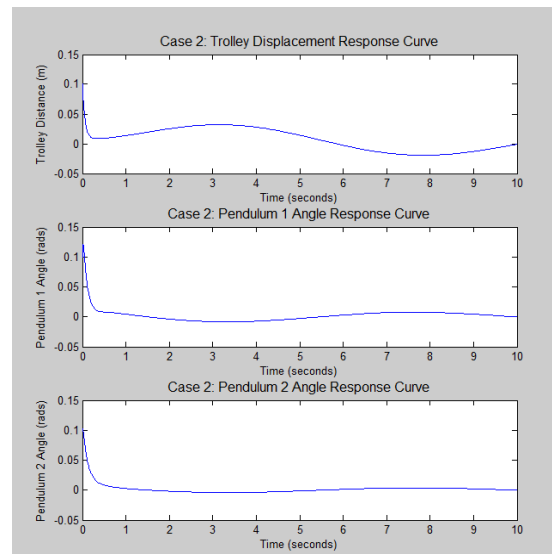


Figure 4: Simulation Results with Kalman Filter

V. CONCLUSION

The purpose of this project was to design a Kalman filter for the double inverted pendulum. Noise was introduced and so filtering was required. The parameter estimation was done by a Kalman filter. A Kalman filter was designed and implemented in Simulink™. The results showed that the system was able to balance the pendulum in reduced time but that the trolley was in motion longer to keep the pendulums balanced. This may be due to the process noise and measurement noise that was introduced to the system. The Kalman filter was able to reach a steady state after a long period of time. This may not be ideal but due to noise issues this is an option for controlling this system. In an ideal case the original controller is preferred.

VI. ACKNOWLEDGMENT

The authors gratefully acknowledge the support of the Measurement and Control Engineering Research Center (MCERC) and Idaho State University College of Science and Engineering for using their resources for this work. The support by Parmod Kumar, Dr. Steve Chiu is greatly appreciated.

REFERENCE

- [1] K. Nonaka, Y. Sugahara, K. Furuta M. Yamakita, "Robust State Transfer Control of Double Pendulum," IFAC Symposium Advances in Control Education, pp. 205-208, 1994.
- [2] J. Shao A. Bradshaw, "Swingup Control of Inverted Pendulum Systems," *Robotica*, vol. 14, pp. 397-405, 1996.
- [3] Zheng S., Wang X., Fan L. Wang L., "Fuzzy Control of a Double Inverted Pendulum Based on Information Fusion," in "International Conference on Intelligent Control and Information Processing, China, 2010.
- [4] Huguenin P., and Bonvin D. Srinivasan B., "Global Stabilization of an Inverted Pendulum - Control Strategy and Experimental Verification," *Automatica*, vol. 45, no. 1, pp. 265-269, 2009.
- [5] Eldukhri E. and Pham D., "Autonomous Swing-Up Control of a Three-Link Robot Gymnast," The Institution of Mechanical Engineers, Part I: Journal of Systems and Control Engineering, pp. 825-832, 2010.
- [6] Guohui L., "A Study on Stable Behaviors of Inverted-Pendulum under Microgravity Environments via an Improved LMI Approach," *Microgravity Science and Technology*, pp. 129-139, 2011.
- [7] Nagasaki T., Kaneko K., Yokoi K., and Tanie K. Kajita S., "A Running Controller of Humanoid Biped," in 2005 IEEE International Conference on Robotics and Automation, Barcelona, Spain, 2005, pp. 616-622.
- [8] Naidu S., *Optimal Control System*. Boca Raton, FL: CRC Press, 2003.
- [9] C. Potluri et al., "sEMG Based Fuzzy Control Strategy with ANFIS Path Planning For Prosthetic Hand," in IEEE RAS and EMBS International Conference on Biomedical Robotics and Biomechatronics, Tokyo, September 2010, pp. 413-418.



Investigation and Development of Mathematical Correlations of Cutting Parameters for Machining Titanium with CNC WEDM

Bazani Shaik & S. V. Ramana

Dept. of Mech., G.M.R. Institute of Technology, Rajam, Srikakulam, AP, India
E-mail : bazani_shaik@yahoo.co.in¹, svr.nano@gmail.com²

Abstract - Wire EDM a very thin wire serves as the electrode, the wire is slowly fed through the material and the electrical discharges actually cut the work-piece. Wire EDM is usually performed in a bath of water. To start machining it is first necessary to drill a hole in the work piece or start from the edge. In the present work is aimed at Experimental Investigation and development of mathematical correlations of Titanium material of different thicknesses is machined for determining steps. The cutting speed is noted from the machine display, surface finish is measured on cut using Talysurf. The spark gap is calculated from cutting width. The optimum values of machining current, cutting speed, spark gap, surface roughness and MRR are used for plotting the curves and best fit curve is selected using the Origin 8.0 software, minitab. The mathematical relation is generated for best fit curve and statistically analysis ANOVA is performed to find fitness of the curve. The maximum error obtained from calculated values and experimental values are found to be less than 2%. From these we, conclude that Regression Statistical analysis ANOVA gives better prediction values with less error%.

Key Words: WEDM, Cutting speed, MRR, Spark gap, surface roughness, Mathematical correlations, Regression Analysis.

I. INTRODUCTION

The object of the Present research has been designed as follows:

1. To carry out mathematical modeling for analyzing the WEDM process Characteristics based on the following features:
 - a. Types of pulse generation modules and their effects on the machining efficiency;
 - b. Module of evaluation and control of the metal removal rate characteristics of Wire.
2. To analyze the effect of thickness of Titanium, on the process variables like the optimum values of machining parameters to study the effect of parameters on current, cutting speed, spark gap and Material removal rate will be investigated and best suited values for stable and controlled machining with least wire breakage. The titanium of thickness 5 to 90mm are prepared. The experiments are conducted on the work piece of every thickness by cutting L shape and U shape by varying the machining current from a lower value to a value where the machining is in consistent in 5 maximum achievable discharge current and also on the various machining criteria, like, cutting speed, spark gap, material removal rate and surface finish using the brass (66%Cu & 34% Zn) wire electrode of diameter

0.25mm and to develop mathematical relations for computing the above mentioned cutting parameters.

II. EXPERIMENT

Wire Electrical Discharge Machining (Wire EDM), is a machining process in which a wire carrying electrical charge is used to cut the hard materials. The two major components required for the wire EDM machine the wire electrode and the degree of precision and the amount of material that can be removed. In order to cut complicated or intricate designs with greater precision and 3D profiles, Wire EDM machines requires not only the traditional X and Y axis but also the U and V axis for a standard 4-axis tooling but can also have a 5th axis.

A traveling wire which is continuously fed from wire feed spool and rewound on a take up spool moves through the work piece and is supported under tension between a pair of wire guides which are located at the opposite sides of the work piece. The lower wire guide is stationary where as the upper wire guide which is supported by the U-V table can be displaced transversely, along U and V axes with respect to the lower wire guide. The upper wire guide can also be positioned vertically along the axis by moving, the vertical arm by means of a motor set on the 3- axis.

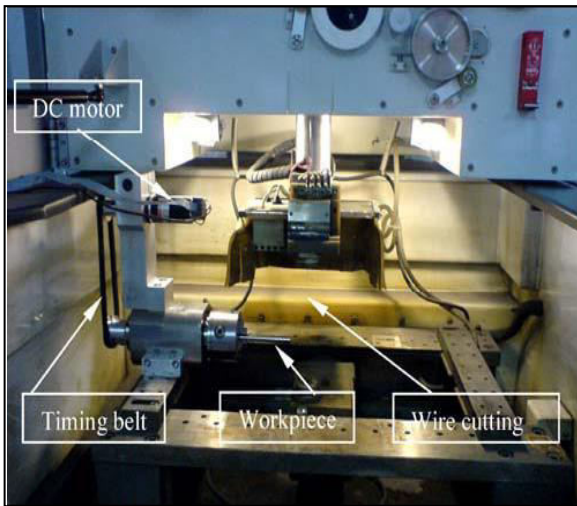


Fig. 1: Wire-cut EDM machine table

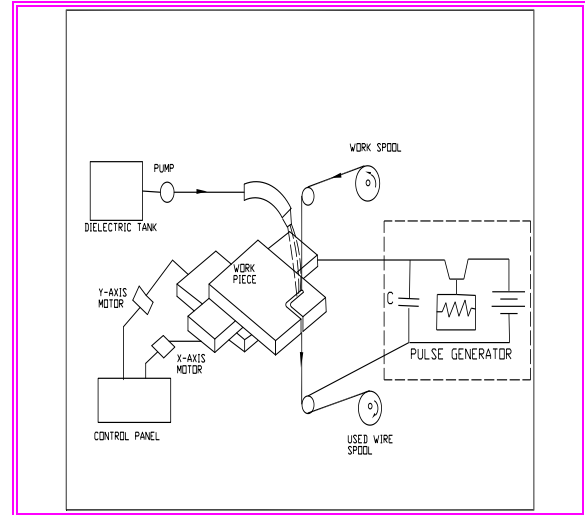
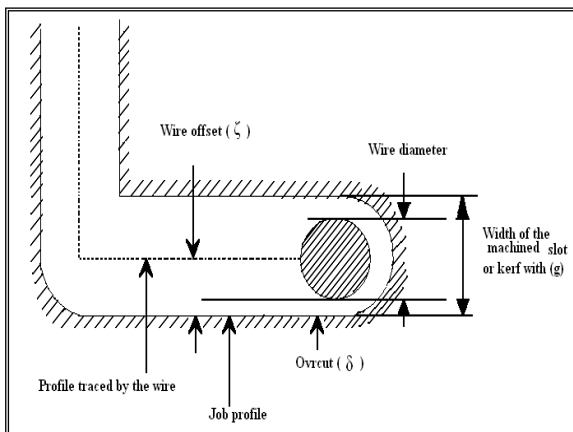


Fig. 3: Schematic view of experimental setup

III. MACHINE SETTINGS

Machine Model	:	ULTRACUT S1
Dielectric	:	De- ionized water
Dielectric conductivity	:	45ohms
Wire diameter	:	0.25 mm
Wire material	:	Brass
Pulse on	:	sparkling during machining Time Pulse on
Pulse off	:	Sparkling during machining Time Pulse off
IP	:	Current in amps
VP	:	Voltage in volts
WP	:	Water pressure kg/mm2
WF	:	Wire feed m/min
WT	:	Wire tension in Newtown's
SV	:	Servo voltage



SF : Servo feed

Fig. 2 : L- Slot generated by WEDM

Results And Discussions

The experiments are conducted on the work piece of every thickness by cutting L shape and U shape by varying the machining current from a lower value to a value where the machining is in consistent in 5 steps. At every machining current, I value the machining criteria is measured. The machining current, I value at which the machining is consistent with continuous cutting, better finish with least wire rupture is selected as optimal. The cutting speed is noted from the machine display, surface finish is measured on cut using Talysurf. The spark gap is calculated from cutting width. The Cutting width $C_w = d + 2 \times S_g$, where d is the wire diameter and S_g is the Spark gap. The MRR is calculated as, $MRR = T \times C_w \times C_s$ where C_s is the cutting speed, mm/min and T is work piece thickness, mm. The optimum values of machining current, cutting speed, spark gap surface roughness and MRR for every thickness are used for plotting the curves and best fit curve is selected using the software. The mathematical relation is generated for this best fit curve and statistical analysis is performed to find the fitness of the curve. Regression analysis done for Effect of current on cutting speed, spark gap surface roughness, MRR and Effect of thickness on current, cutting speed, spark gap, MRR. As the current increases 1.5amp to 2.20amp and cutting speed increases maximum to 4.12amp regression analysis done for experimental data R-Sq-99.8%.error is 0.2%.The Regression values always equal to 1 then the curve becomes best fit curve. As the current increases 1.5amp to 2.20amp and spark gap increases 42.00µm to 60µm.from Regression analysis R-Sq-98.8% error is 1.2%.As the current increases surface roughness increases to 0.50µm to 0.75µm from regression analysis R-Sq-97.6% error is 2.4%.As the current increases MRR increase to 6.864 mm³/min to 94.29 mm³/min for

experimental data regression analysis is R-sq-99.0% error is 1%.The influence of discharge current on job thickness, on the machining criteria such as cutting speed, spark gap, material removal rate Regression analysis done for experimental data.

Using CNC part programming, rectangular slot of 4mm x 6mm and L shaped slot is cut on 5mm thick Titanium work piece by varying discharge current for 5 times. The Fig 2 L- slots are tested for spark gap using shadow graph technique and micro scope. The photograph of experimental setup is shown in Fig. 3. The rectangular slots are tested for surface roughness values using Tally surf. From this, the best value of discharge current is recorded for stable machining with maximum cutting speed and minimum wire breakage. At this value of current, the best value of cutting speed, spark gap is recorded and material removal rate (MRR) is computed. The experiment is repeated for 21 different work piece thicknesses varying from 5mm to 90mm. The best value of discharge current obtained for each thickness and the corresponding cutting speed, spark gap and material removal rate (MRR) are represented in graphical form.

The experimental data thus obtained is subjected to statistical analysis (ANOVA) using the soft ware Origin 8.0. The best fit curve to suit the data is also obtained in the form

$$y = A_2 + \frac{A_1 - A_2}{[1 + \exp(x - x_0) / dx]}$$

and the mathematical correlations for this best fit curve are taken in to consideration.

IV. RESULTS AND DISCUSSIONS

The variation in the discharge current with the increase in work piece thickness is obtained and is shown in Fig. 4.

For a specified set of machining conditions it is observed that with increase in thickness, the required current also increases. This is attributed to the high amount of energy required for high thickness job in which machining is possible only by increasing the current.

$$I = 3.098 - \frac{34.628}{[1 + \exp(T + 456.92) / 152.57]} \tag{1}$$

where I = discharge current, amp

T = thickness, mm

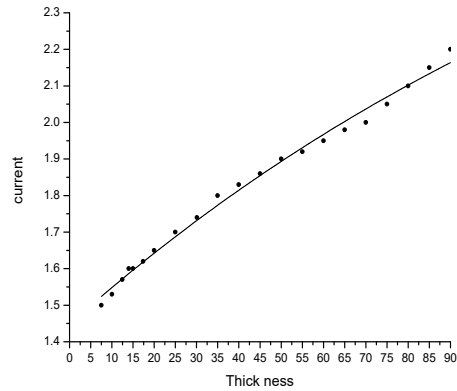


Fig. 4 : Effect of discharge current on thickness

Table 1. Statistical data for Fig. 4

Number of points	21	A1	-31.53
Degrees of freedom	17	A2	3.098
Reduced Ch-sqr	3.92E4	xo	-456.92
Residual sum of Squares	0.0067	dx	152.57
R Value	0.9963		
R-square(COD)	0.9927		
Adj.R-square	0.9914		
Root-MS(SD)	0.0198		

Figure 5 shows the effect of thickness on cutting speed for various sizes of the work pieces. The plot indicates that as thickness of the work piece increases the cutting speed decreases rapidly. For thickness beyond 70mm the cutting speed almost remains constant. If the thickness increases, the volume of metal to be removed increases which demands more energy and it may become a machine constraint. At the same time the spark is jumping to the sides of the wire causing more width of cut, reducing the cutting speed. The data thus obtained is subjected to interpolation and the best fit curve correlation is obtained in the form

$$C_s = 545.58 + \frac{550.714}{[1 + \exp(T + 593.1) / 93.95]} \tag{2}$$

where C_s = cutting speed, mm/min.

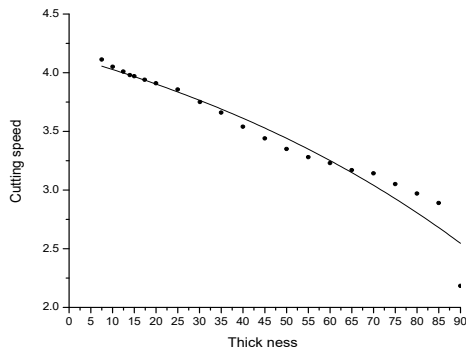


Fig. 5 : Effect of cutting speed on thickness

Table 2 gives the statistical analysis, showing R² value as 0.947 which envisages the fitness of the curve. The standard deviation for this plot is 0.123. From this plot or from the above mathematical correlation, the cutting speed can be predicted for any size of work piece to be machined.

Table 2. Statistical data for Fig. 5

Number of points	21	A1	5.134
Degrees of freedom	17	A2	-545.58
Reduced Ch-sqr	0.015	xo	593.15
Residual sum of squares	0.26	dx	93.95
R Value	0.973		
R-square(COD)	0.947		
Adj.R-square	0.937		
Root-MS(SD)	0.123		

The variation of spark gap with the increase in thickness of work piece is depicted in the Fig. 6. The curve shows an increasing trend in spark gap with increase in thickness of work piece. This may be due to property of spark, which jumps longer at higher current values an essential requirement at higher thickness.

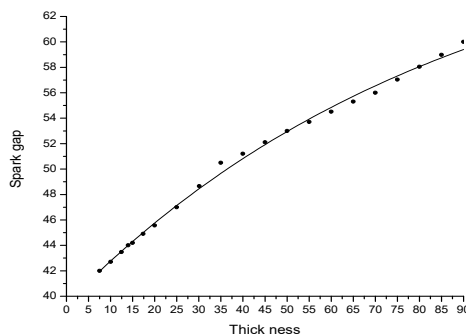


Fig. 6 : Effect of spark gap on thickness

The best suitable curve is drawn and error analysis is carried out using the same Origin 8.0 soft ware. The mathematical correlation obtained is

$$Sg = 70.34 - \frac{1733.54}{[1 + \exp (T + 343.18) / 85.62]} \quad (3)$$

where Sg is the spark gap in micro meters.

Table 3. Statistical data for Fig. 6

Number of points	21	A1	-1663.2
Degrees of freedom	17	A2	70.34
Reduced Ch-sqr	0.126	xo	-343.18
Residual sum of Squares	2.151	dx	85.62
R Value	0.998		
R-square(COD)	0.9968		
Adj.R-square	0.9963		
Root-MS(SD)	0.3557		

The statistical analysis presented in Table 3 shows the values of R² = 0.9968 and standard deviation as 0.3557 are obtained and are tabulated in Table.3. The correlation is useful in finding the spark gap in turn cutting width, to compute the MRR and program the wire off set during CNC part programming, and hence higher accuracy can be achieved.

The change in MRR with increase in thickness is shown in the Fig. 7. The plot shows a constant rise with a positive slope. This may due to the increase in cutting speed and spark gap.

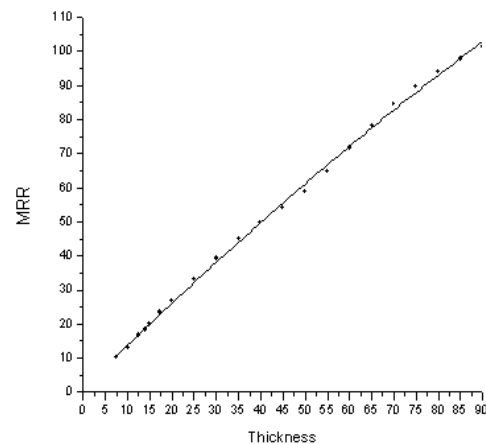


Fig. 7 : Effect of MRR on thickness

The best fit curve is taken along with mathematical correlation is

$$MRR = 109 - \frac{19.38}{[1 + \exp(I + 29.52) / 54.74]} \quad (4)$$

where MRR is material removal rate, mm³/min.

The statistical data obtained in the error analysis (ANOVA) gives $R^2 = 0.9999$ which indicates the fitness of the curve and correlation. The standard deviation obtained is 0.00967. The results of the analysis are presented in Table 4. The above correlation is be useful in determining the maximum achievable MRR and can also be used for cutting time and cost calculations.

Table 4. Statistical data for Fig. 7

Number of points	21	A1	-8.48
Degrees of freedom	17	A2	10.90
Reduced Ch-sqr	10.126	xo	-29.52
Residual sum of squares	0.00151	dx	54.74
R Value	0.9999		
R-square(COD)	0.9999		
Adj.R-square	0.9999		
Root-MS(SD)	0.00967		

V. CONCLUSIONS

The influence of parameters, like discharge current, job thickness, on the machining criteria such as cutting speed, spark gap, surface finish, material removal rate are determined. Titanium material of different thicknesses is machined for determining the optimum values of machining parameters to study the effect of parameters on current, cutting speed, spark gap and Material removal rate will be investigated and best suited values for stable and controlled machining with least wire breakage. Variations and effect of cutting speed, Spark gap, surface roughness, MRR with respect to machining current. Regression Analysis are used for predicting current, cutting speed, spark gap, Surface roughness, MRR. The developed prediction system is found to be capable of accurate process parameters prediction.

The maximum error obtained from calculated values and experimental values are found to be less than 2%. From these we, conclude that Regression Statistical analysis ANOVA gives better prediction values with less error%. The Regression Analysis has predicted the machining values with less error percentage.

REFERENCES

- [1] Liao Y.S., Yub Y.P. --“Study of specific discharge energy in WEDM and its application” International Journal of Machine Tools & Manufacture 44 (2004) pp 1373–1380.
- [2] Fuzhu Han, Jun Jiang, Dingwen Yu - “Influence of discharge current on machined surfaces by thermo-analysis in finish cut of WEDM” International Journal of Machine Tools & Manufacture 47 (2007) pp 1187–1196.
- [3] Puri A.B. Bhattacharyya B. --“An analysis and optimization of the geometrical inaccuracy due to wire lag phenomenon in WEDM” International Journal of Machine Tools & Manufacture 43 (2003) pp 151–159.
- [4] Mu-Tian Yan , Pin-Hsum Huang -- “Accuracy improvement of wire-EDM by real-time wire tension control” International Journal of Machine Tools & Manufacture 44 (2004) pp 807–814.
- [5] K. Kanlayasiri , S. Boonmugb --“Effects of wire-EDM machining variables on surface roughness of newly developed DC 53 die steel: Design of experiments and regression model”-Journal of Materials Processing Technology 192–193 (2007) pp 459–464.
- [6] Shajan Kuriakose, Shunmugam M.S.-- “Characteristics of wire-electro discharge machined Ti6Al4V surface” Journal of Materials Letters 58 (2004) pp 2231-2237.
- [7] Ch.V.S.PameswaraRao, Dr.M.M.M. Sarcar -- “Evaluation of Optimal Parameters for machining Brass with Wire cut EDM” -Journal of Scientific and Industrial Research ISSN 0022-4456 Volume 68, Number 1, Jan-2009 pp 32-35.



Robust Adaptive Control For Two Robot Manipulators Handling An Object

E. Balasubramanian, S. Riyaz Ahammed & S. Abilash

Dept. of Mechanical Engineering, Vel Tech Dr. RR & Dr. SR, Technical University, Avadi, Chennai, India
E-mail : esak.bala@gmail.com, riyaz.veltech@gmail.com & abilash_selvaraj@yahoo.com

Abstract - The kinematics and dynamic relations of manipulators as well as the object are studied. The combined dynamics of the system is obtained with the help of coalescing the dynamics of manipulators and the object. In order to avoid the complex calculations of regressor, a robust adaptive control law is developed. The advantages of the proposed controller are: the control law is described with the help of simple scalar functions and it involves only four parameters to be estimated which is independent of number of robots. This control approach is also valid when more number of links are considered for each of the robot. Simulation and stability analysis are presented to validate the proposed control.

Key words - Collaborative manipulators; robust adaptive control; regressor;

I. INTRODUCTION

Moving long and heavy objects in a desired path and also precise positioning and orienting the objects need a collaborative action between two robot arms. Owing to the serial structure of the robot manipulators they are called “handicapped operators” because they are unable to perform intricate assembly tasks. Collaborative manipulators have many advantages compared to single arm manipulators such as increased load carrying capacity, greater dexterity and manipulability, reduced need for extra auxiliary equipments, efficient use of available workspace and increased productivity by operating each robot in parallel to achieve different tasks at the same time. Earlier many control methods such as master/slave approach [1] and hybrid control [2] methods have been developed for the control of collaborative action and of the object. They have failed due to inappropriate handling of parametric and non parametric uncertainties. In this circumstance adaptive and robust control algorithm came into picture.

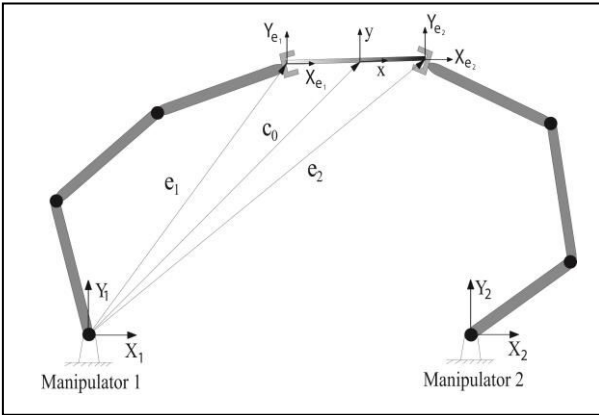
Many studies have been focused on the development and implementation of adaptive and robust control algorithms [3], [4], [5], [6] and [7] for two manipulators handling an object. All of these studies need the use of the regressor matrix to simplify the control algorithm and help in achieving the stability proof for the linearized robot dynamics [8]. However, it should be noted that the regressor based approach has difficulties in implementing in practical problems as it involves more computations. Furthermore, the

recompilation of the regressor at the servo control rates increases the computational effort in practical applications [9]. An off-line computational scheme of regressor is thus proposed to calculate the regressor [10] to reduce the on-line computational complexity which uses the position, velocity and acceleration information of the desired trajectory. However, the computation of regressor could not be avoided when there is a change in the robot structures or desired trajectory. Considering the aforementioned difficulties, for a single manipulator case various control strategies have been developed (see, for example, [11] and also [9] and [10]) which avoids the regressor. It is worth mentioning that until now the adaptive and robust control approaches are still dominant to deal with various uncertainties in the modeling. Some of the relevant literature includes [12], [13], [14] and recently [15]. However, for adaptive approach, it is evident from [16] that, in general nine parameters are required to be estimated for a planar robot manipulator with three links. These parameters gets increased if the number of robots increases and also inclusion of additional links in each robot. In order to avoid this difficulty, Leung and Su [11] developed adaptive algorithm for a single robot with two links. This approach involves computation of simple scalar functions and it involves only four parameters to be estimated which is independent of number of robots. This control approach is also valid when more number of links are considered for each of the robot. Hence, the algorithm developed for the single manipulator is extended to the two manipulator-object system. However, it is to be noted that the typical parameter adaptive algorithm requires at least [16] ten parameters

to be estimated for each robot. This paper presents a study on the collaborative action of two planar manipulators each with three rigid links used to move an object in the desired pose (position and orientation). The remaining content of the paper is organized as follows. In section 2, kinematics and dynamics of manipulators and object are reviewed. A robust adaptive control algorithm is suggested and corresponding stability analysis is presented in section 3. To show the effectiveness of the controller simulations are carried out and the results are discussed in section 4. Section 5 concludes the present study.

II. KINEMATICS AND DYNAMICS OF MANIPULATORS AND OBJECT

The present study considers two planar manipulators moving the rigid object is considered. In order to develop the complete system of dynamic equations, in the following sections, kinematic and dynamic relations of the manipulators and object will be derived and subsequently combined dynamics will be developed. The kinematic relations of each manipulator can be written with respect to transformation matrices of each links. Fig. 1 shows two planar manipulators with corresponding end-effectors grasping an object. The coordinate frame X_1Y_1 and X_2Y_2 shown in Fig. 1 are fixed frames and xy -frame is a moving coordinate frame which is attached to the beam. $X_{e1}Y_{e1}$ and $X_{e2}Y_{e2}$ are the end-effector frames attached at each end of the end-effectors. The end-effector position ns and orientations $e_1 = \{x_1, y_1, \theta\}^T$ and $e_2 = \{x_2, y_2, \theta\}^T$, are represented with respect to a reference frame X_1Y_1 , respectively.



A. Differential kinematics of manipulators

The general differential kinematic relation of manipulators [17] relates the end-effector velocity and joint velocity through Jacobian.

$$\{\dot{q}\} = \{J^{-1}\} \{\dot{e}\} \quad (1)$$

Differentiating (1) gives

$$\{\ddot{q}\} = \{J^{-1}\} \{\ddot{e}\} + \{\dot{J}^{-1}\} \{\dot{e}\} \quad (2)$$

The eqs. (1) and (2) will be used later for the development of combined dynamics of the system.

B. Manipulators dynamics

The general manipulator dynamics is given by [17],

$$M_i(q_i)\ddot{q}_i + C_i(q_i, \dot{q}_i) \dot{q}_i + G_i(q_i) = \tau_i + J_i^T f_i \quad (3)$$

Since we have two manipulators and the assembled form can be given as,

$$M_r \ddot{q} + C_r \dot{q} + G_r = \tau + J^T f \quad (4)$$

where

$$M_r = \begin{bmatrix} M_1 & 0 \\ 0 & M_2 \end{bmatrix}; C_r = \begin{bmatrix} C_1 & 0 \\ 0 & C_2 \end{bmatrix}; J = \begin{bmatrix} J_1 & 0 \\ 0 & J_2 \end{bmatrix}$$

$$G_r = \begin{bmatrix} G_1 \\ G_2 \end{bmatrix}; \tau = \begin{bmatrix} \tau_1 \\ \tau_2 \end{bmatrix}; f = \begin{bmatrix} f_1 \\ f_2 \end{bmatrix}; q = \begin{bmatrix} q_1 \\ q_2 \end{bmatrix};$$

$M_i(q_i)$ ($i = 1, 2$) represents symmetric positive definite inertia matrix, $C_i(q_i, \dot{q}_i) \dot{q}_i$ is the vector due to coriolis and centrifugal components, $G_i(q_i)$ represents the vector of gravitational components, τ_i is the vector of input torque applied at each joint of the manipulator, f_i is the interaction forces/moment between the manipulator and object, J_i is Jacobian matrix of manipulator and q_i is the vector of joint angles.

C. Kinematics of the object

Consider a beam of length L and mass m which is rigidly grasped by the two manipulators. The mass center position and orientation (pose) with respect to reference frame X_1Y_1 is represented as $c_0 = \{x_0, y_0, \theta\}^T$. All kinematic relations are written with respect to X_1Y_1 frame.

The left end pose (Position and Orientation) of the beam is given by,

$$\{e_1\} = \{c_0\} - \left\{ \frac{L}{2} \cos \theta \quad \frac{L}{2} \sin \theta \quad 0 \right\}^T \quad (5)$$

The right end pose of the beam is given by,

$$\{e_2\} = \{c_0\} + \left\{ \frac{L}{2} \cos \theta \quad \frac{L}{2} \sin \theta \quad 0 \right\}^T \quad (6)$$

$$\{\dot{e}\} = \begin{pmatrix} 1 & 0 & \frac{L}{2} \sin \theta \\ 0 & 1 & -\frac{L}{2} \cos \theta \\ 1 & 0 & -\frac{L}{2} \sin \theta \\ 0 & 1 & \frac{L}{2} \cos \theta \\ 0 & 0 & 1 \end{pmatrix} \begin{Bmatrix} \dot{x}_0 \\ \dot{y}_0 \\ \dot{\theta} \end{Bmatrix}$$

$$\{\dot{e}\} = [R] \{\dot{x}_{rd}\} \quad (7)$$

Where

$$C_{rd} = \{0 \ 0 \ 0\}^T; G_{rd} = \begin{Bmatrix} 0 \\ mg \\ 0 \end{Bmatrix}$$

$$M_{rd} = \begin{bmatrix} m & 0 & 0 \\ 0 & m & 0 \\ 0 & 0 & \frac{mL^2}{12} \end{bmatrix}; \ddot{X}_{rd} = \begin{Bmatrix} \ddot{x}_0 \\ \ddot{y}_0 \\ \ddot{\theta} \end{Bmatrix}$$

$$F_{rd} = \begin{bmatrix} 1 & 0 & 0 & 1 & 0 & 0 \\ 0 & 1 & 0 & 0 & 1 & 0 \\ \frac{L}{2}\sin\theta & -\frac{L}{2}\cos\theta & 1 & -\frac{L}{2}\sin\theta & \frac{L}{2}\cos\theta & 1 \end{bmatrix}$$

Differentiating (7) gives,

$$\{\ddot{\theta}\} = [\dot{R}]\{\dot{x}_{rd}\} + [R]\{\ddot{x}_{rd}\}$$

The eqs. (7) and (8) will be used for the development of combined dynamics of the system.

D. Object dynamics

The Euler – dynamic model of the rigid object is represented by,

$$M_{rd} \ddot{X}_{rd} + C_{rd} \dot{X}_{rd} + G_{rd} = F_{rd} (-f) \quad (9)$$

E. Combined dynamics

The manipulators dynamics (4) is represented in joint space and the object dynamics (9) is given in Cartesian space. Hence, initially the object dynamics will be converted into joint space with the help of kinematic relations of manipulators as well as the object. Finally the object dynamics will be combined together with manipulators dynamics formulates the combined dynamics of the system.

Using (1), (7) can be written as,

$$\dot{X}_{rf} = R^\dagger J \dot{q} \quad (10)$$

Differentiating (10) gives,

$$\ddot{X}_{rf} = \dot{R}^\dagger J \dot{q} + R_1^\dagger (\dot{J} \dot{q} + J \ddot{q}) \quad (11)$$

Substituting (11) into (9) for the joint space model of the object,

$$M_{rd} \dot{R}^\dagger J \ddot{q} + M_{rd} (\dot{R}^\dagger J + R_1^\dagger \dot{J}) \dot{q} + G_{rd} = F_{rd} (-f) \quad (12)$$

Then (4) and (12) can be combined together formulates the joint space dynamics model of the system dynamics given by,

$$M_{js} \ddot{q} + C_{js} \dot{q} + G_{js} = \tau_{js} \quad (13)$$

where,

$$M_{js} = (M_r + J^T F_{rf}^\dagger M_{rf} R^\dagger J)$$

$$C_{js} = C_r + J^T F_{rf}^\dagger M_{rf} (\dot{R}^\dagger J + R^\dagger \dot{J})$$

$$G_{js} = G_r + J^T F_{rf}^\dagger G_{rf}$$

F_{rf}^\dagger and R^\dagger are the pseudo inverse matrices. The system of dynamics developed in joint space (13) has following properties [11] which will be useful for stability analysis.

Property 1: M_{js} is symmetric positive definite matrix.

Property 2: The matrix M_{js} and C_{js} in (13) satisfies the following,

$$X^T (M_{js} - 2C_{js}) X = 0 \quad \forall X \neq 0 \quad (14)$$

Where X is the any arbitrary vector. That is $M_{js} - 2C_{js}$ is skew symmetric matrix.

Property 3: Since the matrices M_{js} , C_{js} and G_{js} in (13) are the functions of sine and cosine of manipulator joint angles and velocities, they are bounded. Then, there exist arbitrary positive constants ρ_{ii} ($i=1,2,3$), the boundedness of each matrices can be described as follows:

$$\|M_{js}\| \leq \rho_{11}$$

$$\|C_{js}\| \leq \rho_{22} \dot{q}$$

$$\|G_{js}\| \leq \rho_{33}$$

III. DEVELOPMENT OF CONTROLLER

The development of control law involves satisfying the following objectives.

- The object should move from the initial pose to the desired final pose.
- Two manipulators will be also moved to the desired joint angle from the given joint angle.

A. Robust adaptive control

The proposed robust adaptive controller is in the following form [11],

$$\tau_{js} = -K_{dd} M_{js} S_{\theta 1} - \left(\begin{matrix} \tilde{\rho}_{11} \|\dot{q}_r\| + \\ \tilde{\rho}_{22} \|\dot{q}\| \|\dot{q}_r\| + \\ \tilde{\rho}_{33} + \tilde{\rho}_{44} \|\dot{q}\| \end{matrix} \right) \text{sat} \left(\frac{S_{js}}{\emptyset} \right)$$

where K_{dd} is the positive definite matrix and ρ_{ii} , $i=1,2,3,4$, are the adaptive control gains. The sliding surface can be chosen as,

$$S_{js} = \dot{q} - \dot{q}_r \quad (16)$$

$S_{\theta 1}$ is the measure of algebraic distance of the current state to the boundary layer which is given by,

$$S_{\theta 1} = S_{js} - \emptyset \text{sat}(S_{js}/\emptyset) \quad (17)$$

Where \emptyset is the boundary layer thickness. Also, S_{js} is defined as follows,

$$\begin{aligned} \text{sat}(S_{js}/\emptyset) &= \text{sgn}(S_{js}) \quad \text{if } |S_{js}| > \emptyset \\ &= S_{js}/\emptyset \quad \text{if } |S_{js}| \leq \emptyset \end{aligned} \quad (18)$$

Where $\beta_{ii} > 0$, $i=1,2,3,4$ are the arbitrary constants which determines rates of adaptation. The control law (15) has two terms. The first term is representing proportional and derivative control. The adaptive control gains ρ_{ii} , $i=1,2,3,4$ are represented in the second term which are used to recover and cancel the unknown nonlinear dynamics. It should be emphasized here that the control laws (15) and the adaptive parameters given in (19) involve multiplication of simple scalar functions and the detailed description of model is not necessary.

The adaptive parameters are given by,

$$\begin{aligned} \dot{\hat{\rho}}_{11} &= \beta_{11} \|S_{\theta 1}\| \|\ddot{q}_r\|; \quad \dot{\hat{\rho}}_{22} = \beta_{22} \|S_{\theta 1}\| \|\dot{q}\| \|\ddot{q}_r\| \\ \dot{\hat{\rho}}_{33} &= \beta_{33} \|S_{\theta 1}\|; \quad \dot{\hat{\rho}}_{44} = \beta_{44} \|S_{\theta 1}\| \|\dot{q}\| \end{aligned} \quad (19)$$

Therefore, the suggested controller will avoid the complex calculations of regressor, computationally fast, structurally simple and easy to implement in real time applications.

B. Stability analysis

In order to prove the proposed controller, Lyapunov based stability analysis has been carried out. Differentiating the sliding surface (16) with respect to time gives,

$$\dot{S}_{js} = \ddot{q} - \ddot{q}_r \quad (20)$$

Multiplying both sides of (20) by M_{js} and using (13), (20) can be rewritten as,

$$M_{js} \dot{S}_{js} = \tau_{js} - C_{js} \dot{q} - G_{js} - M_{js} \ddot{q}_r \quad (21)$$

Adding and subtracting $C_{js} \dot{q}_r$ in (21) gives,

$$M_{js} \dot{S}_{js} = \tau_{js} - M_{js} \ddot{q}_r - C_{js} S_{js} - G_{js} - C_{js} \ddot{q}_r \quad (22)$$

$$V(t) = \frac{1}{2} S_{\theta 1}^T M_{js} S_{\theta 1} + \frac{1}{2} \sum \frac{(\rho_{ii} - \hat{\rho}_{ii})^2}{\beta_{ii}} \quad (23)$$

Since $S_{\theta 1} = S_{js}$ [11], differentiating (23) with respect to time gives,

$$\dot{V}(t) = \left(S_{\theta 1}^T M_{js} \dot{S}_{js} + \frac{1}{2} S_{\theta 1}^T \dot{M}_{js} S_{\theta 1} + \sum \frac{(\rho_{ii} - \hat{\rho}_{ii})(-\dot{\hat{\rho}}_{ii})}{\beta_{ii}} \right) \quad (24)$$

Utilizing (15) and (22), (24) becomes,

$$\dot{V}(t) = \left(S_{\theta 1}^T \left(\begin{array}{c} -K_{dd} M_{js} S_{\theta 1} - \\ \left(\begin{array}{c} \hat{\rho}_{11} \|q_r\| + \\ \hat{\rho}_{22} \|\dot{q}\| \|q_r\| + \\ \hat{\rho}_{33} + \hat{\rho}_{44} \|\dot{q}\| \end{array} \right) \text{sat}\left(\frac{S_{js}}{\emptyset}\right) + \end{array} \right) + \right. \\ \left. \left(S_{\theta 1}^T (-M_{js} \ddot{q}_r - C_{js} S_{js} - G_{js} - C_{js} \ddot{q}_r) \right) \right. \\ \left. + \frac{1}{2} S_{\theta 1}^T \dot{M}_{js} S_{\theta 1} + \sum \frac{(\rho_{ii} - \hat{\rho}_{ii})(-\dot{\hat{\rho}}_{ii})}{\beta_{ii}} \right) \quad (25)$$

Since $\|S_{\theta 1}\| = S_{\theta 1}^T \text{sat}(S_{js}/\emptyset)$ [11], utilizing property 3 and after some manipulation (25) becomes,

$$\dot{V}(t) \leq \left(\begin{array}{c} -S_{\theta 1}^T K_{dd} M_{js} S_{\theta 1} - \left(\begin{array}{c} \hat{\rho}_{11} \|q_r\| + \\ \hat{\rho}_{22} \|\dot{q}\| \|q_r\| + \\ \hat{\rho}_{33} + \hat{\rho}_{44} \|\dot{q}\| \end{array} \right) \|S_{\theta 1}\| + \\ \left[\rho_{11} \|\ddot{q}_r\| + \rho_{22} \|\dot{q}\| \|\ddot{q}_r\| \rho_{33} \right] \|S_{\theta 1}\| + \\ + \frac{1}{2} S_{\theta 1}^T \dot{M}_{js} S_{\theta 1} + \sum \frac{(\rho_{ii} - \hat{\rho}_{ii})(-\dot{\hat{\rho}}_{ii})}{\beta_{ii}} \\ - S_{\theta 1}^T C_{js} S_{\theta 1} + \emptyset \rho_{22} \|\dot{q}\| \|S_{\theta 1}\| \end{array} \right) \quad (26)$$

Using property 2 and defining $\rho_{44} = \emptyset \rho_{22}$, also utilizing adaptive parameters (19), above equation yields into,

$$\dot{V}(t) = -S_{\theta 1}^T K_{dd} M_{js} S_{\theta 1}$$

Since $K_{dd} M_{js}$ is symmetric positive definite matrix then, there exists a constant γ such that $\gamma I_d \leq k_{dd} M_{js}$. Then (27) can be rewritten as,

$$\dot{V}(t) \leq -\gamma \|S_{\theta 1}\|_2^2 \leq 0 \quad (28)$$

In order to achieve the stability it is necessary to show that $S_{\theta 1} \rightarrow 0$ as $t \rightarrow \infty$. This can be achieved by applying Barbalat's lemma to the following continuous non-negative function

$$\dot{V}_1(t) = V(t) - \int_0^1 (\dot{V}(\tau) + \gamma \|S_{\theta 1}(\tau)\|_2^2) d\tau \quad (29)$$

$$\dot{V}_1(t) = -\gamma \|S_{\theta 1}(t)\|_2^2 \quad (30)$$

Since S_{js} is bounded and correspondingly errors are bounded. Thus, all the feedback signals are bounded. Therefore, it can be seen from (22) that, S_{js} is also bounded because M_{js} is already given as bounded property (property3) which proves $\dot{V}_1(t)$ to be uniformly continuous function of time. Since $V_1(t)$ is bounded below by 0 and

$\dot{V}_1(t) \leq 0$ for all t , use of Barbalat's lemma proves that $\dot{V}_1(t) \rightarrow 0$ and from (30) that $\|S_{\theta 1}(\tau)\| \rightarrow 0$ as $t \rightarrow \infty$.

IV. SIMULATION

The simulation is carried out by considering the parameters of manipulators and beam given in Table 1 and 2. The beam is moved from the initial position of center of mass and orientation (0.51m; 0.36m; 90°) to final position and orientation (0.55 m; 0.36m; 90°) is considered for the simulation. Correspondingly, the first manipulator is moved from (0°; -45°; -45°) to (-10.35°; -21.5°; -58.2°) and also the second manipulator is moved from the initial joint angles (0°; 45°; 45°) to final joint angles (10.35°; 21.5°; 58.2°). The control parameters are chosen as $K_{dd} = 500$ and $\lambda_{js} = 20$. The adaptive gains are chosen as $\beta_{11}=\beta_{22}=\beta_{33}=\beta_{44}= 0.01$. The initial adaptive parameters are taken as $\tilde{p}_{11}(0) = \tilde{p}_{22}(0) = \tilde{p}_{33}(0) = \tilde{p}_{44}(0) = 1$. In order to reduce the chattering effect, the boundary layer thickness is chosen as $\phi_L=0.05$. The position of the object along X direction is shown in Fig. 2 where it reaches desired value within 0.5secs. It can be seen from the Figs. 3 and 4 that the motion of object along Y direction and orientation about Z axis is maintained at its desired value. Each joint of the manipulators are reached towards its set point value within 0.5secs which are shown in Figs. 5 - 10. In all the figure captions, “ $M_i J_j$ ” represents the j-th Joint of i-th Manipulator where (i=1, 2) and (j=1, 2, 3)

TABLE I. PARAMETERS OF THE MANIPULATOR

Link	Length	Mass	Moment of Inertia
	m	kg	$Kg-m^2$
1	0.3	1.0	0.30
2	0.3	1.0	0.30
3	0.05	0.4	0.15

TABLE II PARAMETERS OF THE BEAM

Parameter	Value
Mass (m)	1.0 kg
Length (L)	0.1 m
Moment of Inertia (I)	0.2 kg-m ²

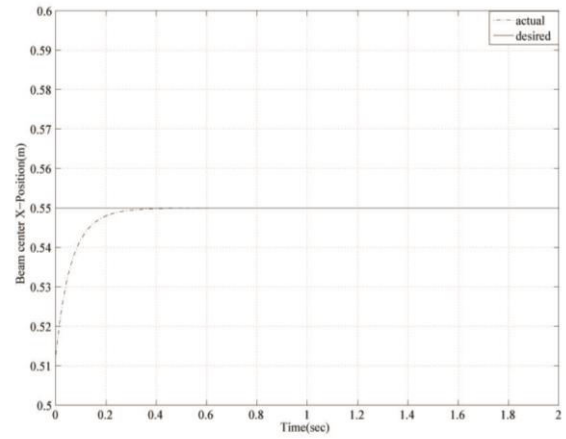


Figure 2. X movement of the beam

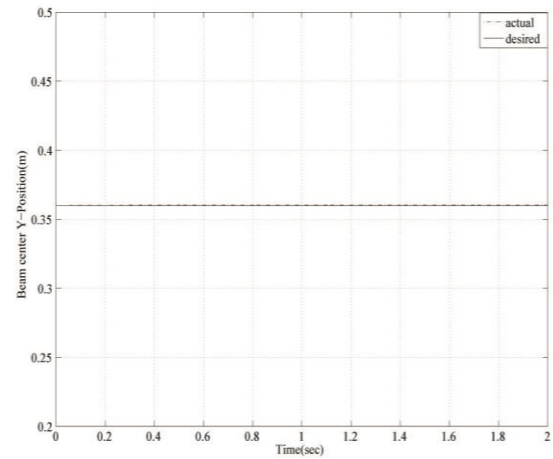


Figure 3. Y movement of the beam

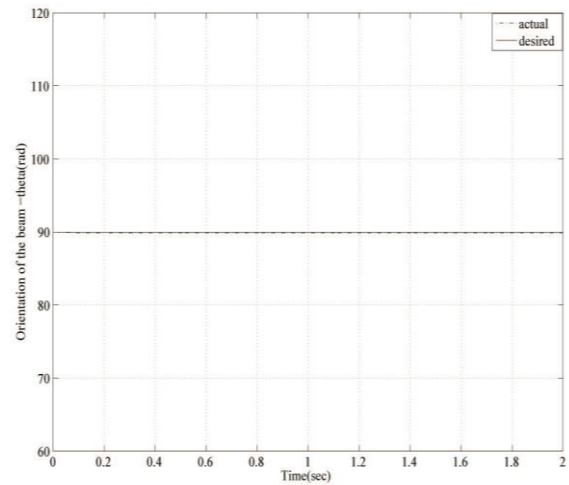


Figure 4. Orientation of the beam

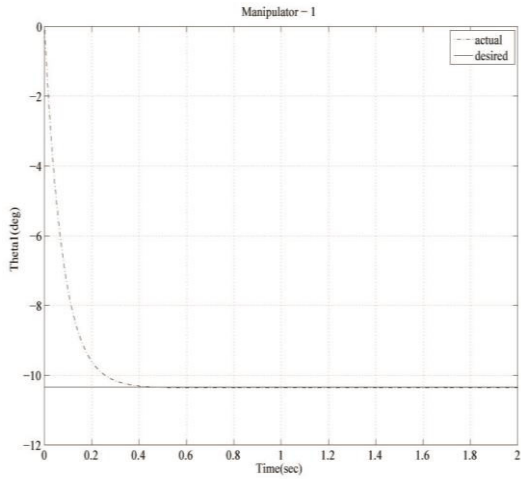


Figure 5. M1J1 angular motion

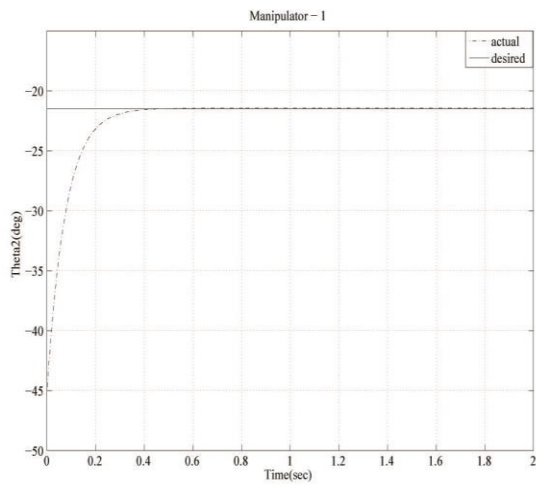


Figure 6. M1J2 angular motion

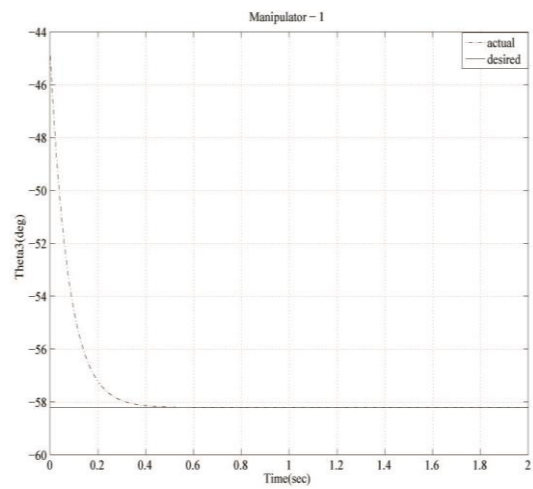


Figure 7. M1J3 angular motion

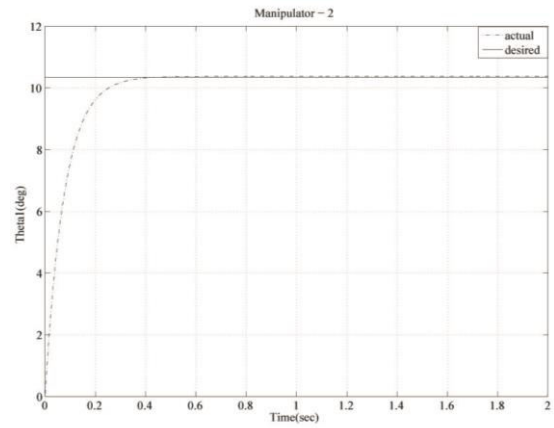


Figure 8. M2J1 angular motion

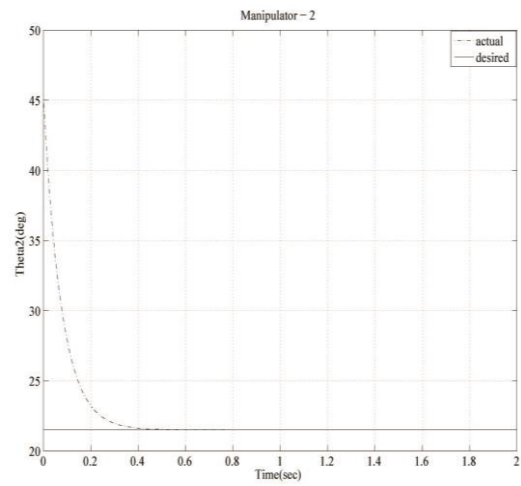


Figure 9. M2J2 angular motion

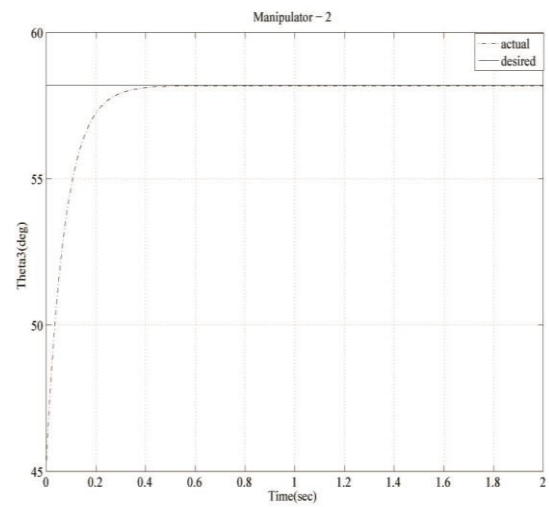


Figure 10. M2J3 angular motion

V. CONCLUSION

In this paper, a robust adaptive control law for the case of two manipulators collaboratively handling a long object is presented. The proposed controller avoids the computation burden caused by the complex regressor and also the structure of the control law is defined with the help of estimation of four parameters. The controller is structurally simple, computationally fast and easy to implement in real time applications. Lyapunov based stability analysis and simulations are carried out. These results validate the effectiveness of the controller.

VI. REFERENCES

- [1] Y. F. Zheng and F. R. Sias, "Two robots arms in assembly," in Proc. IEEE Int. Conf. on Robotics and Autonomous System, 1986, pp. 1230-1235.
- [2] S. Hayati, "Hybrid position/force control of multi-arm cooperating robots," in Proc. IEEE Int. Conf. on Robotics and Automation, 1986, pp. 82-89.
- [3] Y. R. Hu and A. A. Goldenberg, "An adaptive approach to motion and force control of multiple coordinated robots," in Proc. IEEE Int. Conf. on Robotics and Automation, 1988, pp. 1633-1637.
- [4] I. Uzmaya, R. Burkan, and H. Sarikaya, "Application of robust and adaptive control techniques to cooperative manipulation," Control Engineering Practice, vol. 12, pp.139-148, 2004.
- [5] W. Gueaieb, F. Karray, and S. Al-Sharhan, "A Robust hybrid intelligent position/force control scheme for cooperative manipulators," IEEE/ASME Transactions on Mechatronics, vol. 12, no. 2, pp. 109-125, 2007.
- [6] M. Zribi, M. Karkoub, and L. Huang, "Modelling and control of two robotic manipulators handling a constrained object," Applied Mathematical Modelling, vol. 24, no. 12, pp. 881-898, 2000.
- [7] J. H. Jean, and L. C. Fu, "An adaptive control scheme for coordinated multimanipulator system," IEEE Transaction on Robotics and Automation," vol. 9, no. 2, pp. 226-231, 1993.
- [8] J. J. E. Slotine, and W. Li, "On the adaptive control of robot manipulators," Int. J. Robotics Res., vol. 6, no. 3, pp. 49-59, 1987.
- [9] Y. D. Song, "Adaptive motion tracking control of robot manipulators: non-regressor based approach," in Proc. IEEE Int. Conf. on Robotics and Automation, 1994, pp.3008-3013.
- [10] N. Sadegh and R. Horowitz, "Stability and robustness analysis of a class of adaptive controller for robotic manipulators," Int. J. of Robotics Research, vol. 9, no. 3, pp.74-92, 1990.
- [11] T. P. Leung, and C. Y. Su, "Adaptive control for a constrained robot without using a regressor," Transactions of the Institute of Measurement and Control, vol. 18, no. 5, pp. 267-275, 1996.
- [12] W. Gueaieb, F. Karray, and S. Al-Sharhan, "A Robust adaptive fuzzy position/force control scheme for cooperative manipulators," IEEE Transactions on Control Systems Technology, vol. 11, pp.516-528, 2003.
- [13] W. Gueaieb, F. Karray, and S. Al-Sharhan, "A Robust hybrid intelligent position/force control scheme for cooperative manipulators," IEEE/ASME Transactions on Mechatronics, vol. 12, 109-125, 2007.
- [14] M. Azadi, M. Eghtesad, and A. Ghobakhloo "Robust control of two 5 DOF cooperating robot manipulators," Proc. of the IEEE Int. Workshop on Advanced Motion Control, 2006, pp.653-658.
- [15] N. Yagiz, Y. Hacıoglu, and Y. Z. Arslan, "Load transportation by dual arm robot using sliding mode control," J. of Mechanical Science and Technology, vol. 24, pp.1177-1184, 2010.
- [16] M. Zribi, M. Karkoub, and L. Huang, "Modelling and control of two robotic manipulators handling a constrained object," Applied Mathematical Modelling, vol. 24, pp.881-898, 2000.
- [17] J. J. Craig, "Introduction to Robotics: Mechanics and Control," Prentice Hall, Third edition, 2004.



A Nonlinear Model to Study Selectively Deformable Wing of an Aircraft

M. Thangavel¹ & C. Thangavel²

¹Sona College of Technology, Salem, Tamilnadu, India

²VMKV Engineering College, Salem, Tamilnadu, India

E-mail : drnthangavel@gmail.com¹, ctphd2011july@gmail.com²

Abstract - Aeroelasticity of an aircraft includes the study of dynamics of prime movers, structural dynamics, and aerodynamics. Research efforts are on in every area to improve the overall performance of an aircraft. In this paper preliminary studies conducted on the dynamics of selectively deformable wing using an under actuated nonlinear model is reported. First, the literature related to the design and analysis of selectively deformable structure (SDS) wing is reviewed. Second, a single degree of freedom (DOF) model to represent a fixed wing and a two DOF under-actuated model to represent SDS are discussed and their mathematical models are derived. Third, the effect of deformable wing portion on the wing dynamics is studied by varying the excitation frequency and stiffness of the model. Fourth, an experimental setup consisting of two rigid links connected by spring and subjected to sinusoidal displacement is investigated. Final section summarizes the research and provides directions for future work.

I. INTRODUCTION

In the last hundred years airplane technology has grown from strut and wire biplanes propeller driven to jet propelled airplane, Anderson [1]. With the intense study on aerodynamics, the advancement of composite materials, control, sensing, and communication technologies supersonic and hypersonic airplanes are realized. The availability of analysis tools like FEA and CFD has helped in carrying out structural, aeroelasticity analysis of aircraft structures resulting in improved lift/drag ratio, high aspect ratio wing design and light weight high-speed airplanes. Presently, research efforts are undergoing to realize the desired aeroelastic deformation through surface morphing, all movable control surfaces with variable stiffness effects and with selectively deformable structures. The following describes the literature related to aeroelasticity.

Amiryants et al. [2] investigates the morphing of airframe structures using selectively deformable structures (SDS). The main objective of SDS research is to develop a structure which has a minimal Poisson's effect: results in a deflection along the direction of the acting load. Simpson et al.[3] provide a review of research project on "active aeroelastic aircraft structures" (3AS). The aim of the project are as follows:

- Aerodynamic drag reduction.
- Structural weight reduction.
- Advanced sizing design and exploitation.
- Tool reduction.

- Reduced maintenance.
- High aeroelastic efficiency.
- Improved aeroelastic stability and dynamic loads suppression.

Braidruski et al. [4] experiments the usefulness of SMA actuators for morphing wing to reduce fuel consumption and to improve aerodynamic performance. They have used a morphed wing proto-type combined with three sub-systems namely flexible extrudes, rigid intrude and an actuator group control inside the wing box. Kuzmina et al. [5] presents an overview of the aeroelastic deformation using an adaptive stiffness attachments of all moveable aerodynamic surfaces. Amiryants et al.[6] presents the investigations on aerodynamic control using differential leading edge, forward aileron, special combination of spoiler and aileron Nagel et al.[7] presents the results of using active composites to enable shape control of the wing while retaining the stiffness and strength requirements. Amiryants [8] presents a comparison of control effectiveness of hinge-less connection of aileron using selectively deformable structure with traditional control devices. It is shown SDS is highly effective for wide range of mach numbers and dynamic pressure. Ahn et al.[9] presents the tilt-rotor technology developed for smart UAV. Their objective is to develop high speed VTOL aircraft and to tailor the technology for the domestic aerospace industry. Mauchar et al.[10] investigates use of active trailing edge of rotor blade control to minimize noise and vibration, also to reduce fuel consumption. Livne [11] presents an extensive

review on aeroelasticity. He has discussed comprehensively the various issues and remedies, numerical simulation, modeling for capturing local and global behavior, order reduction of large FE and CFD models, sensitivity analysis of coupled structure, aerodynamic optimization with FE/CFD models, aeroservoelasticity and aeroservoelastic optimization, morphing, smart airplanes, accounting for uncertainty in aeroelastic analysis and design, multidisciplinary design optimization, aeroelasticity of selected non-conventional configurations, aeroelastic challenges associated with supersonic and hypersonic flight, flopping flight and UAVs.

From the literature it is clear that massive work have been done to improve aeroelasticity. Recently, research efforts are on in the areas of surface morphing to improve aerodynamics, and minimization of control effort required to effect changes in the wing geometry using selectively deformable structure (SDS). Therefore, availability of an effective model to study SDS dynamics would greatly help in evolving better design for the SDS based wing. In this work a preliminary study has been conducted to understand the usefulness of duffing's equation to study SDS dynamics.

The organization of the paper is follows. In section one, literature related to aeroelasticity have been reviewed. Section two presents the dynamics of SDS using an under-actuated beam like model. Section three reports the simulation conducted on the fixed wing and SDS models. Section four presents the experimental results conducted on simple beam and selectively deformable beams. Final section summarizes the research work and outlines the plan for future work.

II. THE MODEL

A defense aircraft need to be accelerated and decelerated fast and at the same time wing geometry need to be modified to improve aerodynamic effectiveness. Compliance in the wing would help in reducing the control effort required to change the wing geometry. However, the effects of compliance on wing dynamics need to be understood, and for this purpose some simple models of wings are assumed and studies are carried out. Fig. 1 and 2 shows the models of fixed wing and selectively deformable wing respectively. Fixed wing is represented by a simple cantilever beam and SDS wing is represented by a two DOF under-actuated beam and both are subjected to excitation. The following describes the two models.

Model – 1

Figure 1 shows the model representing the fixed wing. It consists of a single beam with one end fixed and a sinusoidal base excitation.

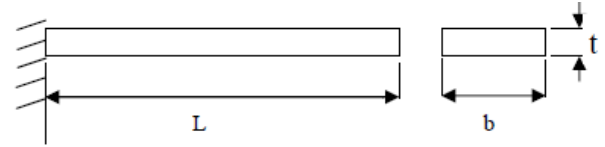


Fig. 1: Cantilever beam model to represent fixed wing.

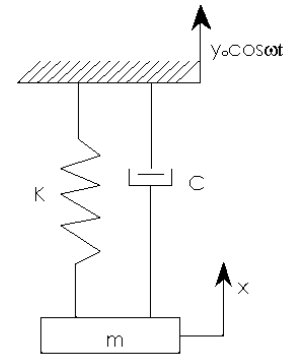


Fig.1a : Equivalent model to represent the fixed wing.

The equation of motion for the above model is given by,

$$m\ddot{x} = -c(\dot{x} - \dot{y}) - k(x - y)^3 \quad (1)$$

Now

$$z = x - y \quad (2)$$

Would results in

$$\begin{aligned} m\ddot{z} + c\dot{z} + kz^3 &= -m\ddot{y} \\ m\ddot{z} + c\dot{z} + kz^3 &= m\omega^2 y_0 \cos \omega t \end{aligned} \quad (3)$$

Where the parameters of the system are, m, c, k, E, l, I – mass, damping coefficient, equivalent stiffness, young's modulus, length, area moment of inertia of cross section of the beam respectively. [$k = 3EI/l^3$]
x, y, z – displacement at the tip, excitation amplitude, relative displacement between the mass and support respectively.

The above equation can be converted into two first order differential equations,

$$z_1 = \dot{z} \quad (4)$$

$$\dot{z}_1 = \frac{1}{m} [m\omega^2 y_0 \cos \omega t - cz_1 - kz^3] \quad (5)$$

Model - 2

Figure 2 shows the under-actuated model representing the SDS wing. It consists of two beams connected by compliant arrangement and its fixed end actuated by a sinusoidal excitation.

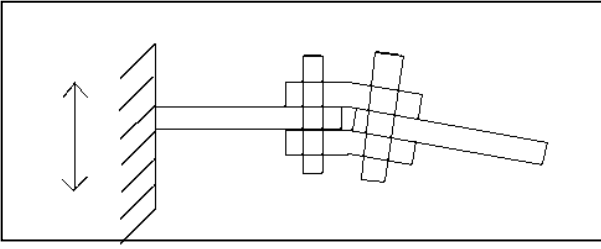


Fig. 2 : An under-actuated model to represent SDS wing

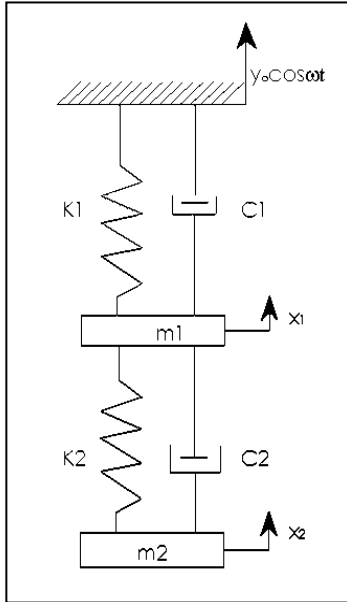


Fig. 2a. The equivalent model for representing SDS wing

The equation of motion for the above model is given by,

$$m_1 \ddot{x}_1 = -c_1(\dot{x}_1 - \dot{y}) - k_1(x_1 - y)^3 - c_2(\dot{x}_1 - \dot{x}_2) - k_2(x_1 - x_2)^3 \quad (6)$$

$$m_2 \ddot{x}_2 = -c_2(\dot{x}_2 - \dot{x}_1) - k_2(x_2 - x_1)^3 \quad (7)$$

Where, m_1, m_2 - mass of the beam 1 and 2

k_1, k_2 - stiffness of the beam 1 and the compliant arrangement

c_1, c_2 - damping coefficient of beam 1 and the compliant arrangement

y_0 - excitation amplitude

x_1, x_2 - displacement of m_1, m_2

\dot{x}_1, \dot{x}_2 - velocity of m_1 and m_2

\ddot{x}_1, \ddot{x}_2 acceleration of m_1 and m_2

Now letting, $z = x_1 - y$ (8)

$\dot{z} = \dot{x}_1 - \dot{y}$ (9)

$$W = x_1 - x_2 \quad (10)$$

$$\dot{W} = \dot{x}_1 - \dot{x}_2 \quad (11)$$

$$\ddot{x}_2 = \ddot{x}_1 - \ddot{W} \quad (12)$$

Where,

z, \dot{z}, \ddot{z} relative displacement, velocity and acceleration between the beam and the mass 1 and 2

w, \dot{w}, \ddot{w} relative displacement, velocity and acceleration between the beam and the mass 1 and 2

Would result in the following two 2nd order equations,

$$m_1 \ddot{z} + c_1 \dot{z} + k_1 z^3 + k_2 w^3 + c_2 \dot{w} = -m_1 \ddot{y} \quad (13)$$

$$m_2 \ddot{w} + c_2 \dot{w} + k_2 w^3 = m_2 \ddot{x}_1 \quad (14)$$

Again letting,

$$\dot{z} = z_1 \quad (15)$$

$$\dot{w} = w_1 \quad (16)$$

Will result in four first order equations,

$$\dot{z} = z_1 \quad (17)$$

$$\dot{z}_1 = \frac{1}{m_1} [m_1 \omega^2 y_0 \cos \omega t - c z_1 - k z_1^2 - c_2 w_1 - k_2 w^3] \quad (18)$$

$$\dot{w} = w_1 \quad (19)$$

$$\dot{w}_1 = \frac{1}{m_2} [m_2 \left\{ \frac{1}{m_1} [m_1 \omega^2 y_0 \cos \omega t - c z_1 - k z_1^2 - c_2 w_1 - k_2 w^3] \right\} - m_2 \omega^2 y^2 \cos \omega t - c_2 w_1 - k_2 w^3] \quad (20)$$

Extensive work has been on solving duffing's equation and its dynamics. Harmonic balance in conjunction with Melnikov method [12], nonlinear dampers for improving structural dynamics [13-15] and nonlinear control design for vibration reduction [16]. This work makes an attempt to assess the usefulness of duffing's equation to study the dynamics of SDS wing.

III. SIMULATION

Simulations are conducted to understand the effect of compliance on wing dynamics. In order to make comparison between fixed wing and selectively deformable wing both the model lengths are kept equal. For fixed wing there will be single stiffness and for SDS there will be two stiffnesses namely the stiffness of the link 1 and stiffness of the compliant arrangement. In the SDS model, the link 2 is joined with link 1 through a compliant arrangement and the link 2 is assumed to be rigid. The excitation amplitude for both the models are kept constant and frequency is varied and the maximum velocity and displacement for each frequency are observed and tabulated. The table 1 and 2 show the maximum tip displacement and velocity values for fixed wing and SDS wing for various frequencies.

Sl. No	Excitation frequency, ω rads/sec	Tip Displacement Y_1 in m	Tip Velocity Y_2 in m/sec
1	100	0.5841	20.0766
2	200	0.5913	40.0519
3	300	0.5957	60.0857
4	400	0.5967	80.0862
5	500	0.5951	100.0850
6	600	0.5978	120.0827
7	700	0.5972	140.1059
8	800	0.5957	160.1250
9	900	0.5954	180.1372
10	1000	0.5965	200.1361

Table 1. Simulation results for fixed wing ($m=5\text{kg}$, $k=200\text{N/m}$, $c=10\text{ N/m/sec}$, Initial conditions $x_0=0.2\text{m}$, $\dot{x}=0$, Excitation amplitude, $y_0=0.2\text{m}$, simulation duration= 10secs)

Sl. No	Excitation frequency, ω rads/ sec	Displacement $Y1$ m	Velocity $Y2$ m/sec	Displacement $Y3$ m	Tip Velocity $Y4$ m/sec	Tip Displacement $Y1+Y3$ m
1	100	0.5554	19.9586	0.4618	15.9518	1.0172
2	200	0.5754	40.0015	0.4872	31.9969	1.0626
3	300	0.5851	60.0187	0.4985	48.0129	1.0836
4	400	0.5888	80.0271	0.5039	64.0207	1.0927
5	500	0.5884	100.0347	0.5045	80.0271	1.0929
6	600	0.5925	120.0407	0.5092	96.0317	1.1017
7	700	0.5927	140.0456	0.5103	112.0356	1.1030
8	800	0.5919	160.0464	0.5103	128.0329	1.1022
9	900	0.5917	180.0604	0.5099	144.0437	1.1016
10	1000	0.5932	200.0698	0.5114	160.0511	1.1046

Table 2. Simulation results for SDS wing ($m_1=2.5\text{kg}$, $m_2=2.5\text{Kg}$, $k_1=250\text{N/m}$, $k_2=150\text{N/m}$, $c_1=10\text{ N/m/sec}$, $c_2=10\text{ N/m/sec}$ Initial conditions $x_{10}=0.2\text{m}$, $\dot{x}_{10}=0$, $x_{20}=0.2\text{m}$, $\dot{x}_{20}=0$, excitation amplitude $y_0=0.2\text{m}$ simulation duration= 10secs)

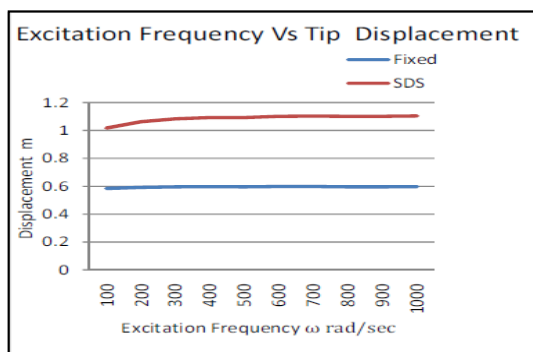


Fig. 3 : Excitation frequency Vs Displacement for fixed and SDS wings.

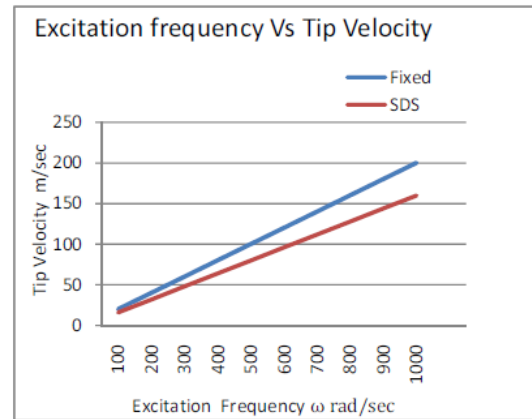


Fig. 4 : Excitation frequency Vs Tip Velocity for fixed and SDS wings

Figs. 3 and 4 show the graphs drawn between frequency Vs displacement and frequency Vs velocity for both type of wings. From the graph we can observe that,

- Compliance in the link reduces the speeding capacity
- For the particular frequency speeding capacity is better
- Compliance in the wing increases displacement again it is more at certain frequency

Stiffness K_2	Displacement $Y1$ m	Velocity $Y2$ m/sec	Displacement $Y3$ m	Tip Velocity $Y4$ m/sec	Tip Displacement $Y1+Y3$ m
100	0.5556	19.9593	0.4622	15.9603	1.0178
110	0.5556	19.9593	0.4621	15.9559	1.0177
120	0.5555	19.9585	0.4620	15.9599	1.0175
130	0.5555	19.9561	0.4620	15.9597	1.0175
140	0.5554	19.9531	0.4619	15.9522	1.0173
150	0.5554	19.9586	0.4618	15.9518	1.0172
160	0.5553	19.9557	0.4617	15.9522	1.0170
170	0.5553	19.9571	0.4617	15.9597	1.0170
180	0.5553	19.9581	0.4616	15.9599	1.0169
190	0.5552	19.9586	0.4615	15.9559	1.0167
200	0.5552	19.9586	0.4614	15.9603	1.0166

Table 3. Displacement and Tip Velocity of SDS wing under stiffness variation while the excitation frequency is kept constant ($m_1=2.5\text{kg}$, $m_2=2.5\text{Kg}$, $k_1=250\text{N/m}$, $k_2=\text{variable}$, $c_1=10\text{ N/m/sec}$, $c_2=10\text{ N/m/sec}$ Initial

conditions $x_{10}=0.2m$, $\dot{x}_{10}=0$, $x_{20}=0.2m$, $\dot{x}_{20}=0$, excitation amplitude=0.2m simulation duration= 10secs)

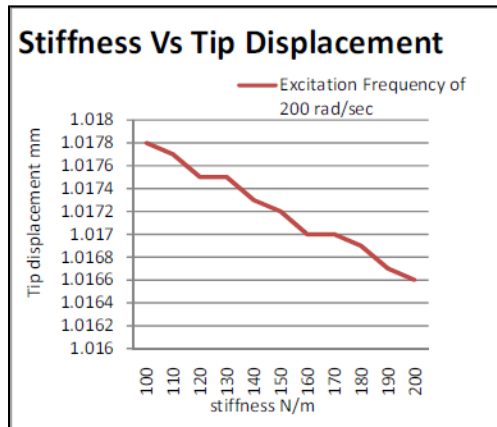


Fig. 5: Stiffness Vs Tip Displacement for SDS wings

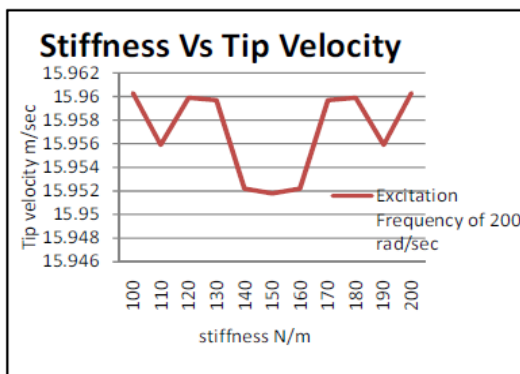


Fig. 6 : Stiffness Vs Tip Velocity for fixed and SDS wings

From the fig.5 it is clear that the increase in stiffness reduces deformation. Fig.6 shows that the tip velocity fluctuates with stiffness variation hinting at wing parameter tuning might improve aerodynamic performance.

IV. EXPERIMENTATION

Here, the effects of compliance on the wing dynamics are studied experimentally. Figs.7 and 8 show the experimental setups for fixed and SDS wings respectively. It consists of a DC motor, variable speed controller, vertical stand with holder, an eccentric cam, fixed beam, selectively compliant beam, and the accelerometer with necessary instruments. Experiments are conducted on fixed wing and compliant wings. The motor speed is varied from 100 rpm to 1000 rpm and the displacement, velocity and acceleration values are noted and tabulated. Compliance in the beam is varied by varying the gap between two beams and the sensor position is also varied and the values are tabulated in tables 4, 5 and 6.



Fig.7: Experimental setup to study fixed wing dynamics.



Fig. 8 : Experimental setup to study SDS wing.

Sl. No	Speed (rpm)	Acceleration (m/s ²)	Velocity (cm/s)	Displacement (mm)	Frequency (hz)
1	100	0.0	0.95	0.423	41
2	200	1.2	0.64	0.430	41
3	300	3.2	1.70	0.891	41
4	400	5.9	2.07	1.000	41
5	500	13.1	4.30	1.745	41
6	600	38.7	7.89	2.295	41

Table 4 : Experimental results for fixed wing (60cm standard steel rule is used as beam)

Sl. No	Speed (rpm)	Acceleration (m/s ²)	Velocity (cm/s)	Displacement (mm)	Frequency (hz)
1	100	0.1	0.30	0.227	41
2	200	0.1	0.81	0.502	41
3	300	1.0	3.08	1.535	41
4	400	7.8	12.36	5.269	41
5	500	4.9	6.90	2.786	41
6	600	4.8	5.10	1.947	41
7	700	5.2	4.39	1.513	41
8	800	6.6	3.90	1.236	41
9	900	9.0	3.94	1.147	41
10	1000	11.9	3.74	1.132	41

Table 5 : Experimental results for SDS wing (30+1+30cm, standard 30cm steels are connected by belt and used as SDS beam)

Sl. No.	Speed (rpm)	Acceleration (m/s ²)	Velocity (cm/s)	Displacement (mm)	Frequency (hz)
1	100	0.2	0.12	0.136	41
2	200	0.0	1.29	0.820	41
3	300	6.0	14.40	6.747	41
4	400	2.5	5.76	2.588	41
5	500	3.2	4.53	1.879	41
6	600	3.7	3.83	1.478	41
7	700	4.8	3.47	1.230	41
8	800	6.1	3.48	1.134	41
9	900	9.3	3.75	1.077	41
10	1000	9.2	4.07	1.139	41

Table 6. Experimental results for SDS wing (30+2+30cm, standard 30cm steels are connected by belt and used as SDS beam)

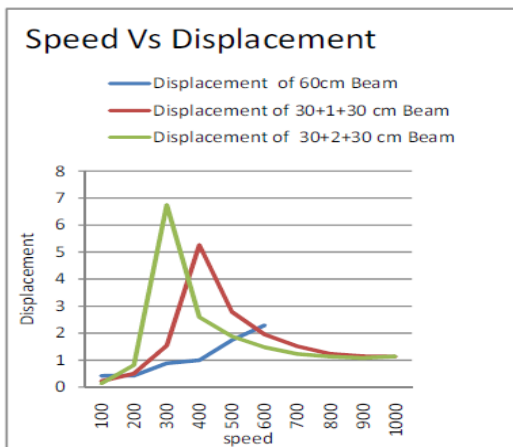


Fig. 9 : Comparison of Speed Vs Displacement

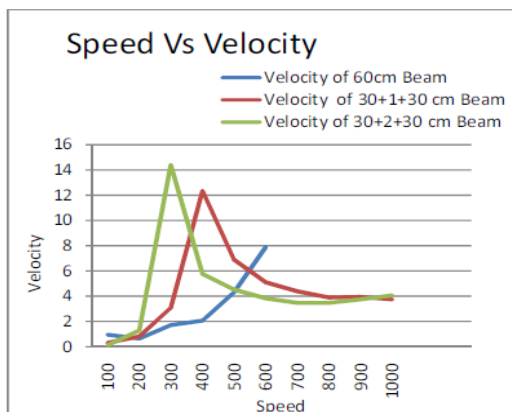


Fig. 10 : Comparison of Speed Vs Velocity

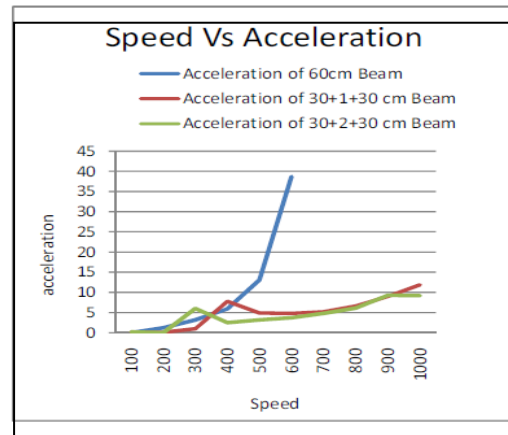


Fig. 11 : Comparison of Speed Vs Acceleration

The experimental data are segregated on the basis of displacement, velocity and acceleration and graphs are drawn as shown in figs 9-11, between speed Vs displacement, speed Vs velocity and speed Vs acceleration respectively. From the graphs it is clear that fixed wings can be accelerated faster than compliant wings. For the compliant wing the displacement is more than the fixed wing. Interestingly, the displacements and velocity of wings are more at certain speed hinting at proper selection of parameters for the wing could improve performance (speeding capability) and also the effort required to effect deformation can be reduced.

V. CONCLUSION

In this paper the suitability of a nonlinear model to study the dynamics of a selectively deformable wing has been investigated. For this purpose a single cantilever beam and a beam with selective compliance representing the aircraft wings are modeled and studied by subjecting them to sinusoidal excitation. The effect of stiffness on acceleration and displacement capability are studied. It is found that stiffer beams (wings) can be accelerated or decelerated faster and undergo less deformation. It is difficult to accelerate the wing with more compliance. Experiments conducted on (stiff) beams and compliant beams conforms the theoretical findings. Further, this preliminary study demonstrates that the dynamics of deformable wing can be studied using a nonlinear model as both (theoretical and experimental) results show comparable dynamic characteristics. In future, the model will be refined further and investigations will be made to arrive at a suitable selectively deformable wing for the aircrafts.

REFERENCES

[1] John D. Anderson, Jr, "Aircraft Performance and Design", Mc Graw-Hill International Editions, Aerospace Science/Technology Series 1999.

- [2] Gennady Amiryants, Fanil Ishmuratov, Victor Malyutin, Victor Timokhin, "Selectively Deformable Structures For Design Of Adaptive Wing Smart Elements" ICAS2010 27th International Congress Of The Aeronautical Sciences.
- [3] John Simpson, Luis Anguita, Bo Nilsson, Vincenzo Vaccaro, Gregorio kawiecki, "Review Of The European Research Project "Active Aeroelastic Aircraft Structures"(3AS) European Conference For Aerospace Sciences (EUCASS)
- [4] V. Brailovski, P. Terriault, T. Georges, D. Coutu, "SMA Actuators for Morphing Wings" 3rd International Symposium on Shape Memory Materials for Smart Systems, Physics Procedia 00 (2010).
- [5] Svetlana Kuzmina, Gennadi Amiryants, Johannes Schweiger, Jonathan Cooper, Michael Amprikidis, Otto Sensberg, "Review And Outlook On Active And Passive Aeroelastic Design Concepts For Future Aircraft" ICAS 2002 CONGRESS pp. 432.1 – 432.10.
- [6] Gennady Amiryants, "Active Aeroelasticity Concept: Novel View, Methodology And Results" ICAS2008, 26th International Congress Of The Aeronautical Sciences.
- [7] B. Nagel, H.P. Monner, E. Breitbach, "Integrated Design Of Smart Composites, Applied To Smart Winglets" ICAS2008 25th International Congress Of The Aeronautical Sciences.
- [8] G.A. Amiryants, F.Z. Ishmuratov, S.I. Kuzmina, "Use Of Aeroelasticity; Multidisciplinary Investigations" ICAS2004 24th International Congress Of The Aeronautical Sciences.
- [9] Ohsung Ahn, J.M. Kim, C.H. Lim, "Smart Uav Research Program Status Update : Achievement Of Tilt-Rotor Technology, Development And Vision Ahead" ICAS2010 27th International Congress Of The Aeronautical Sciences.
- [10] Christoph K. Maucher, Boris A. Grohmann, Peter Jänker, Andree Altmikus, Flemming Jensen, Horst Baier, "Actuator Design For The Active Trailing Edge Of A Helicopter Rotor Blade"
- [11] Eli Livnes, "Future of Airplane Aeroelasticity" Journal Of Aircraft, Vol. 40, No. 6, November–December 2003.
- [12] Michele Bonnin, "Harmonic Balance, Melnikov method and Nonlinear Oscillators Under resonant Perturbation"
- [13] Chion-Fong Chung, Chiang-Nan Chang, " Dynamics of Asymmetric Nonlinear vibration Absorber" Journal of Marine Science and Technology, Vol. 1, No.1, pp. 8-19(2003).
- [14] S.J. Zhu, Y.F. Zheng, Y.M. Fu, "Analysis of non-linear dynamics of a two-degree-of-freedom vibration system with non-linear damping and non-linear spring", Journal of sound and vibration 271 (2004) 15-24.
- [15] Zhu Weiqiu, Wu Qitai, "Jump and bifurcation of duffing oscillator under narrow-band excitation" ACTA MECHANICA SINICA, Vol.10, No.1, February 1994, science press, Beijing, china, Allerton Press, INC., New York, U.S.A.
- [16] Yebin Wang, Kenji Utsunomiya, Scoot A. Bortoff, "Nonlinear Control Design for a Semi-Active Vibration Reduction System" Proceedings of the 30th Chinese Control Conference, July 22-24, 2011, Yantai, China.



Need for Computer Integrated Manufacturing – A Review

Mohd.Abdul Shoeb, Mirza Hussain Baig, Md. Thajuddin & Dr.T. Srihari

Shadan College of Engineering and Technology, Hyderabad, India.

E-mail : mashoeb@ymail.com, ahmedhussain58@ymail.com, srihariwelding@yahoo.com

Abstract - Computer integrated manufacturing (CIM) as a strategy helps to improve the performance of manufacturing firm by integrating various financial areas of manufacturing; both in terms of material and information flow. CIM allows individual processes to exchange information with each other and initiate actions although the main advantage is the ability to create automated manufacturing processes .CIM relies on closed loop control processes based on real time input from sensors .It is also called as “flexible design and manufacturing .”CIM system saves on labour operating the machines it requires extra human labours in ensuring that there are proper safeguards for data signals that are used to control the machine.

I. INTRODUCTION FOR IMPLEMENTATION OF CIM

The justification of CIM systems is one of the foremost important steps in implementing CIM factors such as reduced costs of materials, direct and indirect labour, reduced scrap, rework and inventory labour would justify the scope of CIM implementation.

The implementation of CIM is an example of implementation of information and communications technologies (ICTS) in manufacturing. The CIM as a strategy for integration must physically link parts of the facility and handle the flow of information, especially in context of improving the speed of material flow. The implementation of CIM helps how to overcome the fragmented communication links caused by the diversity of function and size in textile company .Research in CIM design and implementation has mainly been in the area of production .The major issues in CIM are directed related to information systems. The integration of computer aided design and CNC machines made a huge impact on the development of CIM.The heart of CIM is CAM/CAD systems are essentials to reducing cycle times in the organization.

CIM is the architecture for integrating the engineering, marketing, and manufacturing functions through information’s technologies. This indicates the relationship between business process reengineering and computer integrated manufacturing with an objective to achieve the enterprises integration and management for improving productivity and quality. The motivation for CIM has been based on the perceived need for the manufacturing industry to respond to changes more rapidly than in past.

- Babar and Ray propose that while CIM integrates the systems components, it does not necessarily

introduce flexibility into the Systems. The focus should not be on integration alone, but on the simultaneous introduction of flexibility as part and parcel of the integration process in the implementation.

Table-I

AREAS	ISSUES
Strategic	Alignment between business and manufacturing strategies.
Organizational Behavioral	Structure, communication leadership, teamwork, concurrency.
Technological	Networking, communication system, data base, groupware.
Operational	Design, engineering, production planning, accounting.

Table-II

Manufacturing Industry	Implementation		Adaptability	
	Problems	Strategies	Problems	Strategies
Flexible manufacturing systems	Alignment between business and manufacturing	Capital	Top down business oriented strategy	Team efforts
Manufacturing	Lack of information technologies	Organization systems design	Handling variability	Investment in flexible technologies

II. INTEGRATION AND ADAPTABILITY ISSUES IN THE IMPLEMENTATION OF CIM. (3)

Work flow design and Application platform

The workflow design for implementation of CIM can be separated into 4 blocks

- 1) Product design: The product design of CIM for which interactive computer aided design(CAD) systems allows the drawing and analysis tasks to be performed. These computer graphics systems are very useful to get the data out of designers mind into a present form and enable analysis in fraction of time required otherwise and with greater accuracy design process speed up considerably.
- 2) Manufacturing planning: computer aided power planning helps to establish optimum manufacture routines and producing steps, sequence and schedule so that the process is optimum.
- 3) Manufacturing: computer aided manufacturing helps in identifying the problems of manufacturing. Distributed intelligence in the form micro processors could be used to control machines and materials handling and collect the data on currents shops condition.
- 4) Computer aided inspection and reporting so as to provide a feedback loop.
- 5) Control and monitoring .In addition, these workshops can include automated agents and interposes linking. This development will provide a generic platform whereby business can design system to enable “Customer satisfaction” by dividing towards and tracking the completion of workflows. These user designed and basic workflows model important business process, including the pervasive cycle of “Customer makes request”, performer promises CIM technology is designed as a platform which links other preexisting databases. transaction processing and other system with the workflow structure, to fulfill request “Perform report completion” and customer declares satisfaction”.

III. CIM METHODS AND TECHNIQUES:

- 1) *CAD(computer aided design)*CAD also known as computer aided design and drafting (CADD),CAD provides the users with input tools for the purposes of streamlining designs processes ,drafting ,documentation and manufacturing .CAD has been a major driving for research in computational geometry ,computer graphics and discrete differential geometry. Computer aided inspection and reporting so as to provide a feed back

loop.CAD in all manufacturing boost productivity in all workshops applications including metal cutting, handling, and assembly. The features in the CAD systems can be used for the variety of tools for measurements such as tensile strength, and strains and how the elements gets affected in certain temperature.CAD is one of the many tools used by engineers and designers and is used in many ways depending on the profession of the user and type of software in questions.CAD is one part of the digital product development activity within the product lifecycle management processes ,and as such is used together with other tools which are either integrated modules such as computer-aided engineering and finite elements analysis.

- There are several good reasons for using CAD systems to supports the engineering design function.
- To increases the productivity of the designer.

Table - III

Design phase	CAD function
Synthesis	Geometric modeling
Analysis and optimization	Engineering analysis
Evaluation	Design review and evaluation
Presentation	Automated drafting

IV. CAD APPLIED TO FOUR THE SHIGLEY DESIGN PHASES :(2).

- To improve the quality of the design.
- 2) *CAM (computer aided manufacturing)* CAM refers to the use of a computer to assist in all operations of a manufacturing plant, including planning management and storage. Its primary purposes is to create a faster production process and components and tooling with more precise dimensions and materials consistency. The output from the CAM software is usually a simple text file of G-code sometimes many thousands of commands long that is then transferred to a machine tool using a direct numerical control program.CAM is a subsequent computer aided process after computer aided design and sometimes computer aided engineering ,as the mode generated in CAD and verified in CAE can be input into CAM software, which then controls the machine tools .CAM helps in form of manufacturing problems and opportunities, distributed intelligence in the form of microprocessors could be used to control machine and materials handling the data on currents shop conditions.

- CAM is most closely associated with functions in manufacturing engineering, such as process planning and numerical control. The application of CAM can be divided into two categories such as manufacturing planning and manufacturing control.
 - CAM applications for manufacturing planning are those in which the computer is used indirectly to support the production function, but there is no direct connection between the computer and the process
 - CAM system downloads the NC part program directly to the machine tool by means of a telecommunications network. Hence, under this arrangement, product designing programming, and physically production are all implemented by computer.
 - *CAPP (computer aided planning process)* process planning encompasses the activities and functions to prepare a detailed set of plans and instructions to produce a part. Process 3) plans which typically provide more detailed step by step work instructions dimensions related to individual operations, machining parameters, setup instructions the need for CAPP is greater with an increased no. of different types of parts being manufactured with a more complex manufacturing process.
 - Kenneth Crow stated that “Manual process planning is based on a manufacturing engineer’s experience and knowledge of production facilities, equipment, processes, and tooling. Process plan is very time consuming and results vary based on the person doing the planning.
 - According to Engelke, the need for CAPP is greater with an increased number of different types of parts being manufactured, and with a more complex manufacturing process. Computer-aided process planning initially evolved as a means to electronically store process plan once it was created, retrieve it, modify it for new part and print the durability of the vehicles they produce. They are used for design manufacturing for improved design control, better quality and quality control. It is a total company management concept for using human resources more productively. This is not exclusively a software function, but a marriage of people skills, dedication to database accuracy, and computer resources. It is a total company management concept for using human resources more productively.
- 4) *ERP(enterprise resource planning)*:ERP is defined as a method for the effective planning of all resources of a manufacturing company.ERP have enabled the automakers to reduce product development cost and time while improving the safety, comfort and durability of the vehicle they produce.
- They are used for design manufacturing for improved design control, better quality and quality control. This is not exclusively a software function, but dedication to database accuracy, and computer resources. It is a total company management concept for using human resources more productively.
- 5) *CAE (computer aided engineering)*CAE tools are very widely used in the automotive industry. It is dependability is based upon all proper assumptions as inputs and must identify critical inputs.CAE is mostly use in defining the model and environmental factors to be applied to it, analysis solves post processing of results.CAE dependability is based upon all proper assumptions as inputs and must identify critical inputs .Even though there have been many advances in CAE, and it is widely used in the engineering field, physically testing is still used as a final confirmation for subsystems due to the fact that CAE cannot predict all variables in complex assemblies.
- Manufacturing resources planning is defined as a method for the effective planning of all resources of a manufacturing company .Ideally it addresses operational planning in units, financial planning ,and has a simulation capability to answer “what-if “questions and extensions of closed –loop .
 - Computer technology offers the means of imparting intelligence to machines, computer aided equipment can perform many sophisticated machining jobs at much faster speed and with more consistency and accuracy .computer integrated manufacturing promises to boost productivity in all workshops applications including metal cutting, inspection.

V. CIM CONTROL METHODS

CNC (COMPUTER NUMERICAL CONTROL) AND ROBOTICS

DNC (DIRECT NUMERICAL Control)

1) COMPUTER NUMERICAL CONTROL METHOD AND ROBOTICS

- Computer numerical control may be defined as an numerically controlled systems in which a dedicated stored program computer is used to performs store or all of the basic NC functions in accordance with control programs stored in the read write memory of computer .CNC is also called soft wire NC.CNC generally

supports one machine. Software for CNC is written specifically for a particular machine device.

- The various units are discussed below:
- **INPUT UNIT:** It requires all the commands from operator interface and status of the machine in the form of ac or dc and analog signals.
- **CONTROL UNIT:** It takes instruction from the memory unit and interprets them one at a time.
- **MEMORY UNIT:** It stores instructions and data received from the input. It also stores the results of arithmetic operations and supplies information to the output unit.
- **ARITHMETIC UNIT:** It performs calculations and gives results
- **OUTPUT UNIT:** It receives data from memory at the command of control unit. Output signals are used to turn on and off devices, display information, position axes etc.
- **OPERATOR INTERFACE:** Various units which comprises operator interface are as follows:

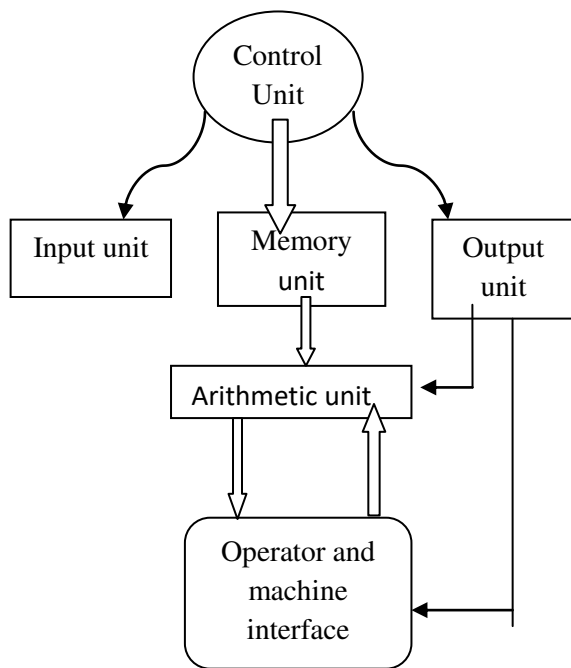
< a> Punched tape

 Magnetic devices

MACHINE INTERFACE : it comprises all devices used to monitor and control machine tools, extreme travel limit, switches, miscellaneous position location, solenoids for hydraulic and air control, control Numerical control is another form of industrial computer control. It involves the use of the computer to direct a machine tool through a sequence of processing steps defined by a program instructions that specifies the details of each step and their sequence. The distinctive feature of NC is control of the relative position of a tool with respect to the object being processed. Computations must be made to determine the trajectory that must be followed by the cutting tool to shape the part geometry .Hence, NC requires the controller to execute not only sequence control but geometry calculations as well Because of its importance in manufacturing. The control objectives might include: to minimize part by determining optimum operating conditions, to maximize machine utilization through efficient scheduling, to

minimize tooling costs by tracking tool supervisory in NC method and techniques.

- Closely related to NC is industrial robotics, in which the joints of the manipulator are controlled to move the end-of-arm through a sequence of positions during the work cycle. As in NC, the controller must perform calculations during the work cycle to implement motion interpolation, feedback control, and other functions. In addition, a robotic work cell includes other equipment besides the robot, and the activities of the other equipment in the work cell must be coordinated with those of the robot.(2)
- Robot controllers can be classified into four categories
 - 1) Limited sequence control
 - 2) Playback with continuous path control
 - 3) Playback with point to point control and
 - 4) Intelligent control.
- Limited sequence control is the most common type .It can be utilized only for simple motion cycles, such as pick-and-place operations. It is usually implemented by setting limits for each sequencing the actuation of the joints to accomplish the cycle.
- Playback robots represent a more – sophisticated form of control than limited sequence robots. Playback control means that controller has a memory to record the sequence of motions in a given work cycle as well as the locations and other parameters associated with each motions and then to subsequently playback the work cycle during execution of the program.(2)
- Continuous path robots have the same playback capability as the previous type .The difference between continuous path and point to point is the same in robotics as it is in CNC.A playback robot with continuous path control is capable of one or both of the following(1)Greater storage capacity. (2)Interpolation calculations



CNC process

EXPLANATION OF CNC

2) DIRECT NUMERICAL CONTROL

DNC may be defined as a system connecting a group of numerically control machines to a common computer memory for part program storage, distribution of machining data, provisions for collection, display or editing part programs, operator instructions or data related to the NC process are also available.

DNC concept is also employed as the heart of the control system of flexible manufacturing systems in which a no of NC machines tools are linked by means of electronic data communication and mechanical automation. Direct control that the PC is interfaced directly to the process and controls its operation in real time. Recent advances in both Pc technologies and available software have challenged this traditional thinking. Starting in the early 1990s, PC s has been installed at an accelerating pace for the direct control of industrial processes. Several factors can be identified that have enabled this trend.

- Wide spread familiarity with PCs
- Availability of high –performance PCs
- Trend toward open architecture philosophy(2)

VI. FEATURES OF DNC:

- Total elimination of punched tape: In DNC system the NC part programs are keyed in directly thus eliminating all the disadvantages of punched tape.
- Storing of the part programs: DNC software can also accomplish post processing functions to convert the program into a form compatible for given machine tool.
- Communications: A communication network is required between central computer and machine tool.
- Processing and reporting: After processing raw data system provides necessary information for the management to take appropriate decisions.

VII. ADVANTAGES OF DNC:

- Elimination of punched tape and tape readers.
- Flexibility in changing programs.
- Storage of NC part programs.
- Reporting of shop performance.
- Convenient editing and diagnostic features.

Flexible manufacturing system

- FMS has been developed to provide some of the economics of mass production to small batch manufacturing. It has brought about radical changes in manufacturing.
- FMS could be considered integration of two areas:
- Flexible manufacturing module (FMM) which can be lathe with a robot.
- Flexible manufacturing cell (FMC) which can be two or more machines tied together with robotic system to manufacture group of designated parts.
- Flexible manufacturing system include automation machine, loading and transfer Of in – process parts, from initial setup through all process steps.

VIII. ADVANCES IN FMS TECHNOLOGY

- Laser checking for part location.
- Special computerized tool setting station.
- Automated tool changers.
- Improved software.
- Work piece transport system

IX. ADVANTAGES OF CIM:

- CIM is more advantageous in design analysis, planning, cost accounting, inventory control.
- They are used for data storage and presentation.
- CIM is most useful where a high level of ICT is used in the company. The availability planning and its data.
- The CIM is implemented for structure, communication, calibration, data base etc.

X. DISADVANTAGES OF CIM ;

- For implementation of CIM strategies there should be alignment between business and manufacturing strategies.
- To be successful, manufacturing enterprises need to not only any have an excellent factory floor, it also needs complete marketing, company planning, and other support.

The issues that get considered under this perspective include the structure of specifications, how the tooling instruction is transmitted, the process of going from the specifications to purchase orders for the various components etc.

XI. DISADVANTAGES OF CIM ;

- For implementation of CIM strategies there should be alignment between business and manufacturing strategies.
- To be successful, manufacturing enterprises need to not only any have an excellent factory floor, it also needs complete marketing, company planning, and other support.

- The issues that get considered under this perspective include the structure of specifications, how the tooling instruction is transmitted, the process of going from the specifications to purchase orders for the various components etc.

CONCLUSION:

In this paper we have introduction an overall approach which will be increasing importance of the computer manufacturing community. The actions approach allows an integrated approach to including humans into computer integrated systems allowing more feasible and effective solutions which are more comprehensive as well as integrating more aspects of a manufacturing enterprise that was previously possible.

In this paper an attempt is made to through light on various CIM methods and technique, theirs applications, advantages and disadvantages. There is a great need to exploit the advantages of the CIM in the manufacturing industry especially in India.(1)

REFERENCES:

- 1) Yam, Peter, CIM –computer integrated man machine manufacturing systems, an introduction”.ICCIM’91 proceedings, Oct, 1991.
- 2) Automation production systems, and computer –integrated manufacturing second edition by mikell p.groover.
- 3) Implementation of computer –integrated manufacturing: a survey of integration and adaptability issues by A.gunasekaran.
- 4) National textile center annual report: September, 2994
- 5) Int.J.computer integrated manufacturing, 1977, vol-10.



Gesture Based Communication

A Gesture Humanoid

G S L K CHAND, G JAGADEESH & Ch SARVANA KUMAR

Department of Electronics And Communication Engineering, ST.MARY'S ENGINEERING COLLEGE,
Department of Master Of Computer Applications, KVR & MKR COLLEGE,
ANNS COLLEGE OF ENGINEERING AND TECHNOLOGY, GUNTUR, ANDHRA PRADESH, INDIA
E-mail : chandugudi@gmail.com, vagankasyapa@gmail.com & chsk85.genius@gmail.com

Abstract - Nowadays new interaction forms are not limited by Graphical User Interfaces (GUIs) making Human Computer Interaction (HCI) more natural. The development of humanoid robots for natural interaction is a challenging research topic. By using gesture based humanoid we can operate any system simply by gestures. The inter-human communication is very complex and offers a variety of interaction possibilities. Although speech is often seen as the primary channel of information, psychologists claim that 60% of the information is transferred non-verbally. Besides body pose, mimics and others gestures like pointing or hand waving are commonly used. In this paper the gesture detection and control system of the humanoid robot CHITTI is presented using a predefined dialog situation. The whole information flow from gesture detection till the reaction of the robot is presented in detail.

Keywords—*Hand gesture, computer vision, HCI, marking menu, UBI hand*

I. INTRODUCTION

Ubiquitous, embedded computing, e.g., in domestic environments requires new human-computer interaction styles that are natural, convenient and efficient. Keyboards and mice are still the most common and most used interfaces between humans and computer systems, no matter if it is just a desktop PC, a notebook or a robot. However there is an increasing interest in developing additional interfaces such as speech recognition, handwriting, gesture recognition and emotion detection, since these ways of interaction may bring more naturalness into the human-computer interface. In addition most people tend to feel more comfortable if they can interact with computers and robots in the same manner humans are communicating with each other. The interesting thing is that psychologists claim that over 60% of interaction signals are transferred non-verbal [5]. This is one of the motivations for the work presented in this paper. Our main goal is to establish a communication interface through gesture recognition between a human and the robot CHITTI, that stands for Robot Human Inter- action Machine. The robot must recognize some gestures made by a human and respond by speaking or making some body movements.

Traditionally there are some techniques for gesture recognition based on the shape of the hand or based on the movement of the human arm and hand. Also there is no tight definition for a gesture. Gestures can be viewed as a non-verbal interaction and may range from simple static signals defined by hand shapes, actions like pointing to some objects, waving a hand or more complex movements to express ideas or feelings allowing the communication among people [8].

Thus for recognizing gestures it is necessary to find a way by which computers can detect dynamic or static configurations of the human hand, arm, and even other parts of the human body. Some methods used mechanical devices to estimate hand positions and arm joint angles such as the glove-based approaches. The main drawback of this interface is that, besides being expensive, the user must wear an uncomfortable glove, having a lot of cables to connect the device to the system that restricts the workspace to a small area and limits the movements of the user. Therefore, one of the best options to overcome the disadvantages of the glove-based methods and to implement less restricted systems is the usage of computer vision to detect and track hands and arms.

Basically, the computer vision approaches concentrate on recognizing static hand shapes (pose gestures) or interpreting dynamic gestures and motion of the hands (temporal gestures). For the static gesture approaches the focus is to identify a gesture by the appearance of the hand, silhouettes, contours, 2D or 3D models, while the methods that consider dynamic gestures are concerned about motion analysis. There are also works like shown below that evaluates both pose gestures and temporal gestures.

Our approach, like many others, aims to support the interaction to a robot and control some movements. But besides that we intend to improve the interaction and communication with a robot, allowing the usage of gestures and dialogs. As an example of some related work, in hand shapes are used to control a walking robot through gestures that indicate commands as stop, go forward, etc. Their system has four modules: a hand detection using skin segmentation, hand tracking, a hand-shape recognizer based on contours and the robot controller. In an integration of gaze and gestures is used to instruct a robot in an assembling task. Basically, pointing hands are detected through skin color and splines for contour descriptions. In [13] an attention model for humanoid robots is defined using gestures and verbal cues. Human motion and gestures are captured using markers attached to the subject body.

In this work we focus on an appearance based method for recognizing gestures that will help improve the interaction with a robot allowing the usage of gestures and dialogs. Our approach also includes a hand tracking module, thus the user can make different sequences of gestures while the robot keeps looking at the user's hand, without having to process the entire image every time in order to detect a hand and then identify a gesture. Not only by hand but also nodding of head etc. The preliminary results are encouraging and for future work we expect to take the motion history into account for recognizing more complex and temporal gestures.

This paper is organized as follows. The first one presents the marking menus applied for detecting the hands of the user. The second one describes the pie and marking menus and the following section explains recognition algorithms. The integration into the control system of the robot is described while finally we presented the conclusions and future work. This also includes the :

A. Marking menus for gesture control

A fundamental concern in all kinds of gestural control is what the command set should be. Exactly what hand posture and movements should be used? A possible strategy is to base the command set on a menu system. The "language" is determined by menu layout and organization, and can be made culturally neutral and self-explanatory. Gestures can be kept relatively simple. The assumption here is that Pie- and marking menus are especially well suited for the purpose, because they offer a possibility for users to develop the skill to work with no feedback from the menus.

B. Pie- and Marking Menus

They are pop-up menus with the alternatives arranged radially, often used in pen-based interfaces. Because the gestures ("marks") are directional users can learn to make selections without looking at the menu items. With expert users, menus need not even be popped up. Hierarchic marking menus are a development of pie menus that allow more complex choices. The shape of the path, rather than the series of distinct menu choices, can be recognized as a selection. If the user, e.g., a novice, works slowly, or hesitates, the underlying menus can be popped up to provide feedback.

C. The Prototype

Following we chose a scenario for the first prototype that is well known to most: remote control of appliances in a domestic environment. A hierarchic menu system for controlling the functions of a TV, a CD player, a VCR, and a lamp is under development and some initial user trials have been performed. The prototype has been set up similar to a home environment in an open lab /demo space at CID.

In order to maximize speed and accuracy, gesture recognition is currently tuned to work only against a uniform background within a limited area, approximately 0.5 by 0.65 m in size, at a distance of approximately 3 m and under relatively fixed lighting conditions.

D. The Recognition Algorithms

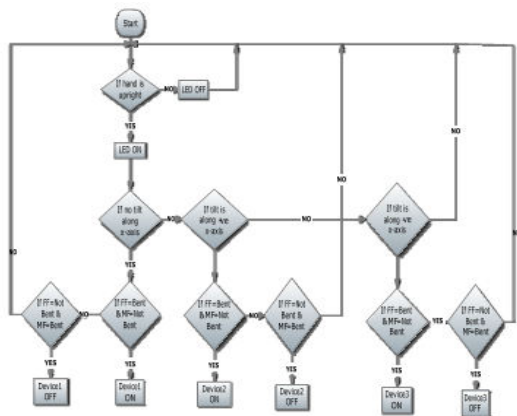
The computer vision system for tracking and recognizing the hand postures that control the menus is based on a combination of multi-scale color feature detection, view based hierarchical hand models and particle filtering. The hand postures or states are represented in terms of hierarchies of multi-scale color image features at different scales, with qualitative inter-relations in terms of scale, position and orientation. In each image, detection of multiscale color features is performed. The hand postures are then simultaneously detected and tracked using particle filtering, with an

extension of layered sampling referred to as hierarchical layered sampling. To improve the performance of the system, a prior on skin color is included in the particle filtering. white ellipses show detected multi-scale features in a complex scene and the correctly recognized hand posture is superimposed in gray.

II. UBI HAND

It is a wireless control of home appliances via hand gestures by using humanoid It works as given in below flow chart

III. FLOWCHART WORKING



A. INTEGRATION

The experiments of the presented approaches have been performed on the humanoid robot CHITTI. The robot consists of a humanoid upperbody and head with 24 degrees of freedom: 7 for the movement of the body and neck, 6 for eye movement and 11 for emotional expressions.

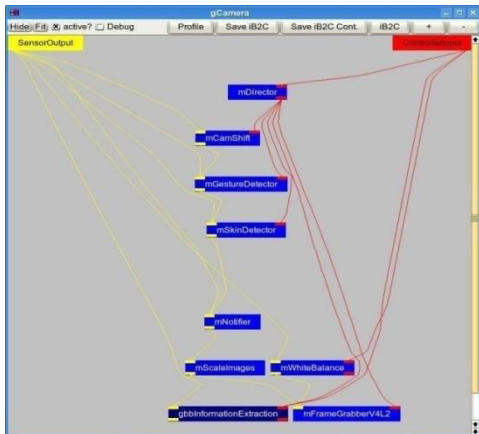


Fig. 2. Screenshot of the Camera group with GestureDetector and CamShift module. The

image shows the tool mcabrowser which can be used for run-time analysis of the control architecture.

	Open Hand	Closed Hand	Positive
Open Hand	0.917	0.00	0.00
Closed Hand	0.00	0.850	0.00
Positive	0.00	0.00	0.883
V	0.00	0.00	0.050
L	0.00	0.050	0.00

Figure 3 shows an interaction between the robot and a human during the experiments.

IV. CONCLUSION

Future work concerning the gesture based interaction will focus on the integration of verbal and non-verbal interaction signals into multimodal dialog situations.

V. ACKNOWLEDGEMENT

We thank mainly our parents who supported not only by financially but also technically. My sincere thanks to my sister who helped me a lot in this project

REFERENCES

- 1). Bretzner, L., Laptev, I. & Lindeberg, T. (2002) Hand Gesture Recognition using Multi-Scale Colour Features, Hierarchical Models and Particle Filtering. Submitted to 5th Intl. Conf. on Automatic Face and Gesture Recognition.
- 2). Callahan, J., Hopkins, D, Weiser, M. & Shneiderman, B. (1988) An Empirical Comparision of Pie vs. Linear Menus. Proceedings of CHI'88, pp. 95-100.
- 3). Freeman, W.T. & Weissman, C.D. (1994) Television Control by Hand Gestures. In 1st Intl. Conf. on Automatic Face and Gesture Recognition.
- 4). Guimbretière, F. & Winograd, T. (2000) FlowMenu: combining Command, Text and Data Entry. Proceedings of UIST'2000, pp. 213-216.
- 5). Kurtenbach, G. & Buxton, W. The Limits of Expert Performance Using Hierarchic Marking Menus. Proceedings of CHI'94, pp. 482-487.

- 6). Jacob Fraden, "Handbook of Modern Sensors: Physics, Designs, and Applications", Springer publications 2010 edition
7. K. Mianowski, N. Schmitz, and K. Berns. Mechatronics of the humanoid robotroman. In Sixth International Workshop on Robot Motion and Control (RoMoCo), Bukowy Dworek, Poland, June 11-13 2007.
8. V. I. Pavlovic, R. Sharma, and T. S. Huang. Visual interpretation of hand gestures for human-computer interaction: A review. In IEEE Transactions on Pattern Analysis and Machine Intelligence, volume 19, pages 677–695, 1997.
9. F. Quek. Gesture, speech and gaze cues for discourse segmentation. In IEEEConference on Computer Vision and Pattern Recognition, pages 247–254, 2000.
10. D. J. Sturman and D. Zeltzer. A survey of glove-based input. In IEEE Computer Graphics and Applications, volume 14, pages 30–39, 1994.
11. S. Waldherr, S. Thrun, and R. Romero. A gesture-based interface for human-robot interaction. In Autonomous Robots, volume 9, pages 151–173, 2000.



Micro Robots For Minimally Invasive Surgery

– A Review

Deiva Ganesh. A¹ & Thangavel. M²

Engineering Design, Sona College of Technology, Salem-636 005, TamilNadu, India.
Department of Mechanical Engineering, Sona College of Technology, Salem-636 005, TamilNadu, India.
Email: amdganesh@yahoo.co.in

Abstract - Micro robots for medical applications need to be compatible with human body, remotely controllable, smooth in movement, less painful to the patients and capable of performing the designated functions. In this paper, state of the art in the design, fabrication and control of micro robots are presented. First the benefits of micro robots in medical applications are listed out. Second, the predominantly used micro robot designs are discussed. Third, the various fabrication process used in micro robot construction are presented. Fourth, the different approaches used for its operation and control are narrated. Finally, the current trend in micro robot technology is summarized and the plan for future work is spelt out. .

I. INTRODUCTION

Worldwide research on micro robots has shown much progress and developments in the ongoing efforts to decrease damage to human body during an operation and to reduce operation time.

Since the 1980's, medicine has seen a dramatic shift towards the use of minimally invasive procedures because of the many advantages this technology presents. Especially, micro robots that can move along blood vessels and treat specific parts of body have received much attention. The ultimate objective of the micro robot is to approach its destination accurately and quickly.

Minimally invasive procedures are linked with a variety of patient-oriented benefits ranging from reduction of recovery time, medical complications, infection risks, and postoperative pain to increased quality of care, including preventative care. The following areas are the important applications [4]:

- The circulatory system
- The central nervous system
- The urinary system and the prostate
- The eye
- The ear
- The fetus

Bradley and Nelson describe [1] that the Operations performed by micro robots will potentially entail several different steps: a) processing previously acquired

medical data (primarily images), simulation and planning of interventions; b) computer design of the optimal configuration of the micro robot customized for the specific patient anatomy and for the planned therapy at the target site; c) delivery of devices within the body to the desired site; d) extremely precise execution of the intervention; e) disassembly, recovery or biodegradation of the devices. The literature related to these issues will be discussed in this paper.

The paper is organized as follows. Section one gives an introduction to the review on the micro robots for minimally invasive surgery. In section two, various micro robot designs are discussed. In the third section, micro robot fabrication techniques are studied. Section four and five give the study of actuators, control of the micro robot respectively. In the next section current technology is discussed. Final section summarizes the review and outlines the plan for future developments.

II. MICRO ROBOT DESIGNS

Micro-robots for medical use can be categorized into two main groups, those that are designed for swimming and those that crawl, gripping the inner pipe walls. The first group might suit medical applications where almost no flow is applied on the robot, while crawling micro-robots may theoretically withstand even massive bloodstream flow present in the human blood vessels [30].

Bradley and Nelson [1] focus on the challenging design issues present themselves when envisioning a medical micro robot for in-vivo applications. Devices

must be small, reliable and biocompatible. They must carry the necessary tools and subsystems on-board. They must be inserted into, steered inside and removed from the target area of the patient’s body in a “minimally-invasive” way. It is difficult to resolve all these issues at once, also because much depends on the particular application.

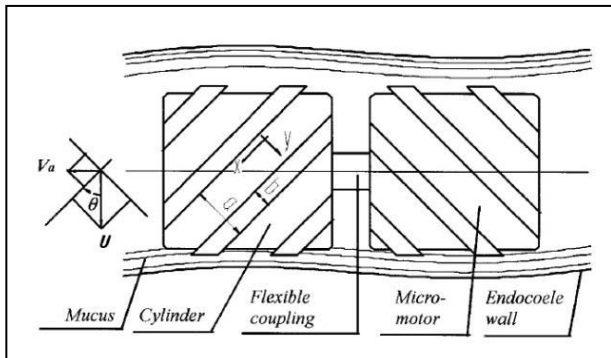


Fig.1 Schematic diagram of medical micro robot by Zhou and Quanl [2, 26]

A schematic diagram of the medical micro robot is shown in Fig.1. Zhou and Quanl [2],[26] designed a medical micro robot consists of a right spirally grooved micro motor, a left spirally grooved cylinder and a flexible coupling. The coupling links the shaft of the micro motor and the cylinder. When the power supply is switched on positively, the cylinder rotates in a clockwise direction and the shell of the micro motor rotates in an anticlockwise direction. The direction of the generated axial thrust force of the spirally grooved cylinder is the same as that of the spirally grooved micro motor and therefore the micro robot moves forward. When the power supply is switched on negatively, the micro robot moves backward.



Fig.2 An autonomous crawling Micro- robot

The new robot consists of a central torso from which tiny arms stretch out, allowing the robot to strongly grip the vessel walls [30]. The operator can manipulate the robot to move in increments, and its unique structure allows it to crawl within a variety of vessels with differing diameters. As indicated, different human

body's cavities differ from each other in diameter, making it extremely important for the robot to be able to adjust accordingly. The robot has been fabricated using MEMS technology and as depicted, having a diameter of 1[mm] and can be further reduced. Miniaturization is made possible since actuation and control are not onboard. Furthermore, the robot advances regardless of the magnetic field actuation direction, which dismisses the need for exact localization and direction retrieval. The small cross sectional area of the robot allows fluids to flow with minimal interference, thus in vascular motion can be made feasible.

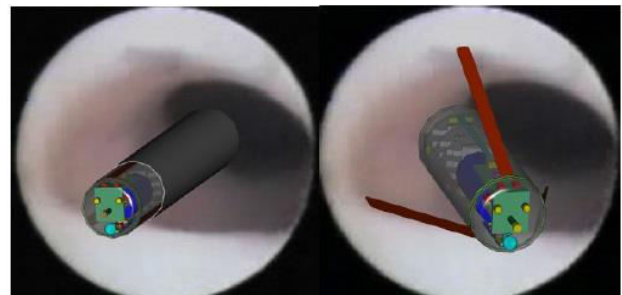
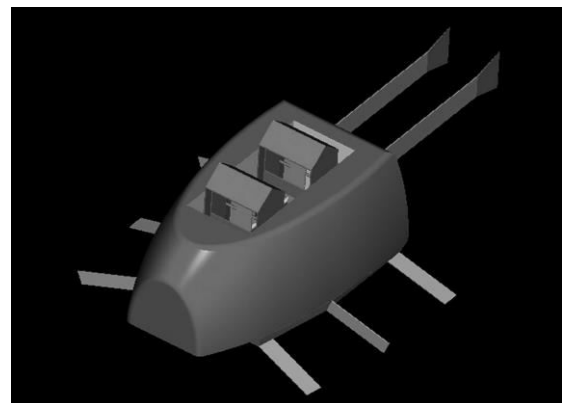


Fig.3 Illustration of the Swimming micro robot by Kosa and Jakab [3]

One of the applications of a flagellar swimmer is interventions in the ventricular system in the brain. Kosa and Jakab [3] presented a swimming micro robot. Fig. 3 illustrates the introduction of the swimming robot into the ventricular space. The critical components in the robot are the following:

- Three flagellar swimming tails that pop out of the robot's body after introduction into the ventricle. The propulsion enables swimming in 5 degrees of freedom.
- Power source made of batteries or magnetic coils for RF induction.
- Custom designed IC for command, control and communication.



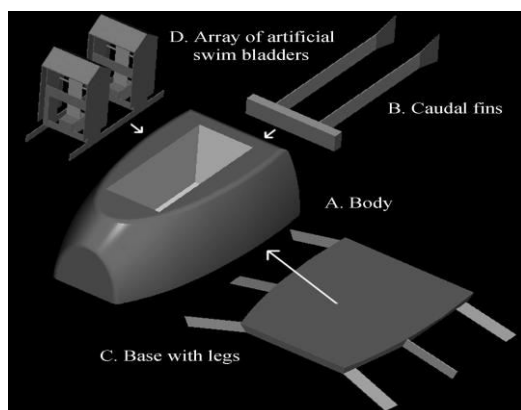


Fig.4 Fish-like micro robot by Zhang and Xiang [9]

Zhang and Xiang [9] designed a new type of hybrid fish like micro robot. It consists of a body, a pair of caudal fins, a base with legs, and an array of artificial swim bladders, as shown in Fig.4. The caudal fins generate the propulsion for swimming motion. The legs are used for walking. And the artificial swim bladders are the floatage adjuster.

III. MICRO ROBOT FABRICATION

One enabling technology for medical micro robots is Micro-Electro-Mechanical-Systems (MEMS), now a commercial technology with various sub-fields and a large variety of application areas. Usually, it is a combination of their low cost, low power consumption and small size that makes a MEMS based design the better choice compared to conventional technology. But MEMS can also be an enabling technology, opening new frontiers to science one of which is the topic of this paper, the use of untethered micro robots for biomedical applications in the human body.

Micro-electro-mechanical systems (MEMS) is a technology of miniaturization that has been largely adopted from the integrated circuit (IC) industry and applied to the miniaturization of all systems (i.e., not only electrical systems but also mechanical, optical, fluidic, magnetic, etc). Behkam and Sitti [7] presented that Miniaturization is accomplished with micro fabrication processes, such as micromachining, that typically use lithography, although other non-lithographic precision micro fabrication techniques exist (FIB, EDM, laser machining). Kovacs [24] and Madou [25] provide a comprehensive discussion of micro machining processes and MEMS devices.

Bradley and Nelson have described another design challenge for a sub-mm sized micro robot. It is the high degree of integration that is needed. Most MEMS devices are designed to be components that are inserted

into larger sized electro-mechanical systems. Even the system-on-a-chip type devices with integrated mechanical and electronic components need to be physically interfaced for power supply and data I/O. In contrast, the sub-mm sized medical micro robot must be micro-manufactured to its final form. Yesin and Nelson [26] have presented the emerging technology of Hybrid MEMS, where individual MEMS components are combined through a robotic micro assembly process, promises a solution. In a Hybrid MEMS design, different and incompatible manufacturing technologies (e.g. Lithography, LIGA, MOEMS, Nano systems) can be used together.

IV. ACTUATORS

In the micro robot fields, smart materials (like ionic conducting polymer film (ICPF), piezo- electric elements, pneumatic actuator, and shape memory alloy) provide the way for a great variety of micro robot design. Zhang and Xiang [9] describe, In the last decade, ICPF actuators have been widely researched. An ICPF actuator consists of a perfluoro- sulfonic acid membrane with chemically plated gold as electrodes on both sides. It bends by applying a low voltage between the electrodes. The actuator is soft and works in water or a wet environment. The ICPF actuator has several advantages. It bends with low voltage (above 1 V). It bends silently, responds quickly and consumes little energy. Its density is near to water. The electromagnetic field of the ICPF actuator is practically undetectable. However, as an emerging technology, ICPF has some disadvantages, such as weak propulsion and lack of long-term stability. ICPF actuators are used as artificial muscles to drive robots. Because of its fast response, the ICPF actuator is widely used in swimming micro robots as oscillating or undulation fins. ICPF actuators are also used for biped walking underwater robot. A kind of ICPF micro leg with 2-DOF has been developed. Kim, Ryu, and Jeong [28, 29] have developed a ciliary motion based 8-legged walking micro robot.

V. CONTROL OF MICRO ROBOT

The important and challenging part of this technology is control of the micro robots. Magnetic actuation is the widely used method of controlling the medical robots. It should be noted that the low frequency magnetic field does not have any medical implications.

A. Wireless Actuation

Magnetic actuation technology has been applied in biological systems for many years when wireless actuation is needed. Nagy and Ergeneman [31] focus on the micro robots for wireless magnetic control. A

common application area is targeted drug delivery where magnetized carrier particles that are coated with various chemical agents are concentrated on specific target regions of the body using external magnetic fields. A similar idea is used in magnetic cell separation where magnetized particles that are selectively attached to a targeted group of cells through their chemical composition are used to sort apart the cells. Amblard and Yurke [15] presented the study on Magnetic manipulators. Individual magnetic beads of a few microns diameter have also been steered inside cells for the study of their mechanical properties as well as for the manipulation of individual DNA molecules. Vikomerson and Lyons [32] presented another area with similar requirements on field control is magnetically assisted stereo taxis to guide catheters inside the brain. There is a disadvantage in terms of the necessary external magnetic field strengths as the robot's size goes smaller.

An important issue related to the control of a magnetic micro robot is the nonlinear nature of the field and field gradients that are created by electromagnet coils or by permanent magnets. For example Bradley and Nelson [1] present the Helmholtz coil configuration consists of two identical coils that are placed on the same axis and separated by a distance equal to the radius of the coils. This arrangement generates a uniform field close to the centre of the coil pair when current passes in the same direction in both coils.

A similar configuration called the Maxwell coil can generate a uniform gradient near the centre. Fig.5 shows superimposed magnetic field generated by concentric Helmholtz and Maxwell coils. This configuration enables independent control of magnetic force (thrust) and torque (orientation) on the micro robot. Both of these coil types are commonly used in MRI systems. The magnetic steering principle was demonstrated using a small scale system.

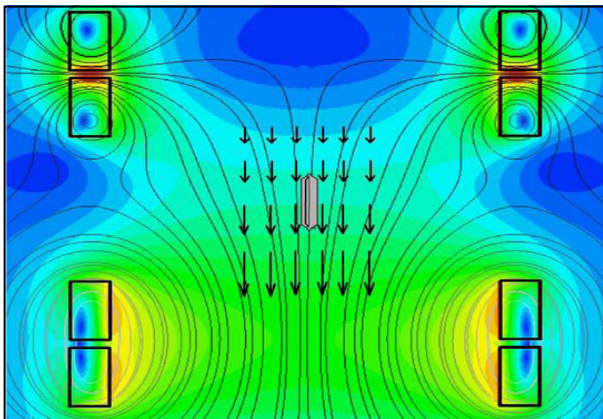


Fig.5 Superimposed magnetic field generated by Maxwell and Helmholtz coils.

The micro robot was put inside a plastic, maze-like structure with 1000 μm wide, water-filled channels.

The maze was inserted at the centre of a pair of concentric Maxwell and Helmholtz coils that were actuated to rotate around the maze. The current through the coils were regulated to control the force and torque (i.e. the forward thrust and orientation) on the robot independently. Numerous trials with the system confirmed that the independent orientation/thrust control principle was successful. Recent efforts are towards applying this principle in a larger scale in combination with on-board magnetic actuators.

B. Piezoelectric Effect

Savvas and Loizou [13] focus on the piezoelectrically driven micro robots. The piezoelectric effect is a phenomenon observable in many crystalline and ceramic materials. When pressure, and therefore strain, is applied to the crystal, a voltage is generated. The deformation of the crystal lattice causes the dipoles, usually randomly distributed through the crystal, to align, creating a charge difference between one side of the material and the other. Piezoelectric materials are often used in micro scale robots. They offer many advantages for small scale applications. Piezoelectric materials can be made in a variety of shapes and sizes, increasing their range of applications. They are also very efficient at converting electrical potential into pressure. They are now without their downsides. For one thing, piezoelectric materials offer only linear motion, they do not rotate. They also only create very small deformations, meaning that a mechanical amplifier is necessary when large displacements are needed. Piezoelectric materials require large voltages to operate, which requires additional volume and weight for electronics.

Another method of controlling micro-nano robots is remote powering. But it is not used in biomedical robotics field. The main limitation is battery technology is not advanced enough to optimize the energy vs. weight ratio at such small scales.

Tendick and ShankarSastry [35] have reviewed the problems in control of the micro robots. Especially, safety is a critical issue in surgical systems. Davies [50] presented many of the factors

that should be considered to minimize risk to the patient (or the surgeon) and gives guidelines for the design of safe systems. System design practices include redundant sensors, hardware and software checks, and a simple user interface. As much as possible, the system should be designed to have passive constraints or limits that cannot be defeated by the failure of active components or software. These include kinematic constraints to restrict motion to a safe region and actuator force capabilities that do not exceed task requirements.

VI. MICRO ROBOT TECHNOLOGY

Perrard and Nicolas [11] presented that the control of a team of micro-robots that operates inside a human body deals with a kind of smart medicine that only acts where and when it is needed. This is done under the acknowledgement of the physician itself, who supervises and allows the different steps of the processing of a particular kind of mission. Today, such micro-robots do not exist. Energy batteries, communication modules, among others, are not ready and the main controller itself is not reality (only coordinated programs exist into the simulator). However, in order to avoid most technical problems, the design of such micro-robots is chosen as simple as possible. In the same way, the embedded controller of each micro-robot must be very simple, in order to use micro-electronic batch processes. In this situation, micro-electronic will not be the only investigated way. Maybe, biological substrates will be useful.

For any robot, whether operating on the surface or subsurface, the power needed for operation becomes a problem. Micro-robots optimally function with little or no battery weight. So the use of remote powering is of interest.

Currently for robotic surgical systems, areas of research include using miniaturized motors to decrease the size of the robotic tower, evaluating the potential for mounting the robotic tower to the ceiling or wall to increase access points to the patient, and real-time or non-real-time image integration into the endoscopic view. Biomedical micro-robotics is one of the next major challenges in the field of robotics. It combines the established theory and techniques of robotics (e.g. motion control, path planning, remote operation or sensor

fusion) with the exciting new tools enabled by MEMS technology in order to significantly improve the quality of our lives. International robotics research efforts are already shifting towards this direction. Micro robots can serve as a near-term goal for wireless biomedical applications, and their design will be based on the task they need to accomplish and the type of environment in which they will operate. Bradley and Nelson [4] have described, initially micro robots will perform simple tasks; as technology advances, we will be able to design and fabricate more complicated devices that perform sophisticated tasks such as targeted drug delivery etc.

Researches are going on to design new medical micro robots and giving better control and actuating methods for those robots.

VII. CONCLUSION

In this paper, the review of the design, fabrication and control of the micro robots and current micro robot technology have been presented. Most of those existing devices are operated by giving external power sources. The next step in the evolution of medical procedures will be from minimally invasive approaches towards extremely targeted, localized and high precision endoluminal techniques performed by micro robots. Developing this technology requires that we address issues such as localization and power. Effective collaboration between medical and robotics experts is needed and presently we are working on the development of remotely controllable self power micro robot.

REFERENCES

- [1] Bradley J., Nelson ETH Zurich, "Microrobotics in Medicine" Institute of Robotics and Intelligent Systems Zurich, Switzerland, Review of Biomedical Engineering, 2008.
- [2] Y S Zhou^{1*}, Y X Quan¹, K Yoshinaka² and K Ikeuchi² "A new medical microrobot for minimal invasive surgery" Proc. Instn Mech engrs Journal of Engineering in Medicine, vol.215, pp. 215-220, 2001.
- [3] Kósa G, Jakab P, Nobuhiko Hata, József F, Zipi Neubach Z, Shoham M, "Flagellar Swimming for Medical Micro Robots: Theory, Experiments and Application" In: 2nd IEEE international

- conference on biomedical robotics, p. 258-263, 2007.
- [4] Bradley J. Nelson, Ioannis K. Kaliakatsos, and Jake J. Abbott² “Micro robots for Minimally Invasive Medicine”. The annual review of Biomedical engineering, pp.55-85, 2010.
- [5] Taheri A, Meysam, Moosavy S, “A Numerical Strategy to Design Maneuverable Micro-Biomedical Swimming Robots Based on Bio mimetic Flagellar Propulsion”, World Academy of science and technology, Vol .54, pp.500-504, 2009.
- [6] Dumsong E, Afzulpurkar N, Tuantranont A and Punyasai C, “Design and Simulation of Wireless, Walking Scratch- Drive Micro-Robot”, 10th Intl. Conf. On Control, Automation, Robotics and Vision, p.588-592, 17-20 Dec, 2008.
- [7] B. Behkam, M. Sitti, “Design Methodology for biomimetic propulsion of miniature Swimming Robots,” J. Dynamic Systems Measurement and Control, Vol. 128, pp.136-43, 2006.
- [8] J. B. Moidel, J.D. Ozer, O. Kuter-Arnebeck “Water Actuation of Micro Robotics”, Journal of Micro/ Nano Robotics, pp.43-48, 2006.
- [9] Wei Zhang_ Shu-Xiang Guo “A New Type of Hybrid Fish-like Micro-robot”, Intl. Journal of Automation and computing, Vol.4, pp.358-365, 2006.
- [10] S. Guo, Y. Hasegaw, T. Fukuda, and K. Asaka, “Fish –Like underwater microrobot with multi DOF,” Proc. of 200 International Symposium on Micromechatronics and uman Science, pp. 63-68, 2001.
- [11] Christophe Perrard, Nicolas Andreff “Control of a team of micro-robots for non-invasive medical applications”, Proc. 6th National conf. On control Architecture of robots, CAR’11, July 2011.
- [12] Huaming Li and Jindong Tan Mingjun Zhang “Dynamics Modeling and Analysis of a Swimming Microrobot for Controlled Drug Delivery”. Proc. IEEE International conference on Robotics and Automation, pp.1768-1773, 2006.
- [13] Savvas G. Loizou, Kostas J. Kyriakopoulos, “Motion Planning of Piezoelectrically Driven Micro-Robots via Navigation Functions” Springer, 1997.
- [14] Dario, P., Guglielmelli, E., Allotta, B. and Carrozza, M. C. “Robotics for medical applications”. IEEE Robotics AutomnMag., Vol.3, pp.44-56, 1996.
- [15] F. Amblard, B.Yurke, A. Pargellis, S. Leibler, “A Magnetic Manipulator for Studying Local Rheology and Micromechanical Properties of Biological Systems”. Review of scientific instruments, vol.67, pp.818-827,2000.
- [16] P. Dario, M.C. Carrozza, L. Lencioni, B. Magnani, C. Filippeschi, M.G. Trivella, A. Pietrabissa, “A Microrobot System for Lower Gastrointestinal Inspection and Intervention”. Sensors and Microsystems, pp.14-21, Singapore, 1996.
- [17] Peter J. Berkelman, Louis L. Whitcomb, Russell H. Taylor, and Patrick Jensen “A Miniature Microsurgical Instrument Tip Force Sensor for Enhanced Force Feedback During Robot-Assisted Manipulation”. Proc. IEEE Transactions on Robotics and Automation, Vol.19, no. 5, pp.917-922, Oct, 2003.
- [18] Yuan Zheng, George Bekey, Arthur Sanderson “Robotics for biological and medical applications”, Intl. Journal of Emerging Medical Technologies, Jan27, 2006.
- [19] Guo S, Pan Q. Mechanism and control of a novel type microrobot for biomedical application. In: IEEE international conference on robotics and automation; p. 187–92, 2007.
- [20] Hülsen H, Trüper T, Fatikow S, “Control System for the automatic Handling of biological Cells with mobile Micro robots”, Proc. American Control Conference, pp.3986-3991, July 2, 2004.
- [21] ArthurW. Mahoney John C. Sarrazinb, Eberhard Bamberg b and Jake J. Abbott “Velocity Control with Gravity Compensation for Magnetic Helical Microswimmers”, In: Advanced Robotics, no.25, pp.1007-1028, 2011.
- [22] Joo Han Kim*, Se Hyun Rhyu, In Soung Jung, Jung Moo Seo “An investigation on development of Precision actuator for small robot”, Proc. 9th WSEAS Intl.Conf. on Robotics, Control and Manufacturing technology, pp. 62-66,2008.
- [23] Joseph JV, Arya M, Patel HRH, “Robotic surgery: the coming of a new era in surgical innovation”, Expert Rev. Anticancer Ther. 5(1):7–9, 2005.
- [24] G. T. A. Kovacs, “Micromachined Transducers Sourcebook”. WCB/McGaw-Hill, ISBN, 0-07-290722-3, 1998.

- [25] M. Madou, "Fundamentals of Microfabrication". Boca Raton, FL: CRC Press, Inc., ISBN, 0-893-9451-1, 1997.
- [26] K.B. Yesin, B.J. Nelson, "Robust CAD Model Based Visual Tracking for 3D Microassembly Using Image Space Potentials". Proc. IEEE International conference on Robotics and automation, pp.1868-1873, 2004.
- [27] Carrozza MC, Dario P, Jay LPS. Micromechatronics in surgery. Trans. Inst. Meas. Control 25(4):309–27, 2003.
- [28] B. Kim, J. Ryu, Y. Jeong, Y. Tak, B. Kim, J. Park. "A Ciliary Motion Based 8-legged Walking Micro Robot Using Cast IPMC Actuators", In Proceedings of 2002 International Symposium on Micromechatronics and Human Science, Japan, pp.85-91, 2003.
- [29] B. Kim, J. Ryu, Y. Jeong, Y. Tak, B. Kim, J. Park. A Ciliary Based 8-legged Walking Micro Robot Using Cast IPMC Actuators", In Proceedings of IEEE Intl. Conf. On Robotics and Automation, Taipei, vol. 3, pp.2940-2945, Sep.2003.
- [30] ViRob- "An Autonomous Crawling Micro-robot". The Technion, Technology institute, Israel, May, 2008.
- [31] Nagy Z, Ergeneman O, Abbott JJ, Hutter M, Hirt AM, Nelson BJ. "Modeling assembled-MEMS microrobots for wireless magnetic control", Proc. IEEE Int. Conf. Robot. Autom., Pasadena, Calif., May 19–23, pp. 874–79, 2008.
- [32] Vilkomerson D, Lyons D. 1997. "A system for ultrasonic beacon-guidance of catheters and other minimally invasive (in the original title, they write "minimally-invasive") medical devices", IEEE Trans. Ultrason. Ferroelectr. Freq. Control 44(2):496–504.
- [33] B. Behkam and M. Sitti. "Modeling and Testing of a Biomimetic Flagellar Propulsion Method for Microscale Biomedical Swimming Robots", ASME J. Dyn. Syst. Meas. Control, 2006.
- [34] Guo S, Pan Q, Li D. "Mechanism and control of a spiral type of microrobot in pipe. In: IEEE conference on robotics and biomimetics", p.43-48, 2008.
- [35] Frank Tendick, S. Shankar Sastry, Ronald S. Fearing and Michael Cohn, "Applications of Micromechatronics in Minimally Invasive Surgery" Proc. IEEE/ASME transactions on mechatronics, vol. 3, no. 1, p. 34-42, March 1998.
- [36] Guo S, Sawamoto J, Pan Q. "A novel type of microrobot for biomedical application". In: International robots and systems, p. 1047-1052, 2005.
- [37] Abbott JJ, Nagy Z, Beyeler F, Nelson BJ. "Robotics in the small-part I: micro robotics". IEEE Rob Autom Mag 2007, 14: p. 92-103.
- [38] Honda T, Arai KI, Ishiyama K. "Micro swimming mechanisms propelled by external magnetic fields", IEEE Trans. Magn. 32(5):5085–87, 1996.
- [39] Dogangil G, Ergeneman O, Abbott JJ, Pan'e S, Hall H, 2008. "Toward targeted retinal drug delivery with wireless magnetic microrobots", Proc. IEEE/RSJ Int. Conf. Intell. Robots Syst., Nice, Fr., Sept. 22–26, pp. 1921–26, 2008.
- [40] T. Fukuda, A. Kawamoto, F. Arai, and H. Matsuura, "Mechanism and swimming experiment of micro mobile robot in water," Proc. of IEEE Int'l Workshop on Micro Electro Mechanical Systems (MEMS'94), pp.273-278.
- [41] J. Edd, S. Payen, B. Rubinsky; M.L. Stoller and M. Sitti, "Biomimetic propulsion for a swimming surgical micro-robot," IEEE/RSJ Intelligent Robotics and Systems Conference, vol. 3, pp. 2583 – 2588, October 2003.
- [42] S. Guo, Y., Okuda and, K. Asaka, "Hybrid type of underwater micro biped robot with walking and swimming motions" In Proceedings of IEEE Intl. Conf. On Mechatronics and Automation, Ontario, Canada, pp.81-86, 2005.
- [43] K.B. Yesin, K. Vollmers, and B.J. Nelson, "Modeling and control of untethered biomicrobots in a fluidic environment using electromagnetic fields," Int'l J.Robotics research, vol.25, no.5-6, pp.527-536, 2006.
- [44] C. Haber, D. Wirtz, "Magnetic Tweezers for DNA Micromanipulation", Review of Scientific Instruments, vol.7, no.12, pp.4561-4570, 2000.
- [45] Ritter, E. G. Quate, and G. T. Gillies, "Nonlinear magnetic stereotaxis: Three-dimensional, in vivoremote magnetic manipulation of a small object in canine brain". Medical physics, vol.17, no.3 pp.405-415,1990.
- [46] Haga Y, Esashi M. "Biomedical microsystems for minimally invasive diagnosis and treatment", Proc. IEEE 92(1):98–114, 2004.

- [47] Y. Zhang, Q. Wang, P. Zhang, X. Wang, and T. Mei, "Dynamic analysis and experiment of a 3mm swimming microrobot," Proc. of the 2004 IEEE/RSJ International Conference on Intelligent Robots and Systems, pp. 1746-1750, 2004.
- [48] Byun D, JonghoChoi, Kyoungae Cha "Swimming micro robot actuated by two pairs of Helmholtz coils system", Journal of Mechatronics, pp. 357-364, 2011.
- [49] ZHOU Yinsheng¹, HE Huinong¹, GU Daqiang¹, AN Qi² & QUAN Yongxin¹ "Noninvasive method to drive medical micro-robots" Chin. Sci. Bull., vol.45, pp.617-620, 2000.
- [50] B. L. Davies, "A discussion of safety issues for medical robots," in Computer-Integrated Surgery: Technology and Clinical Applications, R. H. Taylor, S. Lavallee, G. C. Burdea, and R. Mosges, Eds. Cambridge, MA: MIT Press, 1996, pp. 287–298.
- [51] Bahareh Behkam, Metin Sitti "Coli Inspired Propulsion For Swimming Micro robots", Carnegie Mellon University, Proc. International Mechanical Engg. Conference and R&D Exposition, Nov 13-19, 2004.
- [52] G. Kósa, M. Shoham and M. Zaaroor., "Propulsion Method for Swimming Micro Robots", IEEE Transaction on Robotics, vol. 23, pp. 137-150, Jan. 2007.



Mechanical Design of Omni-Directional Robot Suitable for Swarm Based Application

M. Thangavel & T. Vinny Daniel David

Dept. of Mechanical Engineering, Sona College of Technology, Salem-636005, TamilNadu, India
E-mail : drmthangavel@gmail.com, vinnydanieldavid@gmail.com

Abstract - In this paper, a robot design suitable for swarm based application is presented. Initially, the literatures related to legged robot design are reviewed and the behaviors of swarm of ants under extreme situations are studied. Based on the study, the functional requirements of a swarm robot entity are identified. Initially, a robot design with multidirectional capability is evolved. The various locomotion parameters namely obstacle crossing ability, slip during locomotion, and drive torque required are determined. Then, the robot design is further improved to realize Omni-directional capability. Since the wheel constitutes an important component of the robot, mechanical designs of the wheel with curved leg geometry is carried out. Finally, a physical model of the Omni-directional robot is constructed and its obstacle crossing ability is demonstrated.

Key words - *Omni-directional Robot, Swarm Robot, wheel design, obstacle crossing ability.*

I. INTRODUCTION

Swarm robots are most suitable for defense and space applications as they possess redundancy, scalability (failure tolerant) and can function under decentralized control. Presently group of humans are employed to perform variety tasks namely providing security to a country, to important localities, for surveying a territory, carrying out agricultural activities etc. For the above tasks a swarm of robots can also be employed. However, to employ robots for swarm applications, they need to possess simple control architecture and configuration design and at the same time able to realize the objective by a collective behavior through effective communication and adapting to the situation at hand. It demands the need for the design of a simple yet Omni-directional robot with multi-robot co-ordination and swarm intelligence. The following describes the literature related to swarm robots and mobile robot design.

Globus et al. [1] elaborates on the usefulness of modular robots for space exploration and especially for lunar operations. They proposed the use of evolutionary approaches for generating appropriate solution for varying types of problems. Major design control and environmental challenges (dust) to be tackled are also spelt out. Khursid and Bing-rong [2] discusses the usefulness of robots in demining, surveillance, logistics and rescue operations. They focus on issues of the requirements of robots for use in war and peace. Higgins et al. [3] presents the various security challenges for swarm robots namely resource constraints, physical capture and tampering, lack of hierarchical control,

jamming of communication between robots by the attacker, lacking in mobility, difficulty in identifying the own group from the hostile one, intrusion by opponent group of robots etc. they also discuss the application of swarm robots in military, monitoring environmental pollutants, disaster relief, and healthcare. Grob and Dorigo [4] focus on the hardware and control that enable a group of 16 robots called swarm-bot to realize self accessibility. They provide the hardware details like the various sensors, number of DOF of s-bot, and the algorithm to enable accessibility between robots. Trianni et al. [5] presents an evolutionary based approach for realizing hole avoidance by a swarm of robots through collaboration (physical connection between robots). They use appropriate fitness function for identifying the nearest suitable robot to get connected. Rovetta and Paul [6] present design methodologies for a swarm of autonomous space robots suitable for planetary mapping and rover guidance. Weisbin et al. [7] reviews the literature related to rover construction using wheels, legs, tracks and the associated control systems. Hettiarachchi and Spears [8] presents an energy based method for evaluating obstacle avoidance capability of swarm of robots. Michud [9] built a mobile robotic platform that combines wheels, legs, and tracks to move in three dimensional environments. Vijay Kumar et al. [10] presents the design and control of wheel-legged robot satisfying the requirements on weight, stability, and obstacle crossing ability. It consists of body frame, three wheels driven by dc motors, four legs powered by eight servo motors. Buehler et al. [11] presents the design and development of a six-legged robot with one actuated DOF per leg. Quinn et al. [12-15] initially

developed wheg-1 robot without body flexion which is capable of moving over various terrains and climbing over obstacles similar to a cockroach. The design constitutes three evenly spaced spokes with torsion compliance in the axle which permits the vehicle's gait to passively adapt to irregular terrain. The robot design is further improved by including body flexion which enhanced its performance. Further, Quinn and co-workers presented an autonomous vehicle that has the capability of moving in land and seashore also has been developed. It uses tripod gait for land locomotion and specially designed front and rear whogs for swimming. Turning is realized by two servo motors, situated one at the front and the other at rear. Davies and Hirose [16] developed a belt-driven mechanism with a long leg-stroke along with a mechanism to control the orientation of the passive wheels for stair-climbing applications. Takahashi et al. [17] developed a 4-leg-wheel hybrid locomotion. Leg load distribution is realized by a twisting joint at the centre of the body, and a forward/and backward shift of the body. Experiments are done to validate the design and control. Eich et al. [18] arrived at an optimal structure of the quadruped robot by minimizing the sum of joint torques. Minimization of the joint torque results in a reduced joint acceleration during walking and reduction in energy consumption. Tzvi et al. [19] presents the design and analysis of a hybrid mobile robot consisting of a mobile manipulator and a gripper. The whole system moves using a tracked wheel. Its capability to move over uneven terrain is demonstrated. Wang and Li [20] derived the inverse kinematics model of a mobile robot and its usefulness in steering under different mode are demonstrated. Ceccaralli et al. [21-22] designed a four bar mechanism to be used in a stair climbing robot over which a wheel can be attached for its motion. Also presents the design of a tripod walking robot that uses single DOF for each leg. Feasibility of the design is validated by MATLAB simulation. Chugo et al. [23] presents the mechanical design of a new step-climbing vehicle that uses passive linkages. Thangavel and Vinny [24] presented the conceptual and mechanical design of wheeled-leg robot and the effect of passive compliance on actuator reduction. From the literature it is clear that most of the mobile robots found in the literature are having more number of legs and hence need more number of actuators and their coordination and are not the suitable candidate for swarm based systems. Therefore, a simple robot design with a few actuators is desirable. In this paper an attempt is made to arrive at a suitable robot design for swarm based applications.

This paper is organized as follows. Section one reviews the literature related to mobile robot design and control. In section two, a simple study is conducted to understand swarm behavior under extreme situations. In

section three, robot design with multi-directional capability is described. Section four presents the mechanical design of three legged wheg. Section five advances the conceptual design of Omni-directional robot. The final section spells out the major conclusion arrived.

II. STUDY OF SWARM BEHAVIOR

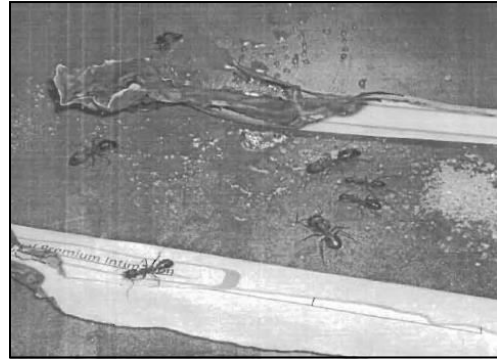


Fig.1: Retreating in every possible direction under threat

A Swarm of ants were tested under various conditions and their behavior was noted down. These aspects have been considered while designing the swarm robot. Figures 1 shows the behavior of the ants under extreme conditions. The ants normally move as a swarm, but when threatened by a distress situation (fire in this case) they tend to retreat in all possible directions. From the swarm behavior it is clear that the robot should also have the capability to move in all directions. The following describes an attempt to evolve a robot which is simple in design and also capable of moving in all directions.

III. ROBOT DESIGN WITH MULTIDIRECTIONAL CAPABILITY

In this section a robot design with wheg is presented and the expressions for determining its rolling resistance, obstacle crossing ability and slip are derived.

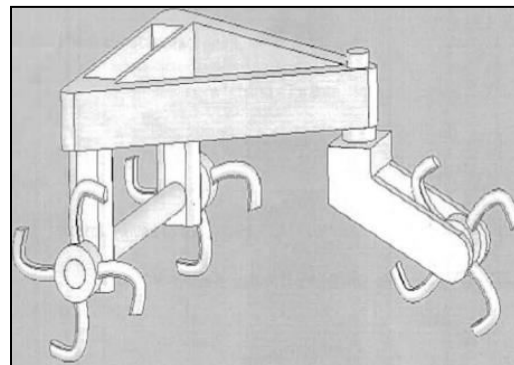


Fig. 2 : Robot design using wheg

Figure 2 shows the conceptual design using wheg. This configuration consists of a triangular shaped frame as body, with one actuator in the rear and two in the front. One actuator in front helps in turning the robot while others are used to drive the system. The one actuator in the rear is able to power both the rear wheels with the help of a simple gear drive. One actuator in the front is used to turn robot while the other is used to provide torque to the front wheel.

3.1 Rolling Resistance for Wheg

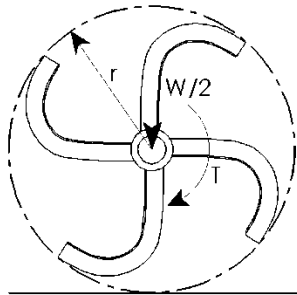


Fig. 3 : Rolling Resistance for wheg with front wheel drive.

Taking moment about contact point O,

$$W*r*\sin \alpha - T = 0$$

$$T = w*r*\sin \alpha \quad (3.1)$$

Where,

T = torque given to the wheel

W = weight of the robot

r = radius of the wheel

From the above equation if $\alpha = 90^\circ$ the drive power required will be,

$$T = w*r \quad (3.2)$$

Since $\sin \alpha = 1$, when $\alpha = 90^\circ$.

The wheel will be able to climb over the obstacle, since it is possible to produce the said torque (T)

3.2 Length crossing ability of Wheg

The following evaluations help us to calculate the length of the obstacle for which the wheg will be able to jump over without any additional rolling resistance.

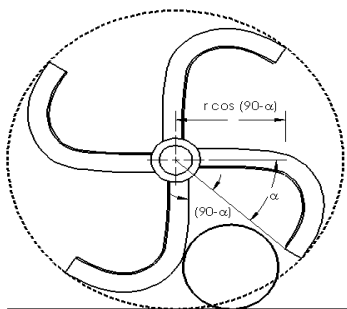


Fig.4: Determination of length crossing ability of Wheg.

Let the distance moved by the legged wheel is $r*\alpha$.

If there are 'n' number of wheels,

$$D = n*r*\alpha \quad (3.3)$$

The distance moved by the wheel tip

$$C = r - (r*\cos \alpha) \quad (3.4)$$

The obstacle length that the legged wheel can cross is,

$$L = (n*r*\alpha) + (r - C)$$

$$L = n*r*\alpha + r - r*\cos \alpha \quad (3.5)$$

The obstacle length that the wheg can cross over is given by the above expression.

3.3 Obstacle Crossing Ability of Wheg

Here, expressions for calculating the height of the obstacles that the wheg can climb over are evaluated theoretically and used for determining the design of the robot. Figure 5 shows the diagram used for deriving the expression.

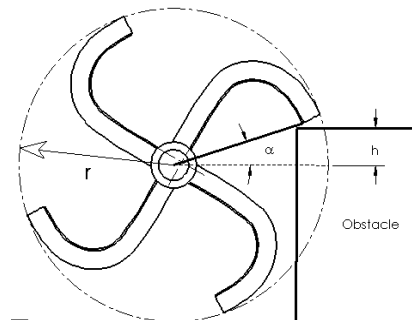


Fig. 5 : Obstacle crossing ability of Wheg

Assuming that enough drive torque is available to climb maximum height, the obstacle height climbed can be calculated from the expression,

$$H = r(1 + \sin \alpha) \quad (3.6)$$

3.4 Amount of Slip

There will be cases where the leg could miss the obstacle causing slip during forward movement. Here, the amount of slip when the leg misses the obstacle is calculated,

$$S = r*\alpha - (r - r*\cos \alpha)$$

$$S = r*(\alpha - 1 + \cos \alpha) \quad (3.7)$$

From the above equation, the amount of slip when the leg misses the obstacle can be calculated.

3.5 Drive Power Required for the Robot

The expressions to calculate the drive power required to drive the whole robot over an inclined surface is evaluated.

From the free body diagrams of the robot shown in fig.6

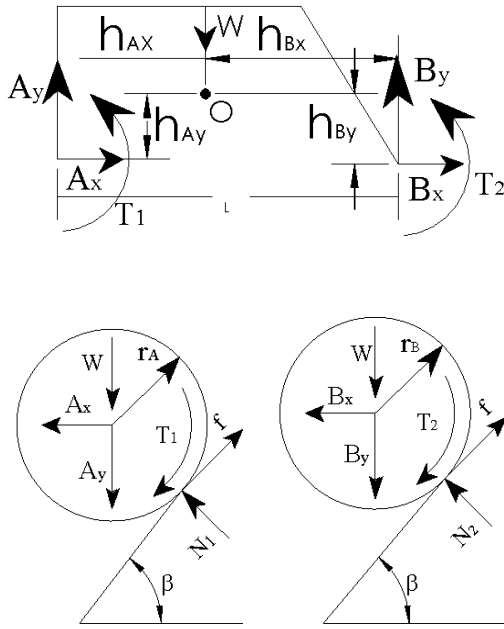


Fig. 6 : Drive power required for the robot on inclined surface

Taking moment about contact point 'O',

$$(A_x * W \sin \beta) r_A - T_1 = m(k^2 + d^2) \alpha_1 \quad (3.8)$$

$$(B_x * W \sin \beta) r_B - T_2 = m(k^2 + d^2) \alpha_2 \quad (3.9)$$

From the free body diagram of the body,

According to Newton's law,

$$A_x + B_x - w \sin \beta = m_{\text{vehicle}} * \ddot{X}_{\text{vehicle}} \quad (3.10)$$

We know that,

$$\ddot{\theta}_A = -\ddot{X} / r_A$$

$$\ddot{\theta}_B = -\ddot{X} / r_B$$

Determination of Normal Forces

$$N_1 - A_y - W \sin \beta = 0 \quad (3.11)$$

$$N_2 - B_y - W \sin \beta = 0 \quad (3.12)$$

From the free body diagram of the body,

By Newton's Law,

$$A_y + B_y - W \cos \beta = 0 \quad (3.13)$$

Taking moment about centre of gravity,

$$A_x * h_{Ay} + B_x * h_{By} + A_y * h_{Ax} + B_y * (L - h_{Ax}) + T_1 + T_2 = 0 \quad (3.14)$$

Where,

A_x, A_y, B_x, B_y = forces along the horizontal and vertical direction.

T_1, T_2 - torque required at the position A and B.

$h_{Ax}, h_{Ay}, h_{Bx}, h_{By}$ = distance between the position A and B to the C.O.M.

N_1, N_2 = Normal forces.

From the above equation the drive force required to drive the robot over an inclined surface can be calculated.

3.6 Experimental Evaluation of Wheg Design

For the designed wheg the various parameters namely the obstacle crossing ability, length of the obstacle and height of the obstacle for which there is no rolling resistance are determined experimentally. The experimental procedure has been detailed in the following pictures by using prototype design of the wheg (fig 7).

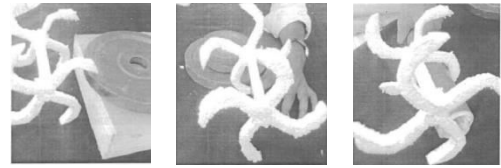


Fig. 7 : Prototype design of the wheg for obstacle crossing ability, length of the obstacle and height of the obstacle

3.7 Comparison of Calculated Theoretical and Experimental Values

In table 1, the values calculated using the analytical method and the experimentally obtained values are compared find out the genuineness of the obtained analytical expressions.

For diameter = 175mm, $\alpha = 25^\circ$

Measured Parameters	Theoretical In (mm)	Experimental In (mm)
Length of obstacle	113	110
Height of obstacle	75	70
Obstacle crossing ability	125	120

Table 1 : Evaluation of wheg.

Thus the theoretical values calculated are found to be in close agreement with the experimentally calculated values. The small difference in the values could be due to measurement errors.

IV. ANALYSIS OF LEG GEOMETRY

From the theoretical evaluation derived earlier it is found that a three legged wheg is more effective than a four legged one. It possess better obstacle crossing

ability (both length and height). In this section mechanical design of whieg with three legs is attempted

Figure 8 shows the whieg model with three curved legs.

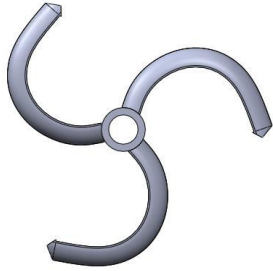


Fig. 8 : Whieg design with three curve shaped legs

4.1 Stress

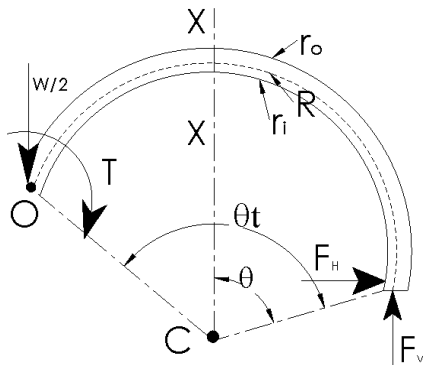


Fig. 9 : Free body diagram for the leg while climbing over an object.

Considering the circular cross-section for the leg [25]

$$r_n = \frac{(r_o^{1/2} + r_i^{1/2})^2}{4} \quad (4.1)$$

$$e = R - r_n \quad (4.2)$$

$$R = r_i + d/2 \quad (4.3)$$

$$A = \pi d^2/4 \quad (4.4)$$

Bending moment at the section located by angle 'θ'

Stress at outer fiber.

$$\sigma_o = F_H/A - M*(r_o - r_n)/A*e*r_i \quad (4.5)$$

Stress at inner fiber.

$$\sigma_i = F_H/A + M*(r_n - r_i)/A*e*r_i \quad (4.6)$$

R= Radius of centroidal axis.

ri= Radius of inner fiber.

ro= Radius of outer fiber.

rn= Radius of neutral axis.

A= Area of circular cross section of the leg.

σi, σo= Stress at the inner and outer fiber.

M= Bending moment with respect to centroidal axis.

FH, Fv= Force along the horizontal and vertical direction.

e= Distance from the centroidal axis to the neutral axis.

From the above equation, stress acting at the designated section in the leg can be determined.

4.2 Deflection

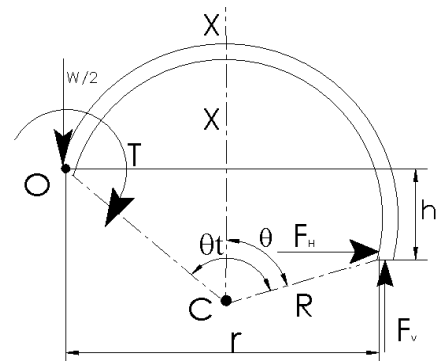


Fig. 10 : Deflection of whieg model-1 in the case of applied force.

$$F_v * r + F_H * h = T \quad (4.7)$$

$$F_v = W_{robot}/2 \quad (4.8)$$

$$F_H = (T - W_{robot} * r/2)/h \quad (4.9)$$

Bending moment at the location formed by the angle 'θ' [26].

$$M = F_H(R - R \cos \theta) + F_v * R \sin \theta \quad (4.10)$$

$$\frac{\partial M}{\partial F_v} = R \sin \theta \quad (4.11)$$

$$\Delta V = \int_0^{\theta_t} M * \left(\frac{\partial M}{\partial F_v} \right) * R * d\theta \quad (4.12)$$

Assuming $F_H=0$,

$$\Delta V = \int_0^{\theta_t} F_v * \left(\frac{R * \sin \theta * R * \sin \theta}{EI} \right) * R * d\theta \quad (4.13)$$

$$\Delta_V = \frac{F_V * R^3}{2EI} \left[\theta_t - \frac{\sin 2\theta_t}{2} \right] \quad (4.14)$$

Deflection in the horizontal direction,

$$\frac{\partial M}{\partial F_H} = R - R \cos \theta \quad (4.15)$$

Assuming $F_V=0$

$$\Delta_H = \int_0^{\theta_t} F_H * \left(\frac{(R - R \cos \theta) * (R - R \cos \theta)}{EI} \right) * R * d\theta \quad (4.16)$$

$$\Delta_H = \frac{F_H * R^3}{EI} \left[\theta_t + \frac{\theta_t - \frac{\sin 2\theta_t}{2}}{2} - 2 \sin \theta_t \right] \quad (4.17)$$

$$\Delta = \sqrt{\Delta_V^2 + \Delta_H^2} \quad (4.18)$$

From the above calculations the deflection of three legged whег model shown in figure 10 can be calculated

From the expressions it can be inferred that for the same loading condition, the stress developed in the leg depends on the geometric parameters of the leg. An important point to be considered for leg geometry selection is that it should minimize the vertical oscillation of the body during locomotion to enhance the energy efficiency.

V. WHEG DESIGN WITH BIDIRECTIONAL CAPABILITY

As the three legged whег is more effective than a four legged one, bi-directional capability is provided. Figure 11 shows the shape of the three legged bi-directional whег model. Further, it improves the performance. This design modification facilitates easy reversal of the direction of motion with equal ease. Further it retains the turning ability of the robot. This greatly reduces the complexity of the drive system used for turning since the robot will be able to move in both the directions efficiently. An internal bend is provided at the bottom of the leg to improve grip during robot motion.

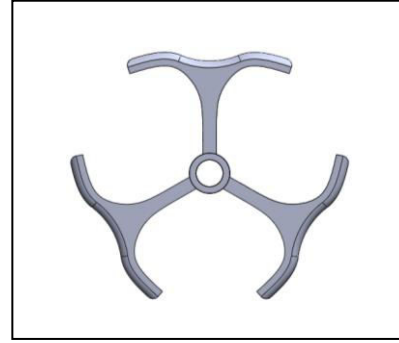


Fig. 11 : Three legged bi-directional whег model.

5.1 Physical model of the robot

Fig.12 shows the prototype built using the selected design with the objective of gaining experience in design and construction. In future a robust model will be built using stronger material.



Fig. 12 : Prototype built using the selected design

VI. CONCLUSION

In this paper two robot configurations have been evolved and evaluated for swarm based applications. The first design is evolved using triangular body and whег and is direct driven with front wheel steering. It has less rolling resistance and good obstacle crossing ability but it does not have Omni-directional capability. Leg geometry is found to have influence on the deformation and stress induced in the leg and the leg with curved geometry is selected as it would help in realizing smooth robot body movement. Finally, a front leg driven robot design with modified whег is found to possess all the desired features and is selected. In future, a robust robot model with passive compliance at the hip joint will be built and its obstacle crossing ability and Omni-directional capability will be experimented.

ACKNOWLEDGEMENT

The First author (Dr. M. Thangavel) gratefully acknowledges the funding provided by ISRO through RESPOND Project to carry out this project.

REFERENCES

- [1] Al Globus, Greg Hornby, Greg Larchev, Matt Hancher, Howard Cannon, and Jason Lohn “Teleoperated Modular Robots for Lunar Operations” American Institute of Aeronautics and Astronautics.
- [2] Javaid Khurshid, Hong Bing-rong “Military Robots- A Glimpse from Today and Tomorrow” 2004 8th International Conference on Control, Automation, Robotics and vision. Kunming, China, 6-9th December 2004.
- [3] Fiona Higgins, Allan Tomlinson and Keith m. Martin “Survey on Security Challenges for Swarm Robotics” Fifth International Conference on Autonomic and Autonomous Systems, 2009.
- [4] Roderich Groß, Marco Dorigo “Towards group transport by swarms of robots” Int. J. Bio-Inspired Computation, Vol. 1, Nos. 1/2, 2009
- [5] vito Trianni, Stefano Nolfi, Marco Dorigo “Cooperative hole avoidance in a swarm-bot” Robotics and Autonomous System 54 (2006) p.p 97-103
- [6] Alberto Rovetta, Elena Cristiana Paul “Trends of space robotics design methodologies for a colony of autonomous space robot explorers” 12th IFToMM World Congress, Besancon (France), June 18-21, 2007.
- [7] C.R. Weisbin, Mel Montemerlo, W. Whittaker “Evolving Directions in NASA’s Planetary rover Requirements and Technology” Robotics and Autonomous System, vol 11, Issue 1, May 1993, p.p 3-11.
- [8] S. Hettiarachchi, W. M. Spears, “Distributed Adaptive Swarm for Obstacle Avoidance” International Journal of Intelligent Computing and Cybernetics.
- [9] Francois Michaud, Dominic Letourneau, Martin Arsenault, Yann Bergeron, Richard Cadrin, “AZIMUT, a leg- Track – Wheel – Robot”, Proceedings of the 2003 IEEE/RSJ Intl. Conference on Intelligent Robots and Systems, Las Vegas. Nevada October 2003.
- [10] Vijay kumar, Terry kientz, Kenneth chin Robert Breslawski, “Mobile Robot for Un –even Terrain”, Proceedings of DETC’ 02, 2002 ASME Design Engineering Technical Conferences and Computers and Information in Engineering Conference Montreal, Canada, September 29 – October 02,2002.
- [11] Martin Buehler, N.Neville, “Towards Running of a six –Legged robot”,12th Yale Workshop on Adaptive and Learning Systems, May 2003.
- [12] John T. Offi, Roger D. Quinn, Daniel A. Kingsley, Roy E. Ritzmann “Improved mobility Through Abstracted Biological Principles” Proceedings of the 2002 IEEE/RSJ, Intl. Conference on Intelligent Robots and Systems, EPFL, Lausanne, Switzerland · October 2002, pp. 2652-2657.
- [13] Roger D. Quinn, Gabriel M. Nelson, Richard J. Bachmann, Daniel A. Kingsley, John T. Offi, Thomas J. Allen, Roy E. Ritzmann “Parallel Complementary Strategies For Implementing Biological Principles Into Mobile Robots” The International Journal of Robotics Research Vol. 22, No. 3–April, March–April 2003, pp. 169-186.
- [14] Jeremy M. Morrey, Bram Lambrecht, Andrew D. Horchler, Roy E. Ritzmann, Roger D. Quinn, “Highly Mobile and Robust Small Quadruped Robots”, Proceedings of the 2003 IEEE/RSJ, Intl. Conference on Intelligent Robots and Systems, Las Vegas, Nevada October 2003.
- [15] Alexander S. Boxerbaum, Philip Werk, Roger D. Quinn, Ravi Vaidyanathan “Design of an Autonomous Amphibious Robot for Surf Zone Operation: Part I Mechanical Design for Multi-Mode Mobility” Proceedings of the 2005 IEEE/ASME, International Conference on Advanced Intelligent Mechatronics, Monterey, California, USA, 24-28 July, 2005, pp. 1459-1464.
- [16] Daniel Davies and Shigeo Hirose, “Continuous High-Speed Climbing Control and Leg Mechanism for an Eight-Legged Stair- Climbing Vehicle”, 2009 IEEE/ASME International Conference on Advanced Intelligent Mechatronics Suntec Convention and Exhibition Center, Singapore, July 14-17, 2009.
- [17] Masashi Takahashi, Kan Yoneda, Shigeo Hirose, “Rough Terrain Locomotion of a Leg-Wheel Hybrid Quadruped Robot”, Proceedings of the 2006 IEEE International Conference on Robotics and Automation, Orlando, Florida - May 2006.
- [18] Markus Eich, Felix Grimminger, Frank Kirchner, DFKI Bremen, Tadayoshi Aoyama, Kosuke Sekiyama, Yasuhisa Hasegawa and Toshio

- Fukuda, “ Analysis of Relationship between Limb Length and Joint Load in Quadruped Walking on the slope”, 2008 IEEE/RSJ International Conference on Intelligent Robots and Systems, Acropolis Convention Center, Nice, France, Sept, 22-26, 2008
- [19] Pinhas Ben-Tzvi, Andrew A. Goldenberg, Jean W. Zu “Design and Analysis of a Hybrid Mobile Robot Mechanism with Compounded Locomotion and Manipulation Capability” Journal of Mechanical Design Transactions of the ASME, JULY 2008, Vol. 130 / 072302-(1-13).
- [20] Jingguo Wang and Yangmin Li “Kinematic Analysis of a Mobile Robot with Two-body Frames” Proceedings of the 2008 IEEE International Conference on Information and Automation June 20 -23, Zhangjiajie, China, pp. 1073-1078.
- [21] A. Gonzalez, E. Ottaviano, M. Ceccarelli “On the kinematic functionality of a four-bar based mechanism for guiding wheels in climbing steps and obstacles” Mechanism and Machine Theory 44 (2009) pp.1507–1523.
- [22] Conghui Liang, Marco Ceccarelli, Giuseppe Carbone “A Novel Biologically Inspired Tripod Walking Robot” Proceedings of the 13th WSEAS International Conference on SYSTEMS, ISBN: 978-960-474-097-0.
- [23] Daisuke Chugo, Kuniaki Kawabata, Hayato Kaetsu, Hajime Asama and Taketoshi Mishima “Mechanical Design of Step-Climbing Vehicle With Passive Linkages” Bioinspiration and Robotics: Walking and Climbing Robots, Book edited by: Maki K. Habib ISBN 978-3-902613-15-8, pp. 544, I-Tech, Vienna, Austria, EU, September 2007.
- [24] M. Thangavel, T. Vinny Daniel David, “Leg design for wheeled-leg robot” International conference on computational vision and robotics 2010, Bhubaneswar, Orissa, India.
- [25] Hall, Holowenko, Laughlin., Theory and Problems of Machine design, Schaum’s outline series, SI (Metric) edition, McGraw-Hill, (1982).
- [26] William A. Nash., Theory and Problems of Strength of Materials, Schaum’s outline series, 3/e, McGraw-Hill, (1994).

